2012-01-01

Analysis And Modeling Of Dust Event Data From El Paso, Texas

Nancy Ivette Rivera Rivera
University of Texas at El Paso, nirivera2@miners.utep.edu

ANALYSIS AND MODELING OF DUST EVENT DATA FROM EL PASO, TEXAS

NANCY I. RIVERA RIVERA M.S.

Environmental Science and Engineering Program

APPROVED:

Thomas E. Gill, Ph.D., Co-Chair

Rosa M. Fitzgerald, Ph.D., Co-Chair

Sergio Cabrera, Ph.D.

David J. Novlan, M.S

Benjamin C. Flores, Ph.D.
Dean of the Graduate School

Dedication

I want to dedicate this work to my family, especially to my Mom Tomasita Rivera Rivera and my Dad Gil. M. Rivera Mercado (that passed away 5 months ago) for all the support, confidence and help they gave me during this journey. To my husband, Gary D. Lynch for all his support and understanding during this process. To my sister and brother, Edda M. Rivera and Gil R. Rivera for all their support. Also I dedicate this work to God because he has always given me the power and determination that I have needed to succeed in all my dreams.

Dedicación

Este trabajo se lo dedico mi familia, en especial a mi mamá Tomasita Rivera Rivera y a mi papá Gil M. Rivera Mercado (que falleció hace 5 meses) por toda la confianza y apoyo que me han brindado en todo este tiempo. A mi esposo Gary D. Lynch por todo su apoyo y comprensión durante este proceso. A mis hermanos, Edda M. Rivera y Gil R. Rivera y sus respectivas familias por todo su apoyo. También le dedico este trabajo a Dios por que el siempre me ha dado la Fortaleza y la Determinación que he necesitado para realizar todos mis sueños.

ANALYSIS AND MODELING OF DUST EVENT DATA FROM EL PASO, TEXAS

by

NANCY I. RIVERA RIVERA M.S.

DISSERTATION

Presented to the Faculty of the Graduate School of

The University of Texas at El Paso

in Partial Fulfillment

of the Requirements

for the Degree of

DOCTOR OF PHYLOSOPHY

Environmental Science and Engineering Program

THE UNIVERSITY OF TEXAS AT EL PASO

December, 2012

Acknowledgements

I want to thank:

- Thomas E. Gill - Co-Chair
- Rosa M, Fitzgerald - Co-Chair
- Sergio Cabrera - Committee member
- David J. Novlan - Committee member

for their advice and all the help that they gave to me during this research. This project was supported in part by NOAA through the Educational Partnership Program for Minority Serving Institutions (EPP/MSI) Cooperative Agreement NA17AE1623.

Abstract

Wind erosion is a dynamic physical process that leads to environmental degradation when strong winds blow on loose, dry, bare soils, creating dust events that can impact human health, visibility and air quality. Since 1932, more than two thousand dust event days were recorded at El Paso, averaging 25 per year. This research analyzes and models data on dust events in the El Paso/Juarez metropolitan area for better understanding of their effects. The meteorological characteristics of these events are analyzed for variables such as the frequency, visibility, and average wind speeds associated with convective and non-convective events. These variables are further correlated with other parameters including particulate matter concentrations, relative humidity and associated precipitation to determine their relationships. Air transport pathways into El Paso during days with dust events (classified as convective and non-convective in nature), as well as days in which dust was not reported, were created with the HYSPLIT model and statistically analyzed. During 2001- 2005, dust events were recorded on 12% of all days; 55% of the events were synoptically-driven, while 45% of the events were convectively-driven. Analyses showed different airflow patterns during dusty days as compared to overall trajectories into El Paso. For synoptically-driven dust events, arriving air masses were strongly associated with a zone of known dust source areas west-southwest of the city, and trajectories were consistent with air parcels moving toward cyclones crossing or developing NE of the Chihuahuan Desert. For convective dust events, trajectories were correlated with air masses arriving from the south and southeast, consistent with monsoon moisture surges bringing thunderstorms. Finally, numerical modeling of weather on a dust event day was performed and analyzed using the Weather Research and Forecasting (WRF)-Chem model. The case study selected was Feb. 4, 2008, where very strong gusty winds across much of northern Mexico, eastern New Mexico and Northwest Texas generated widespread dense blowing dust in the afternoon on. WRF-Chem model results were correlated with TCEQ station data to evaluate the

model's performance for dust storms. The results of these analyses improve the knowledge of how dust storms and airborne particulate matter behave in the El Paso, Texas/ Ciudad Juarez, Chihuahua region and can aid in improving the forecasts of these phenomena.

Table of Contents

Acknowledgements.....v

Abstract.....vi

Table of Contents.....vi

List of Tables.....x

List of Figures..... xii

Chapter 1 1

1.1 Introduction.....1

1.2 Study area……..7

1.3 References……..……14

Chapter 2 26

2.1. Statistical Analysis of historic Dust Events in the Chihuahuan Desert.....26

2.1.1 Introduction.....26

2.1.2 Methodology 28

2.1.2.1 Historic Dust Storm Data…….…28

2.1.2.2 Particulate Matter Data…….31

2.1.2.3 Precipitation Data…….34

2.1.2.4 Relative Humidity Data……....35

2.2.3 Results……...37

2.1.3.1 Particulate Matter…….….37

2.1.3.2 Precipitation ……..…41

2.1.3.3 Relative Humidity …….……...44

2.1.4 Summary …….....48

2.1.5 References ……..…..…50

Figures……....57

Chapter 3 86

3.1 Back Trajectory analysis of air transport patterns that bring dust storms to El Paso, TX ..... …..86

3.1.1 Introduction..... 86

3.1.2 Data and Methodology…….…….89

3.1.2.1 Dust events data extraction …….....89

3.1.2.2 Back Trajectories …….....90
3.1.2.3 Statistical Analysis …….....92
3.1.3 Results…….94
3.1.3.1 Overall data for El Paso, 2001-2005 ……94
3.1.3.2 Convectively-Driven Dust Events ……..103
2.2.4 Summary ……...105
2.2.5 References…….....107
Chapter 4 114
4.1 Modeling analysis of El Paso dust storm meteorological data using the WRF model coupled with Chemistry (WRF-Chem) to simulate the chemistry of the mineral aerosols ……...114
4.1.1 Introduction……..…….....114
4.1.2 WRF and WRF-Chem model Description ……....115
4.1.3 Modeling Research - Case Study ……..……...120
4.1.4 Results ……...123
4.1.4.1WRF-Chem Model.……123
4.1.4.2 TCEQ CAMS Data…….....124
4.1.5 Summary ……125
4.1.6 References…….……..126
Figures…….....129
Tables……..….144
Chapter 5 ……..…156
5.1 Conclusion…….....156
References…….....160
Vita…….....186

List of Tables

Chapter 2

Table I: Example of Statistical analysis done withb the data. 30

Table II: Example of Precipitation Averages table..... .35

Table III: Correlation of the average PM 2.5 and PM 10 for non-convective and convective events and its Anova…….....39

Table IV: Anova correlation of the average PM 2.5 and PM 10 for the hour of the 1st dust observation for the duration of the event versus the visibility……...40

Table V: Correlation between the precipitation averages vs. 2008 dust events……..….42

Table VI: Correlation between the number of dust days in 2010 vs. the average precipitation 3 years prior (2005-2007)…….....43

Table VII: Correlation of RH % and PM 2.5/PM 10 for the hour of the first dust observation for the duration of the event, for all the events..…….…..46

Table VIII: Correlation of RH % and PM 2.5/PM 10 for the hour of the first dust observation for the duration of the event, for Non-Convective events……46

Table IX: Correlation of RH % and PM 2.5/PM 10 for the hour of the first dust observation for the duration of the event, for Convective events……..…47

Chapter 3

Table I: Factors that affect convective and Non-Convective dust events in El Paso, TX…….....88

Chapter 4

Table I: Surface Wind Speed WRF-Chem data, February 4, 2008 event……144

Table II: 3D-Surface Wind Speed WRF-Chem data at different pressure heights,

February 4, 2008 event…….145

Table III: Surface Planetary Boundary Layer Height WRF-Chem data,

February 4, 2008 event…….....146

Table IV: Surface Relative Humidity (%) WRF-Chem data, February 4, 2008 event……....147

Table V: Surface Sea Level Pressure WRF-Chem data, February 4, 2008 event……....148

Table VI: Surface Temperature (K) WRF-Chem data, February 4, 2008 event……..149

Table VII: TCEQ CAMS 12 Data……150

Table VIII: TCEQ CAMS 40 Data……...151

Table IX: TCEQ CAMS 41 Data……..152

TableX: TCEQ CAMS 49 Data……153

Table XI: TCEQ CAMS 72 Data……..154

Table XII: TCEQ CAMS 324 Data……...155

List of Figures

Chapter 1

Figure 1.1: Three Phases of Wind Erosion: Entrainment, transport, deposition. Atmospheric conditions, soil properties, land surface characteristics and land-use practice that control wind erosion process….. 4

Figure 1.2: Chihuahuan Desert Region. After an original map by R. Schmidt (1979). Image retrieaved from http://museum.utep.edu/chih/chihdes.htm.……8

Figure 1.3: Monthly frequency of dust events in El Paso, 1932-2010……...9

Figure 1.4: MODIS Aqua data image…….…….11

Figure 1.5: Haboob Convective Dust Event…….....11

Figure 1.6: Percent of Convective Dust Events……...12

Chapter 2

Figure 2.1: Location of Continuous Air Monitoring Stations…….…..33

Figure 2.2: Visibility vs. PM 2.5, PM 10 Concentrations for all the Events…….....57

Figure 2.3: Visibility vs. PM 2.5, PM 10 Concentrations for Convective Events……58

Figure 2.4: Visibility vs. PM 2.5, PM 10 Concentrations for Non-Convective Events…….59

Figure 2.5: PM 2.5 and PM 10 Concentrations of Convective vs. Non-Convective Events……..…60

Figure 2.6: (a) Seasonality Concentrations PM 2.5/PM 10, Dusty days 2001-2010…….61

(b) PM 2.5/PM 10 Convective vs. Non-Convective, Winter Months 2001-2010……..62

(c) PM 2.5/PM 10 Convective vs. Non-Convective, Spring Months 2001-2010……..63

(d) PM 2.5/PM 10 Convective vs. Non-Convective, Summer Months 2001-2010……64

(e) PM 2.5/PM 10 Convective vs. Non-Convective, Fall Months 2001-2010……...…65

Figure 2.7: Convective vs. Non-Convective PM 2.5 and PM 10 Concentrations at hour of minimum visibility, 2001-2010……66

Figure 2.8: Non-Convective PM 2.5 and PM 10 Concentrations hourly data for the duration of the event, 2001-2010…….……..…67

Figure 2.9: Precipitation vs. hours of dust per year 1932-2010……68

Figure 2.10: Precipitations vs. # of dust events per year 1932-2010……69

Figure 2.11: Correlation of # of dust events in 2003 vs. Average Precipitation (2000-2002)……..70

Figure 2.12: Correlation of # of dust events in 2003 vs. Average Precipitation (1997-2002)…….…..…71

Figure 2.13: Correlation of # of dust events in 2003 vs. Average Precipitation (1990-2000)……..72

Figure 2.14: Correlation of # of dust events in 2008 vs. Average precipitation (2006-2007)……...73

Figure 2.15: Correlation of # of dust events in 2008 vs. Average precipitation (2005-2007)…….…...74

Figure 2.16: Correlation of # of dust events in 2010 vs. Average precipitation (2005-2007)……...…75

Figure 2.17: Correlation of # of dust events in 2010 vs. Average precipitation (2005-2009)……...….76

Figure 2.18: Average Relative Humidity and Precipitation vs. Frequency of Dust Events, 2001-2010…….77

Figure 2.19: Average PM 2.5 (µg/m^3) vs. % of Relative Humidity (2001-2010)……...….78

Figure 2.20: Average PM 10 (µg/m^3) vs. % of Relative Humidity (2001-2010)……..79

Figure 2.21: Average PM 2.5 and PM 10 (µg/m^3) vs. % of Relative Humidity (2001-2010)……...….80

Figure 2.22: Relative Humidity of Convective vs. Non-Convective Dust Events (2001-2010)…….…..81

Figure 2.23: (a) PM 2.5 and Day average RH for Non-Convective dust days (2001-2010)…….82

(b) PM 10 and Day average RH for Non-Convective dust days (2001-2010)…….82

Figure 2.24: (a) PM 2.5 and Day average RH for Convective dust days (2001-2010)……83

(b) PM 2.5 and Day average RH for Convective dust days (2001-2010)……...….83

Figure 2.25: Relative Humidity vs. Visibility, All the events 2001-2010……...……..84

Figure 2.26: Wind and Wind gust comparison at minimum visibility 1932-2010……85

Chapter 3

Figure 3.1: Monthly frequency of dust days at El Paso, TX during 2001-2005, Convective and Non-Convective…….…….90

Figure 3.2: Contour Plot of overall residence time for 2001-2005……...95

Figure 3.3: Contour Plot of overall source contribution for 2001-2005……96

Figure 3.4: Contour Plot of residence times for all days during which dust was observed for 2001-2005……..……..97

Figure 3.5: Contour Plot of residence times for all days during which dust was not observed for 2001-2005……...98

Figure 3.6: Contour Plot of source contributions for all days during which dust was observed for 2001-2005……..…....99

.

Figure: 3.7: Contour Plot differential probability for all dust days during which dust was observed for 2001-2005…….……...101

Figure 3.8: Contour Plot differential probability for all dust free days for 2001-2005……102

Figure 3.9: Contour Plot of differential probability for all dust days during which convectively-driven dust was observed for 2001-2005……..103

Figure 3.10: Contour plot of conditional probability for all days which convectively-driven dust was observed for 2001-2005……..…….104

Chapter 4

Figure 4.1: Principal components of the WRF system (Copied from Skamarock et al., 2005)…….129

Figure 4.2: GOES Visible-Infrared Composite image that shows the dust event from February 4, 2008. Images obtained from the TCEQ website, (http://www.tceq.state.tx.us/assets/public/compliance/monops/air/sigevents/08/080204txw-goes-2225-comp.jpg) 130

Figure 4.3: Structure of the Planetary Boundary Layer (PBL). Adapted from Stull, 1988……...131

Figure 4.4: PBLH and it interaction with the Earth surface forces……132

Figure 4.5: Plot of surface wind speed, 4km; WRF-Chem data, February 4, 2008 event…….133

Figure 4.6: Plot of surface 3D-wind speed, 4km; WRF-Chem data at different pressure levels, February 4, 2008 event……..134

Figure 4.7: Plot of the Planetary Boundary Layer Height (PBLH) (meters), 4km; WRF-Chem data, February 4, 2008 event……...…….....135

Figure 4.8: Plot of Surface Relative Humidity (%), 4km; WRF-Chem data, February 4, 2008 event……...136

Figure 4.9: Plot of Surface Sea Level Pressure (SLP), 4km; WRF-Chem data, February 4, 2008 event……137

Figure 4.10: Plot of Surface Temperature (K), 4km; WRF-Chem data, February 4, 2008 event……..138

Figure 4.11: Wind Speed comparison WRF-Chem model vs. TCEQ stations measurements, February 4, 2008 event……..…….139

Figure 4.12: Temperature comparison WRF-Chem model vs. TCEQ stations measurements, February 4, 2008 event……140

Figure 4.13: Relative Humidity (RH) comparison WRF-Chem model vs. TCEQ stations measurements, February 4, 2008 event……141

Figure 4.14 Changes in PM 2.5 concentrations during the February 4, 2008 event. Data obtained from the TCEQ stations. ……...……..142

Figure 4.15 Changes in PM 10 concentrations during the February 4, 2008 event. Data obtained from the TCEQ stations. ……..…...143

Chapter 1

1.1 Introduction

The term “aerosol” applies to the liquid and particle phase in a system (Prospero *et al*., 1983). Dust is a type of aerosol distinct from smoke, mist, fumes and fogs (Pye, 1987). Dust aerosol particles transported in suspension in the Earth’s atmosphere are mostly much smaller than 100μm; material which is transported for very long distances (thousands of kilometers) is generally smaller than 10 μm and much is smaller than 2 μm (Pye, 1987). “Mineral dust” is a term used to indicate atmospheric aerosols originated from the suspension of minerals constituting the soil or earth crustal materials; it is composed of various oxides (SiO_2, FeO, Fe_2O_3, and others), carbonates ($CaCO_3$, $MgCO_3$), and other more complex minerals such as clay minerals, feldspars evaporite salts, etc. that constitute the Earth's crust. Global mineral dust emissions are estimated of 2000 Mt per year , of which 1500 Mt is deposited to the land and 500 Mt to the ocean (Shao *et al.,* 2011) , of which the largest part is attributed to deserts. Although this aerosol class is usually considered of natural origin, it is estimated that about 25% (Ginoux *et al*., 2012) to 30% Tegen *et al*., 2004) of the mineral dust load in the atmosphere could be ascribed to human activities through desertification and land misuse.

Mineral dust is one of the largest contributors to global aerosol loading and can interact with the earth’s climate system in different ways. It can affect the radiation budget, atmospheric photochemistry, and cloud processes (e.g. Kondratyev *et al*., 1983; Washington *et al*., 2003; Zender and Young, 2005; Grini *et al*., 2005; Mahowald *et al*. 2006; DeMott *et al.,* 2010; Mahowald *et al.,* 2010; Zhang R. *et al.,* 2010; Calvo *et al.,* 2012). The entrainment of mineral

dust into the atmosphere from terrestrial sources also represents an important process of land-atmosphere interaction (Washington et al., 2003). The major sources are usually deserts, dry lake beds and semi-arid surfaces (Calvo *et al.,* 2012). Factors such as surface soil moisture and vegetation cover as well as changes in climatic parameters such as wind speed and precipitation regulate the emission of mineral particles (Grini *et al.,* 2002; Washington and Todd, 2005). Because dust can be transported over thousands of kilometers, it can have an influence at great distances from its original source (Prospero et al., 2002). Dust contributes to the transport of allergens and pathogens, and when inhaled, can cause or aggravate respiratory diseases (e.g. Hernández-Cadena *et al*., 2000; Samet *et al.,* 2000; Pope III *et al.*, 2002; Pope III *et al.,* 2006; Griffin *et al*., 2007; Ho *et al*., 2007; Grineski *et al.,* 2011). Dust storms represent a significant hazard to road and air travel (Okin *et al.,* 2011). Detection of these variable aerosol events is challenging because of its short lifetimes, multiple-scales, and strong impact of local surface and meteorological conditions (Zhao *et al.,* 2010).

Dust storms are mainly caused by specific weather conditions in semi arid to arid areas over the globe (Zhang *et al.,* 1997; Liu et al., 2003; Natsagdory *et al*., 2003; Tegen *et al*., 2004). Researchers found that regional climatic variables like land surface air temperature, lack of precipitation, availability of soil particles and higher wind velocities are favorable conditions for dust storm occurrence and intensity (Gillette and Walker, 1977; Nilgun and Nikcovic, 2000). The wind speed at a particular site depends primarily on the nature and strength of large-scale wind system over the region (Wigner and Peterson, 1987). Strong winds associated with the passage of cold fronts often raise dust for several hours. The most persistent episodes of high winds and blowing dust occur with the presence of a low pressure system (Brandali *et al*., 1977). The

southwestern plains of the U.S. are influenced by one of the planet's key spots for the formation of cyclones, the downwind or lee side of the Rocky Mountains, Colorado (Shultz and Doswell, 2000). Observations made by Wigner and Peterson (1987) and Bernier et al. (1998) suggest that the most intense dust storms in the Southern Great Plains northeast of the Chihuahuan Desert region are associated with the development of lee cyclones (Colorado cyclones). Although dust storms associated with cyclogenesis are the least frequent, they are the most intense, and they are associated with the lowest visibilities, highest particulate concentrations, longest duration, and greatest total mass of sediment moved (Middleton *et al.*, 1986; Lee and Tckaerian, 1995; Wigner and Peterson, 1987).

Wind erosion is a dynamic physical process that leads to soil degradation that occurs when strong winds blow on loose, dry, bare soils (Zobeck and Van Pelt, 2005). The process of wind erosion is controlled by different physical mechanisms as seen in Figure 1.1 (Shao, 2000). Those mechanisms are: (1) entrainment of particles by wind shear at the surface; (2) the transportation of particles in the atmosphere by advection and turbulent diffusion, and (3) the deposition of particles through dry and wet removal. These physical processes are governed by many factors such as atmospheric conditions, soil characteristics, land surface properties, and land-use practices (Shao, 2000). The occurrence of wind erosion is a consequence of two types of forces at work: (1) aerodynamic forces, that attempt to remove particles from the surface and (2) forces, such as gravity and inter-particle cohesion, that resist removal. Wind-blown materials move in three modes: (1) **creep**, where large soil particles (1-2 mm) roll or slide along the surface; (2) **saltation**, where particles between 100μm and 1 mm tend to move in a bouncing

mode; (3) **suspension**, which involves soil particles less than 100µm that travel long distances suspended in the atmosphere (Zobeck and Van Pelt, 2005).

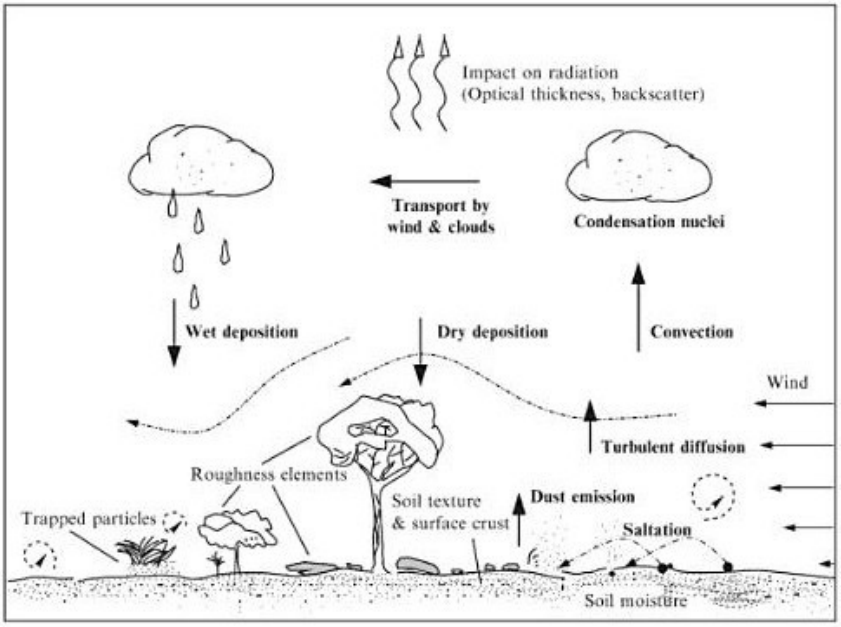

Figure 1.1: Three phases of wind erosion: entrainment, transport and deposition. Atmospheric conditions, soil properties, land-surface characteristics and land-use practice control the erosion process (Modified from Lu, 1999).

Even though wind is the driving force behind the wind-erosion process, the conditions of the soil surface and its surroundings often control whether or not a soil is transported by the wind. In recent years the identification of source areas for dust storms has been an important area for research, where the Sahara Desert and western China are being recognized as the strongest sources globally (Goudie, 2009). Other emitting regions are Lake Eyre and the Great Basin in Australia and deserts in Patagonia and west Argentina (Formenti *et al.*, 2011; Calvo *et al.*, 2012). At a global scale, the dust regions in the northern hemisphere (mainly between 10º and 35º) contribute more aerosols than the ones in the southern hemisphere (Prospero *et al.*, 2002; Formenti *et al.*, 2011; Ginoux *et al.*, 2012).

Recent advances show that dust sources may be more diverse than previously believed (Schepanki *et al.,* 2007). Previous studies have used a variety of data sources, such as ground-based, satellite and meteorological data, to monitor dust storms. Research in the area of West Texas and New Mexico (Kondratyev, *et al*., 1983; Gill. *et al*., 2000; Prospero *et al*., 2002; Rivera Rivera, 2006; Janugani et al., 2009; Rivera Rivera *et al*., 2010; Baddock *et al*., 2011; Lee *et al.,* 2012, Tong *et al*., 2012), has shown that image analysis techniques may help improve our understanding of the dispersion of the dust storms in the areas mentioned above during the windy seasons.

Remote sensing and modeling is used to study dust transport over large and remote places where it is not easy to obtain information using ground-based monitoring platforms (Gill et al., 2000; Rivera Rivera *et al.*, 2009). Remote sensing data may be used to monitor surface features and their changes over large and remote areas, such as desert zones, which are frequently the source of mineral dust emissions. Remote sensors like TOMS, AVHRR, Landsat, GOES-10, SeaWiFS, MODIS, and Meteosat-SEVIRI are some of the platforms used to obtain data that may be used to map the sources of these dust emissions (Ackerman, 1997; Legrand, *et al*., 2001; Doyle and Dorling, 2002; Prospero *et al*., 2002; Miller, 2003; Belsman, 2004; Darmenova, *et al.,* 2005; Connell and Prata, 2006; Christopher *et al*., 2011: Ginoux *et al.,* 2012). Some of these sensors are sensitive to aerosols at different altitudes in the atmosphere. Other studies such as Tong et al. (2012) have used routine aerosol ground monitoring stations measurements like the Interagency Monitoring of Protected Visual Environments (IMPROVE) Network to study the long term dust climatology in Western United States.

All these data have been used to assess the frequency and magnitude of dust events for potential impacts on climate, visibility and health-related air quality issues. Studies conducted by the United States Department of Agriculture's (USDA) Economic Research Service estimated that the off-site costs of wind erosion in the western USA range from $4 to $12 billion per year (Zobeck and Van Pelt, 2005). Off-site impacts from wind erosion are caused primarily by the release of fugitive dust, which may travel long distances imposing cost for cleaning, reducing recreational opportunities, and impairing health (Zobeck and Van Pelt, 2005). Recent research (Samet *et al*., 2000; Pope *et al*., 2002; Yin *et al*., 2005; Grineski *et al.*, 2011) in the US showed that there is a direct link between the exposure to high-levels of air-borne particle concentrations and the increase of mortality from cardiovascular disease, respiratory illness and lung cancer. Many contaminants that pose a significant risk to human health and the environment are associated with dust, including metals, pesticides including dioxins, and radionuclides (Shao, 2000). For these reasons, it is important to determine the areas and the intensity of the dust emissions using both atmospheric modeling and air-quality studies.

This study focuses on the dust climatology in the Chihuahuan desert region in the southwestern U.S. and northwestern Mexico. This area has not been as well characterized for dust emissions as other desert areas in the western U.S. (i.e. Death Valley or Owens Lake in California) (Cahill *et al* 1994; Reheis *et al*., 2002) Chihuahuan desert dust sources have been linked to low-range continental transport, especially seasonally in the spring and winter (Novlan *et al*., 2007). This region encompasses a critical climatic boundary region between the subtropics and the middle latitudes and has been described as a modern semiarid climate that consists of relatively cool, dry winters and warm wet summers (Castalgia and Fawcett, 2006).

Novlan *et al*., (2007) found that dust storm frequency is at its peak during the spring months (March- May). However, dust storms in the area also occur during the summer months and are associated with the North American Monsoon (primarily convective events) (Apodaca and Morris, 2008). Figure 3 shows the monthly frequency of dust events in the region during 1932-2008.

1.2 Study Area

The Chihuahuan Desert is located in the southwestern part of the United States and the northwestern part of Mexico (Figure 1.2). It spans 11 degrees of latitude and approximately 8 degrees of longitude. Aridity in this desert zone stems from a combination of the domination by subtropical high pressure, orographic barriers and continentality. It increases in elevation from 600m above sea level in the northern part to over 2000 m in the south (Warner, 2004). The Chihuahuan Desert is located between two orographic barriers, the Sierra Madre Occidental and the Mimbres Highland to the west and the Sierra Madre Oriental / Sacramento Mountains to the east. Basin and Range topography characterizes the desert. There are very few through-flowing rivers and few areas of erosional lowlands (Schmidt, 1986). As a result, nearly the entire desert has a basin level of 900-1200 m (Schmidt, 1986).

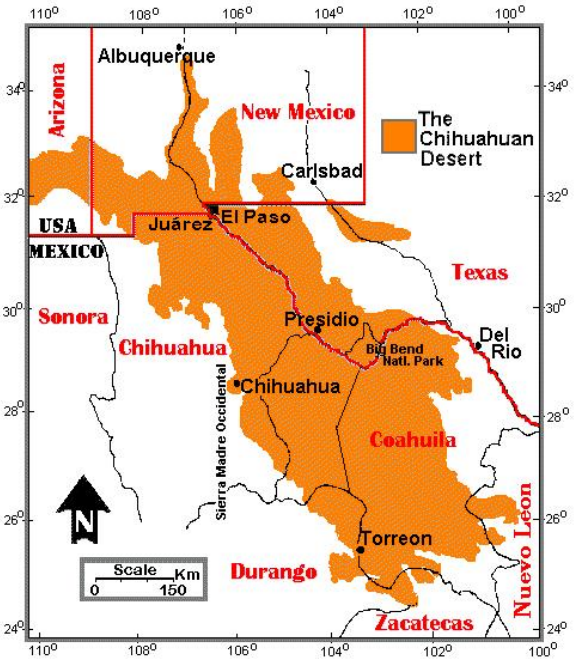

Figure 1.2: Chihuahuan Desert Region. After an original map by R. Schmidt (1979). Image retrieved from http://museum.utep.edu/chih/chihdes.htm

The physical environment of the Chihuahuan Desert is relatively homogeneous. It is surrounded by N-NW trending mountains which have nearly similar heights. Most of the zone lies more or less at an equal distance from the major sources of moisture, these being the Gulf of Mexico, the Gulf of California and the Pacific Ocean. Because it is a subtropical desert, a convective rainfall occurs during the summer months with a significant impact from the moist southwesterly flow of the North American monsoon. The maximum rainfall occurs in July and August. Annual rainfall averages are typically 20-30 cm (Warner, 2004). Natural vegetation is desert scrub in the west, merging with short grass prairie in the east (Lee *et al.*, 2009).

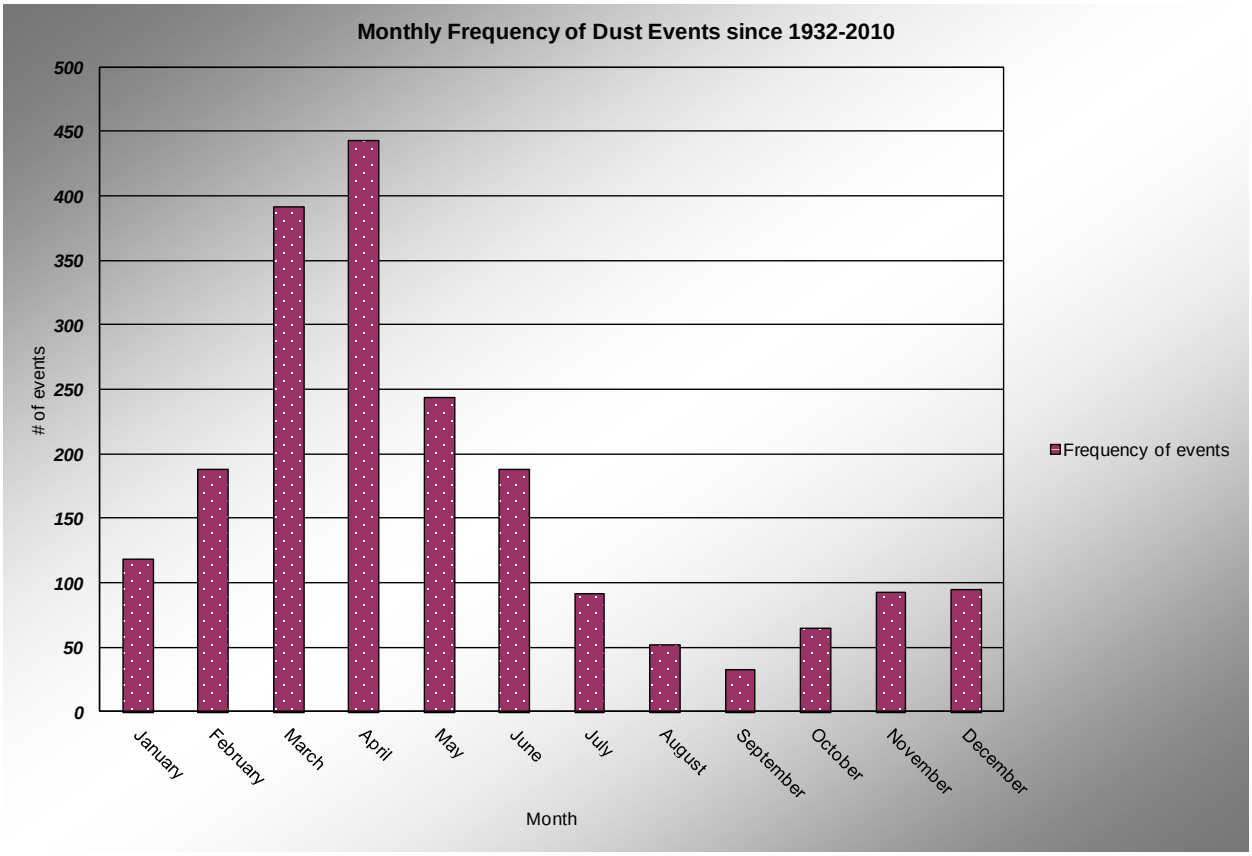

Figure 1.3: Monthly frequency of dust events in El Paso, 1932-2010.

David Novlan from the NOAA/National Weather Service Office in El Paso, TX stated in response to a query from the Texas Commission for Environmental Quality (TCEQ) on dust storms forecasting (adapted from Rivera Rivera, N. I., 2006 M.S. Thesis) that there are two basic categories into which dust storms fall into in the Chihuahuan Desert: Synoptic scale and Mesoscale. Synoptic scale systems (e.g. Cyclones, air masses, hurricanes) typically last for several days to a week; Mesoscale systems usually last hours to a day, and they include thunderstorms and other smaller-scale circulation systems (Moran, 2006). The most persistent episodes of high winds and blowing dust in southwestern North America occur with the presence of a synoptic-scale low pressure system located northeast of the Chihuahuan Desert (Rivera Rivera *et al*., 2009). This surface cyclone is commonly referred to as the ‘‘Albuquerque Low,’’

tracking along the Colorado-New Mexico border into the Texas Panhandle area then northeastward (Novlan *et al*., 2007). These events are driven by the surface pressure gradients, set up by the large scale upper flow aloft, so the characteristic southwest winds of high velocity over 6-12 + hours tap the dust primarily from playa sources throughout the southwest and produce the characteristic swath of dust that emanates from the Chihuahuan Desert and sweeps east northeastward into east southeast New Mexico and eventually into west Texas (Figure 1.4) (Novlan, D., Personal Communication, 2008). The characteristic Haboob (Figure 1.5) of the southwestern North American desert that arises from thunderstorm outflow (very prevalent in the North American monsoon season) is the typical example of the mesoscale dust event on a smaller scale in space and time (Novlan *et al*., 2007). Figure 1.6 shows the percent of dust events that were convective during 1960 to 2006.

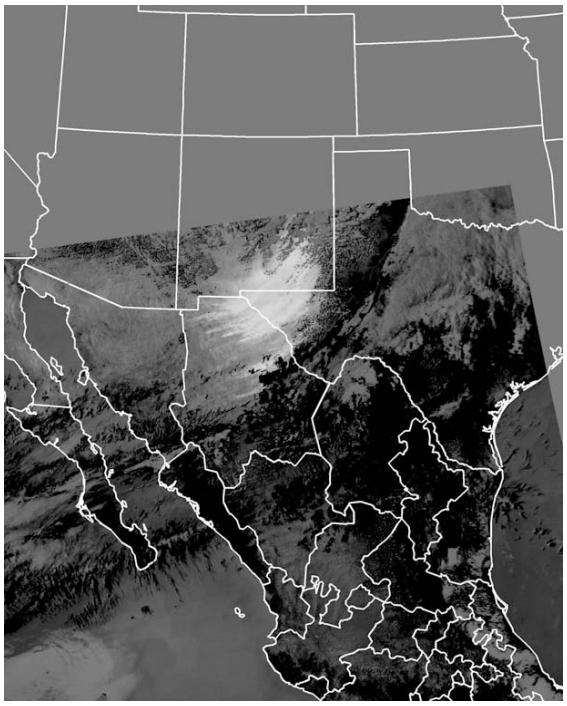

Figure 1.4: MODIS Aqua data image from the 15 April 2003 dust event (20:20 GMT). Difference between bands 31 and 32 (thermal IR bands), showing dust plumes originating in the Chihuahuan Desert area and advecting across western Texas and southern New Mexico (adapted from Rivera Rivera *et al.*, 2009).

Figure 1.5: Haboob (convective) dust event. (Adapted from Novlan *et al*., 2007)

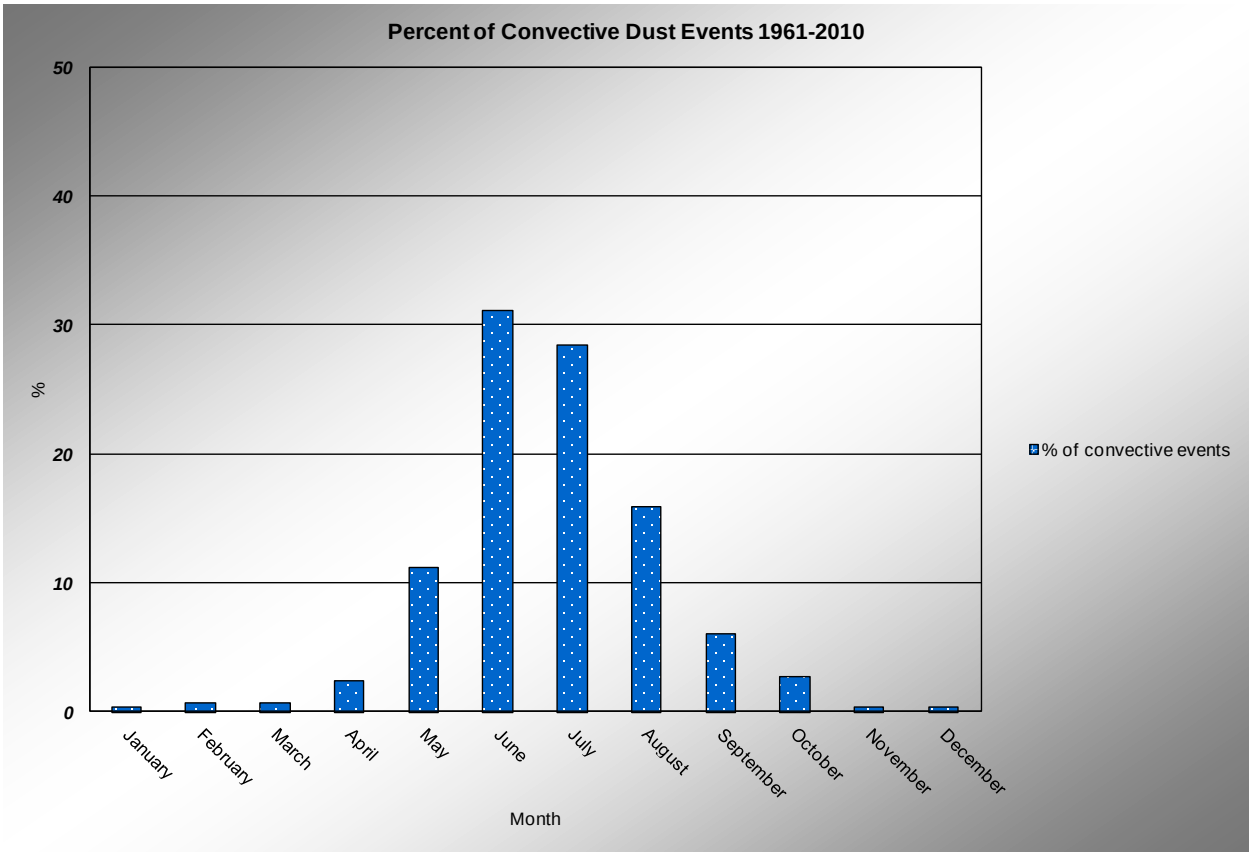

Figure 1.6: Percent of convective dust events at El Paso from 1960-2010

The research contained in this dissertation will continue the Master's thesis work done by Rivera Rivera *et al*., (2006),which focused on characterizing dust sources in the Chihuahuan desert region by analyzing remote sensing data (Janugani *et al*., 2009; Rivera Rivera *et al*., 2009; Rivera Rivera *et al*., 2010). In previous research different dust events were analyzed; the source locations of the dust events were obtained and their land surface was assessed to determine how they corresponded to different land cover surfaces (Rivera Rivera *et al*., 2010; Baddock *et al*., 2011). Most of the source locations were consistent with bare soil, dry playa lakes and agricultural land. These source locations are responsible for poor air quality in far-west Texas, Southern New Mexico and Ciudad Juarez, Chihuahua, Mexico on windy days (Dominguez *et al*., 2007). Further research in Northern Mexico, West Texas and New Mexico is critical because

these areas have major dust outbreaks, regularly in the windy season, that affect the metropolitan area of El Paso, TX/ Ciudad Juarez, Mexico (Novlan *et al*., 2007; Rivera Rivera *et al*., 2009).

1.3 References

Ackerman, S.A. (1997). Remote sensing aerosols using satellite infrared observations. Journal of Geophysical Research, 102 (D14), 17069- 17079.

Apodaca, K., and Morris, V. R. (2008). Analysis of aerosol number size distribution and hygroscopic growth factors as functions of ambient relative humidity during the North American Monsoon. AMS 89th Annual Conference, JP 2.15, Phoenix, AZ.

Baddock, M. C., Gill, T. E. Bullard, J. E., Dominguez-Acosta, M., and Rivera Rivera, N. I. (2011). Geomorphology of the Chihuahuan Desert on potential dust emissions. Journal of Maps, 249-259.

Belsman, L. O. (2004). Satellite data for air quality forecaster. The Aerospace Corporation.

Bernier, S.A., Gill, T.E. and Peterson, R.E. (1998). Climatology of dust in the Southern High Plains of Texas. In: Busacca, A., Lilligren, S. and Newell, K. (eds), Dust aerosols, loess soils and global change: An interdisciplinary conference and field tour on dust in ancient environments and contemporary environmental management, October 1998, Seattle, Washington, Washington State University College of Agriculture and Home Economics Miscellaneous Publication no. 190, pp. 4-7

Brandalli, H. W., Ashman, J. P., and Reinke, D. L. (1977). Pictures of the month; Texas dust moves into Florida. Monthly Weather Review, 105, 1068-1070.

Cahill, T. A., Gill, T. E., Gillette, D. A., Gearhart, E. A., Reid, J. S., and Yau, M-L. (1994) Generation, Characterization, and Transport of Owens (Dry) Lake Dusts, Final Report. Contract No. A132–105, Air Quality Group, Crocker Nuclear Laboratory, Univ. of Calif.

Calvo, A.I., Alves, C., Castro, A., Pont, V., Vicente, A.M., Fraile, R. (2012). Research on Aerosol Sources and Chemical Composition: Past, Current and Emerging Issues. Atmospheric Research, 121, 1-28. doi: 10.1016/j.atmosres.2012.09.021

Castalgia, P. J. and Fawcett, P. J. (2006). Large Holocene lakes and climate change in the Chihuahuan desert. Geology. 34 (2), 113-116.

Christopher, S. A., Gupta, P., Johnson, B., Ansell, C., Brindley, A., Haywood, J. (2011). Multi-sensor satellite remote sensing of dust aerosols over North Africa during GERBIL. Quarterly Journal of Royal Meteorological Society. Vol. 137, No. 658: 1168-1178.

Connell, B.H. and Prata, F. (2006). Detecting volcanic ash and blowing dust using GOES, MODIS, and AIRS imagery. In: 14th Conference on Satellite Meteorology and Oceanography, American Meteorological Society, Preprints, P3.8, 7 pp.

Darmenova, K., Sokolik, I.N. and Darmenov, A. (2005). Characterization of east Asian dust outbreaks in the spring of 2001 using ground based and satellite data. Journal of Geophysical Research, 110, D02204, doi:10.1029/2004JD004842.

DeMott, P.J., Prenni, A.J., Liu, X., Kreidenweis, S.M., Petters, M.D., Twohy, C.H., Richardson, M., Eidhammer, T., Rogers, D.(2010). Predicting global atmospheric ice nuclei distributions and their impacts on climate. P. Natl. Acad. Sci. USA 107, 11217.

Dominguez Acosta, M., (2009). The Pluvial Lake Palomas- Samalayuca Dunes system. Doctoral dissertation, Geology, University of Texas at El Paso, United States.

Doyle, M., Dorling, S., 2002. Satellite and ground based monitoring of aerosol plumes. Water Air and Soil Pollution Focus 2, 615- 629.

Formenti, P., Schuetz, L., Balkanski, Y., Desboeufs, K., Ebert, M., Kandler, K., Petzold, A., Scheuvens, D., Weinbruch, S., Zhang, D.(2011). Recent progress in understanding physical and chemical properties of mineral dust. Atmos. Chem. Phys. 11, 8231-8256.

Gill, T. E., Westphal, D. L., Stephens, G., and Peterson, R. E. (2000). Integrated assessment of regional dust transport from West Texas and New Mexico, Spring 1999. American Meteorological Society, 11th Conference on Air Pollution Meteorology Preprints, 370-375.

Gillette, D. A. and Walker, T. (1977). Characteristic of airborne particles produced by wind erosion of sandy soil, High Plains of West Texas. Soil Science, vol. 123, pp. 97-110.

Ginoux, P., J. M. Prospero, T. E. Gill, N. C. Hsu, and M. Zhao (2012), Global-scale attribution of anthropogenic and natural dust sources and their emission rates based on MODIS Deep Blue aerosol products, Rev. Geophys., 50, RG3005, doi:10.1029/2012RG000388.

Goudie, A. S. 2009. Dust Storms: Recent Developments. Journal of Environmental Management, 90, 89-94.

Griffin, D. W.(2007). Atmospheric Movement of Microorganisms in Clouds of Desert Dust and Implications for Human Health. Clinical Microbiology Reviews. Vol. 20, No. 3, 459-477.

Grineski, S. E., Staniswalis, J. G., Bulathsinhala, P., Peng, Y., Gill, T. E. (2011). Hospital admissions for asthma and acute bronchitis in El Paso, Texas: Do age, sex and insurance status modify the effects of dust and low wind events. Environmental Research, 111, 1148-1155.

Grini, A., Zender, C.S., Colarco, P.R. (2002). Saltation Sandblasting behavior during mineral dust aerosol production. Geophys. Res. Lett. 29, 1868.

Grini, A., Myhre, G., Zender, C. S., and Isaksen, S. A. (2005). Model simulation of dust sources and transport in the global atmosphere: Effects of soil erodibility and wind speed variability. Journal of Geophysical Research, 110, D02205, doi:10,1029/2004JD005037.

Hernández-Cadena, L., Téllez-Rojo, M. M., Sanín-Aguirre, L. H., Lacasaña-Navarro, M.,

Campos, A., Romieu, I. (2000). Relación entre consultas a urgencias por enfermedad respiratoria y contaminación atmosférica en Ciudad Juárez, Chihuahua. Salud Pública de México. Vol. 42, no. 4, 288-297.

Ho, W-C.,Hartley, W. R., Myers, L., Lin, M-H., Lin, Y-S., Lien, C-H., Lin, R-S. (2007). Air pollution, weather, and associated risk factors related to asthma prevalence and attack rate. Environmental Research, 104, 402-409.

Janugani, S., Jayaram, V., Cabrera, S. D., Rosiles, J. G., Gill, T. E. and Rivera Rivera, N. I. (2009). Directional Analysis and Filtering for Dust Storm detection in NOAA-AVHRR Imagery. Proceedings of the SPIE Vol. 7334, 73341G-1.

Kondratyev, K. Ya., Grigoryev, A. A., and Pokrovsky, O. M. (1983). The effects of aerosols on climate and aerosol climatology on the basis of observations from space. Advances in Space Research, 2 (5), 3-10.

Lee, J. A., Gill, T. E., Mulligan, K. R., Domínguez Acosta, M., and Perez, A. E. (2009). Land Use/Land Cover and Point Sources of the December 15 2003 Dust Storm in Southwestern North America. Geomorphology, 105, 18- 27.

Lee, J. A., Baddock, M. C., Mbuh, M. J., Gill, T. E. (2012). Geomorphic and land cover characteristics of Aeolian dust sources in West Texas and eastern New Mexico, USA. Aeolian Research, 3, 459-466.

Lee, J.A. & Tchakerian, V.P. (1995). Magnitude and frequency of blowing dust on the Southern High Plains of the United States, 1947-1989. Annals of the Association of American Geographers,**85**: 684-693.

Legrand, M., Plana-Fattori, A. and N'doumé, C. (2001). Satellite detection of dust using the IR imagery of Meteosat, 1, Infrared difference dust index. Journal of Geophysical Research, vol. 106, no. D16, pp. 18251-18274, doi:10.1029/2000JD900749.

Liu, H.Y., Tian, Y.H., and Ding, D. (2003). Contributions of different land cover types in Otindag Sandy Land and Bashang area of Hebei Province to the material source of sand stormy weather in Beijing. Chinese Science Bulletin 48 (17), 1853–1856.

Mahowald, N. M., Muhs, D. R., Levis, S., Rasch, P. J., Yoshioka, M., Zender, C. S., and Luo, C. (2006). Change in atmospheric mineral aerosols in response to climate: Last glacial period, preindustrial, modern, and doubled carbon dioxide climates. Journal of Geophysical Research, Vol. 111, D10202, doi:10.1029/2005JD006653.

Mahowald, N.M., Kloster, S., Engelstaedter, S., Moore, J.K., Mukhopadhyay, S., Mcconnell, J.R., Albani, S., Doney, S.C., Bhattacharya, A., Curran, M.a.J., Flanner, M.G., Hoffman, F.M., Lawrence, D.M., Lindsay, K., Mayewski, P.A., Neff, J., Rothenberg, D., Thomas, E., Thornton, P.E., Zender, C.S. (2010). Observed 20th century desert dust variability: impact on climate and biogeochemistry. Atmos. Chem. Phys. 10, 10875-10893.

Middleton, N. J., Goudie, A. S., and Wells, G. L. (1986). The frequency and source areas of dust storms. Aeolian Geomorphology, Allen and Unwin, Boston, pp. 237-259.

Miller, S.D. (2003). A consolidated technique for enhancing desert dust storms with MODIS. Geophysical Research Letters, vol. 30, no. 20, pp. 2071, doi:10.1029/2003GL018279.

Moran, J. M., (2006). Weather Studies, Introduction to Atmospheric Science. 3rd Edition American Meteorological Society, Boston, MA.

Natsagdory, L., Jugder, D., and Chung, Y.S., (2003). Analysis of dust storms observed in Mongolia during 1937–1999. Atmospheric Environment vol. 37, no. 9–10, pp. 1401–1411.

Nilgun, K., Nickovic, S., (2000). An illustration of the transport and deposition of mineral dust onto the eastern Mediterranean. Atmospheric Environment vol. 34, pp. 1293–1303.

Novlan, D.J., Hardiman, M., Gill, T.E., (2007). A synoptic climatology of blowing dust events in El Paso, Texas from 1932-2005. Preprints, 16th Conference on Applied Climatology, American Meteorological Society, J3.12, 13 pp.

Okin, G. S., Bullard, J. E., Reynolds, R. L., Ballantine, J-A. C., Schepanski, K., Todd, M. C., Benalp, J., Baddock, M. C., Gill, T.E. and Miller, M. E. (2011). Dust emission: small-scale processes with global-scale consequences. Eos, Transactions of the American Geophysical Union 92(29):241- 242.

Pope III, C. A., Brunnet, R. T., Thun, M. J., Calle, E. E., Krewski, D., Ito, K., and Thurston, G.D. (2002). Lung cancer, cardio-pulmonary mortality, and long-term exposure to fine particulate air pollution. The Journal of the American Medical Association. 287 (9), 1132-1141.

Pope III, C. A. and Dockery, D. W. (2006). Health Effects of Fine Particulate Air Pollution: Lines that Connect. Journal of the Air &Waste Management Association. 56: 709-742.

Prospero, J. M. Charlson, R. J., Mohnen, V., Jaenicke, R., Delany, A. C., Moyers, J., Zoller, W. and Rahn, K. (1983). The Atmospheric Aerosol System: An Overview. Reviews of Geophysics and Space Physics, 21 (7), 1607-1629.

Prospero, J. M., Ginoux, P., Torres, O., Nicholson, S.E., and Gill, T. E., (2002). Environmental characterization of global sources of atmospheric soil dust identified with the Nimbus 7 Total Ozone Mapping Spectrometer (TOMS) absorbing aerosol product. Reviews of Geophysics, 40 (1), 1002, doi:10.1029/2000RG000095.

Pye, K. (1987). Aeolian Dust and Dust Deposits. Academic Press Inc. London. 334.

Reheis, M., Budahn, J. R. and Lamothe, P. J. (2002). Geochemical evidence for diversity of dust sources in the Southwestern United States. Geochimica et Cosmochimica Acta, 66, 1569–1587.

Rivera Rivera, N.I. (2006). Detection and characterization of dust source areas in the Chihuahuan Desert, southwestern North America. Masters Thesis, University of Texas at El Paso, United States.

Rivera Rivera, N. I., Gill, T. E., Gebhart, K. A., Hand, J. L., Bleiweiss, M. P. , and Fitzgerald, R. M. (2009). Wind modeling of Chihuahuan Desert dust outbreaks. Atmospheric Environment, 43, 347-354.

Rivera Rivera, N. I., Gill, T. E., Hand, J. L., and Bleiweiss, M. P. (2010) Source characteristics of hazardous Chihuahuan Desert dust outbreaks. Atmospheric Environment, 44, 2457-2468.

Samet, J. M., Dominici, F., Curriero, F. C., Coursac, I., and Zeger, S. L. (2000). Fine particle air pollution and mortality in 20 US cities, 1987-1994. The New England Journal of Medicine, 343, 1742-1749.

Schepanski, K., I. Tegen, B. Laurent, B. Heinold, and A. Macke (2007), A new Saharan dust source activation frequency map derived from MSG-SEVIRI IR-channels, Geophysical Research Letters, 34(18).

Schmidt, R. H., Jr. (1979). A climatic delineation of the "real" Chihuahuan Desert. Journal of Arid Environments, 2, 243-250.

Schmidt, R. H. (1986). Chihuahuan Climate. Second Symposium on Resources of the Chihuahuan Desert, Chihuahuan Desert Institute, Alpine, Texas, pp. 40-63.

Shao Yaping, Wyrwoll, K.-H., Chappell, A., Huang Jianping, Lin Zhaohui, McTainsh, G.H., Mikami, M., Tanaka, T.Y., Wang Xulong and Yoon Soonchang. (2011). Dust cycle: An emerging core theme in Earth system science. Aeolian Research 2(4):181-204, doi:10.1016/j.aeolia.2011.02.001

Shao, Y. (2000). Physics and Modeling of Wind Erosion. Kluwer Academic Publisher, Dordrecht, Netherlands.

Schultz, D. M. and Doswell, C. A. (2000). Analyzing and Forecasting Rocky Mountain Lee Cyclogenesis Often Associated with Strong Winds. Weather and Forecasting, 15, 152–173.

Tegen, I., Werner, M., Harrison, S.P., Kohfeld, K.E. (2004). Relative importance of climate and land use in determining present and future global soil dust emission. Geophysical Research Letters, 31, L05105. doi:10.1029/2003GL019216.

Tong D.Q., Dan M., Wang T. and Lee P. (2012). Long-term dust climatology in the western United States reconstructed from routine aerosol ground monitoring. Atmospheric Chemistry and Physics 12:5189-5205.

Warner, T. T. (2004) Desert Meteorology. Cambridge University Press. Cambridge, U.K.

Washington, R., Todd, M., Middleton, N. J., and Goudie, A. S. (2003). Dust-storms source areas determined by the Total Ozone Monitoring Spectrometer and Surface Observations. Annals Association of American Geographers, 93 (2), 297-313.

Washington, R., Todd, M.C. (2005). Atmospheric controls on mineral dust emission from the Bodélé Depression, Chad: The role of the low level jet. Geophys. Res. Lett. 32, L17701.

Wigner, K. A. and Peterson, R. E. (1987). Synoptic climatology of blowing dust on the Texas South Plains, 1947-84. Journal of Arid Environment, No. 13, pp. 199-209.

Yin, D., Nichovic, S., Barbaris, B., Chandy, B., and Sprigg, W. A. (2005). Modeling wind-blown desert dust in the southwestern United States for public health warning: A case study. Atmospheric Environment, 39, 6243-6254.

Zhang, X.Y., Arimoto, R., and An, Z.S., (1997). Dust emission from Chinese desert liked to variations in atmospheric circulation. Journal of Geophysical Research - Atmosphere vol. 102 no. D23, 28, pp. 041–28,047.

Zhang, R., Shen, Z., Cheng, T., Zhang, M., Liu, Y. (2010). The elemental composition of atmospheric particles at Beijing during Asian dust events in spring 2004. Aerosol Air Qual. Res. 10, 67-75.

Zhao, T. X-P., Ackerman, S. and Guo, W. (2010). Dust and Smoke Detection for Multi-Channel Imager. Remote Sensing, 2, 2347-2368.

Zender, C. S., and Kwon, E.Y. (2005). Regional contrast in dust emission responses to climate. Journal of Geophysical Research. Vol. 110, D13201, doi:10.1029/2004JD005501.

Zobeck, T.M., and Van Pelt, R.S. (2005). Erosion: Wind-induced. In: Hillel, D., editor. Encyclopedia of Soils in the Environment. Oxford, UK, Elsevier, Ltd., pp. 470-478.

Chapter 2

2.1 Analysis of Historic Dust Events in the Chihuahuan Desert since 1932-2010

2.1.1 Introduction

Atmospheric and land-surface conditions control the frequency and intensity of dust storms (Middleton, 1984; Jauregui, 1989). For example, surface cover, soil moisture, strong winds, and low humidity (among others) are important environmental factors that are often associated with dust events (Warn & Cox, 1951; Jackson *et al*., 1973; Jauregui, 1989). In most cases, the exact influence of each factor on regional dust levels is still poorly understood and even less is understood about the combined effects of multiple environmental factors (Stout, 2001).

Dust emissions from semi-arid regions can vary in time as environmental conditions change with the seasons (Warn & Cox, 1951; Brown *et al*., 1968; Smith *et al*., 1970; Jackson *et al*., 1973; Orgill & Sehmel, 1976; Goudie, 1983; Brazel & Nickling, 1986; Wigner & Peterson, 1987; Lee *et al*., 1994; Stout, 2001). Variations in dust storm frequency have relied heavily on visibility observations (Pecille, 1973; Orgill & Sehmel, 1976; Pollard, 1977; Changery, 1983; Goudie, 1983; Wigner & Peterson, 1987; Lee *et al.*, 1994; Lee & Tchakerian, 1995). Before 1993, visibility was routinely estimated each hour by a National Weather Service observer who attempted to see fixed objects at known distances from the station. When visibility decreased to less than 7 miles, a note was made as to the reason for the reduced visibility (Stout, 2001). In semi-arid agricultural regions, the occurrence of blowing dust was sometimes reported as the

cause for reduced visibility. As a result, the National Weather Service surface observations provide a helpful record of blowing dust that often extends as far back as 1947 (Stout, 2001).

Historical dust event data was analyzed as part of this project. This type of data is important because it can show relations between the dust storms with safety, health, and nuisance (David Novlan, Personal Communication, Zobeck and VanPelt, 2005; Grineski *et al*., 2011; Okin *et al*., 2011). Dust events can disrupt our daily life and put our environment, economy and health at risk. They cause pollution, respiratory disease, ecological disaster, low visibility, interrupted transportation and aviation (Akhlaq *et al.*, 2012).

2.1.2 Methodology

2.1.2.1 Historic dust storm data

A synoptic climatology of significant blowing dust events in El Paso, Texas has been compiled at the National Weather Service office (NWSO) of El Paso, TX, based on observational data from the El Paso International Airport (ELP) collected since 1932 (Novlan *et al.,* 2007). Approximately two thousand cases were documented during that period of time, based on visibility reductions of 7 statute miles or less. These records were maintained on a Microsoft Excel spreadsheet. The data consisted of date, time of first dust observation, restricted visibility, wind direction, wind speed, and duration of the events. In the data, ‘‘dusty days’’ were documented based on at least one hourly observation of blowing sand or dust, with high winds reducing visibility to <10 km. Novlan *et al*. (2007) further classified these events as synoptic-scale (non-convective) or mesoscale (convectively driven events) (Rivera Rivera *et al*., 2009; Rivera Rivera, 2006). Synoptic-scale dust events are least frequent in the region and convectively-driven dust events are more frequent during the late summer (rainy) months, when the Chihuahuan Desert is under the influence of the North American monsoon (Apodaca *et al*.,2007).

“The synoptic type primarily occurs during the months of March and April which are characteristically the two driest months of the year. This dryness combined with the retreat of the Polar Front Jet stream slowly northward but still close enough to steer upper level energy disturbances in the form of upper air toughs of low pressure with associated surface Pacific cold fronts sets the stage for very strong winds aloft. As this type of system approaches the southern New Mexico/Far West Texas area a process call “lee troughing develops” in the lower portions of the atmosphere in which the surface pressure falls faster to the lee of the Rocky Mountains (both Central

and Southern Rockies) setting up a pressure gradient from the higher pressure to the west to the lower pressure out east. One of the typical signatures to look for in this surface pattern is what we refer to as an Albuquerque low, in which the lower pressure at the surface typical tracks along the Colorado/New Mexico Border to the Texas Panhandle near Amarillo.

The Type 2 pattern for blowing dust in the El Paso area is the Mesoscale thunderstorm induced outflow producing localized to often fairly extensive areas of blowing dust (sometimes referred to as Haboobs) in the desert southwest. These may be associated with dry micro bursts (usually dry thunderstorms in June with the inverted "v" sounding signatures) or wet/hybrid micro bursts in July through September. These features usually cover an area say about the size of the city of El Paso or half that amount and may last from 1 to 4 hours in temporal extent. These are associated with significant wind shear hazards" (adapted from Rivera Rivera 2006).

This historic dust event data was analyzed using the Microsoft Excel program. The analyses performed with the data were a statistical analysis, Particulate Matter, visibility, wind speed, precipitation and relative humidity data correlations. Table I shows a basic statistical analysis done with the dust event data. Monthly frequency of dust events, percentage of convective events, and average wind speeds were analyzed. To obtain the monthly frequency of dust events, the number of convective events and the average wind speed during the events, the number of events per month, convective events and wind speed were added respectively from 1932 to 2010. The mean and standard deviation were obtained by using the average and standard deviation functions within the Excel program. The percentage of convective dust events was obtained by dividing the number of convective dust events per month by the total number of convective events.

Table I: Example of statistical analysis done with the data

month	Frequency of events	Mean	St. Dev	# of convective events	% of convective events	Average wind speed
January	118	1.49	1.44	1	0.34	17.04
February	188	2.38	2.05	2	0.68	22.50
March	391	4.95	2.98	2	0.68	24.26
April	443	5.61	3.27	7	2.36	23.74
May	243	3.08	2.49	33	11.15	20.07
June	188	2.38	2.72	92	31.08	16.11
July	91	1.15	1.96	84	28.38	8.29
August	52	0.66	1.41	47	15.88	7.09
September	33	0.42	0.74	18	6.08	5.92
October	65	0.82	1.03	8	2.70	12.02
November	93	1.18	1.38	1	0.34	14.86
December	95	1.20	1.47	1	0.34	17.04
Total	2000	25.32	22.95	296		

2.1.2.2 Particulate Matter data

Particulate matter, or PM, is the term for particulate found in the air, including: dust, dirt, soot, smoke, and liquid droplets. National Ambient Air Quality Standards (NAAQS) regulate ambient air concentrations of particulate in two different size fractions, PM 2.5 and PM 10. PM 2.5 is the fine fraction of particulate that is 2.5 microns or smaller in aerodynamic diameter. PM 10 is the coarse fraction and consists of particulate that is 10 microns or smaller (Watson *et a.,* 1997). Particulate Matter is a significant human health hazard capable of causing long term respiratory ailments and even sudden death (Vedal, 1997; Samet *et al.,* 2000; Pelletier, 2006). It also impacts visibility, contributing to vehicular accidents and the loss of scenic quality (Pelletier, 2006).

The impact of atmospheric aerosols on visibility, through their scattering and absorption of solar radiation, is especially sensitive to fine particles, e.g. those less than 1.0 μm (Watson, 2002; Nicole Pauly, 2009); because these particles, compatible in size to the wavelength of visible solar radiation, have the largest optical extinction efficiency (Wang *et al*., 2012). Meteorological visibility provides a proxy of optical concentration of PM 1.0 (Mahowald *et al*., 2007; Wang *et al*., 2012). Visibility measurements have been used successfully to quantify long-term variation of aerosol during the past four decades (Field *et al.,* 2009; Vautard *et al.,* 2009; Wang *et al.,* 2009).

In this research the historical dust data was correlated with Particulate Matter (PM) data. The particulate matter data was obtained from the Texas Commission for Environmental Quality

(TCEQ) and included PM 2.5 and PM 10 for the CAMS 12 (UTEP) location from 2001 to 2010. Data collected from 2001 to 2010 was used, as this was the only time frame available for the PM data from the TCEQ's. The TCEQ's Continuous Ambient Monitoring Stations (CAMS) document air and water parameters via instruments that measure the following pollutants on an hourly basis: ozone, carbon monoxide, nitric oxide, nitrogen dioxide, oxides of nitrogen, hydrogen sulfide, fine particulate matter (PM 2.5 and PM 10) (TCEQ CAMS website). This data is accessible online at http://www.tceq.state.tx.us/compliance/monitoring/air/monops/hourly_data.html. There, a search can be done for air quality data collected on a specific day, during a particular month, or a definite year and at a specific TCEQ air monitoring site. CAMS 12 is located at 250 Rim Road, El Paso, TX near The University of Texas at El Paso (UTEP) at latitude 31° 46' 05" North and longitude 106° 30' 04" West. Figure 2.1 shows a map with the location of CAMS 12 and a picture of the site. I utilized CAMS 12 instead of the other stations around El Paso, because this station had the most up to date and complete data set for the time frame that was being analyzed. CAMS 12 PM 2.5 and PM 10 daily and hourly averages were linked to the dust storm days from 2001 to 2010 (in the historic dust storm database) and statistically analyzed to correlate PM 2.5 / PM 10 ratios of convective and non-convective events and also to correlate these values with, wind speed, relative humidity and visibility.

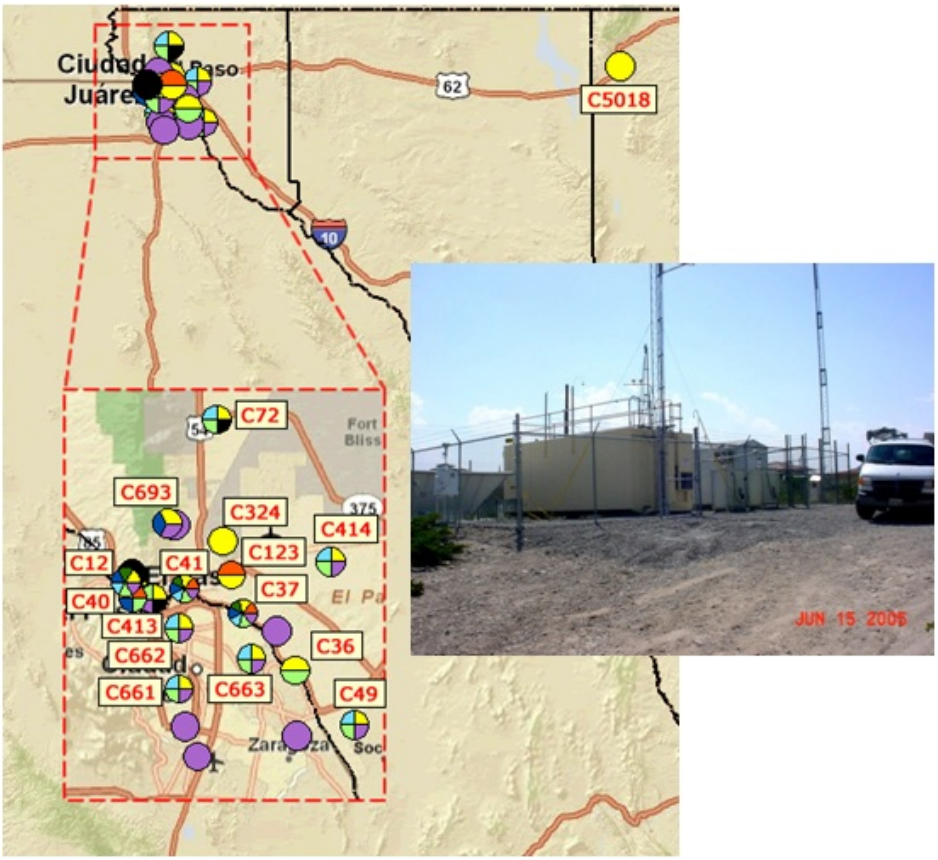

Figure 2.1: Location of the Continous Air Monitoring Station 12 (CAMS 12).

From the dust data set, a correlation was done with the following parameters: PM2.5, PM10, visibility, mean wind speed, and relative humidity. Correlations of PM2.5 and or PM10 with each parameter (visibility, mean wind, peak gust, and relative humidity) could show relations between the dust storms and safety, health, and nuisance (David Novlan, Personal Communication). In addition, evaluating the concentrations of PM 2.5/ PM 10 for each of the variables mentioned above proves valuable as well.

It is initially expected that in non-convective cases a higher PM10 concentration would have lower PM2.5 concentration, as non-convective cases are much larger in space and time and

allow for a greater probability for obtaining larger particles. It is also suspected that the earlier season storms would have a larger concentration of smaller particles; which over a single season might decrease in time, at least for the same source region, as they are depleted from the source soils. The data analysis is stratified by wind direction, wind speed and peak gust.

2.1.2.3 Precipitation Data

Monthly precipitation data from 1932 to 2010 was also used in this research to see if any correlation occurs between the hours of dust storms per year and the number of dust events. Previous studies have found that precipitation totals in the Western United States for periods between 2 month to 2 years prior to dust events are correlated with dust event frequency (eg. Brazel and Nickling, 1987; Littman, 1991; Yu *et al.*, 1993; Bach *et al.*, 1996; Holocombe *et al.*, 1997; Lancaster and Helm, 2000; Okin and Reheis, 2000).

The precipitation data was obtained online from the National Weather Service Forecast Office (WSO) of El Paso, TX (http://www.srh.noaa.gov/epz/?n=elpaso_monthly_precip). Table II shows an example of the monthly precipitation data and its annual averages and its format in the Excel program. The data is divided by the total precipitation of every month per year. The precipitation data is measured by WSO in inches and for the purpose of this research the averages (last five columns on Table II) were converted to centimeters.

Table II: Example of the monthly precipitation data and its annual averages and its format in the Excel program

Precipitation-Total Note: averages and extremes at bottom of table are through the calendar 2008																		
	January	February	March	April	May	June	July	August	September	October	November	December	Annual (cm)	Annual Averages (cm)	previous year average (cm)	previous 3 years average (cm)	previous 5 years average (cm)	previous 10 years average (cm)
YEAR	TOTAL	TOTAL	TOTAL	TOTAL	TOTAL	TOTAL	TOTAL	TOTAL	TOTAL	TOTAL	TOTAL	TOTAL	TOTAL					
1932	0.17	0.68	0.03	T	1.46	0.15	2.28	2.14	2.85	0.53	0	0.65	10.94	2.53	2.28	2.02	1.94	1.84
1933	0.19	0.23	T	0.09	0.04	2.14	1.34	0.27	0.99	0.6	0.04	0	5.93	1.37	2.53	2.07	2.13	2.00
1934	0.01	0.12	0.24	0.05	0.37	0.01	0.19	0.6	0.17	0.44	0.21	0.32	2.73	0.58	1.37	2.06	1.99	1.96
1935	0.24	0.47	0.14	0.02	0.17	0.09	0.16	1.72	1.24	0.14	0.92	0.34	5.65	1.20	0.58	1.49	1.63	1.83
1936	0.57	0.06	T	0.11	0.56	0.34	0.68	1.94	3.52	0.32	1.32	0.51	9.93	2.29	1.20	1.05	1.59	1.79
1937	0.12	0.32	0.48	T	0.19	1.05	0.39	0.36	0.48	1.71	0.22	0.91	6.23	1.44	2.29	1.36	1.59	1.77
1938	1.22	0.17	0.49	T	0.02	2.82	0.6	0.2	2.31	0.19	T	0.28	8.3	2.11	1.44	1.64	1.37	1.75
1939	0.65	0.08	0.44	0.45	0.01	T	0.6	0.91	0.9	0.93	0.75	0.19	5.91	1.36	2.11	1.95	1.52	1.76
1940	0.54	0.41	0.02	0.02	0.43	1.87	1.06	0.78	0.25	0.82	1.25	0.31	7.76	1.64	1.36	1.64	1.68	1.66
1941	0.46	0.46	1.63	1.49	1.23	0.18	1.4	2.13	4.19	1.65	0.48	0.35	15.65	3.31	1.64	1.71	1.77	1.68
1942	0.14	0.72	0.02	1.04	T	0.52	0.68	3.82	1.03	1.53	0	1.26	10.76	2.48	3.31	2.11	1.97	1.78
1943	0.25	0	0.07	T	T	1.63	0.92	0.44	1.36	T	1.53	0.82	7.02	1.98	2.48	2.48	2.18	1.78
1944	0.45	1.42	0.15	T	0.39	1.67	1.52	1.04	0.25	1.3	0.41	0.48	9.08	2.10	1.98	2.59	2.16	1.84
1945	0.11	0.17	0.64	T	T	0.03	0.47	0.84	0.12	4.31	0	0.05	6.74	1.71	2.10	2.19	2.30	1.99
1946	1.23	T	0.04	0.36	1.23	0.2	0.71	1.19	1.51	0.41	0.03	1.31	8.22	1.90	1.71	1.93	2.32	2.04
1947	0.87	T	0.66	0.06	0.68	0.53	0.97	1.63	0.02	0.35	0.53	0.82	7.12	1.64	1.90	1.90	2.03	2.00
1948	0.25	0.63	0.04	0.11	T	0.96	0.82	1.82	0.03	0.18	T	0.86	5.7	1.45	1.64	1.75	1.87	2.02
1949	1.84	0.22	0.04	0.05	0.39	0.51	1.18	0.43	1.74	1.5	T	0.86	8.76	2.02	1.45	1.66	1.76	1.96
1950	0.29	0.26	T	T	0.1	0.11	3.57	0.16	1.32	0.94	0	0	6.75	1.71	2.02	1.70	1.74	2.02

2.1.2.4 Relative Humidity Data

Surface humidity is directly influenced by the precipitation, which affects the material resource of a dust storm. The particle cohesive force and drag force enlarges, leading to an increase of the threshold wind speed, thus reducing the occurrence probability of dust or sandstorm (Fengmei and Chongyi, 2010). The moisture content of the upper soil surface is closely linked to the moisture content of the atmosphere directly above it (J.M. Gregory, pers. comm.) Dry winds remove moisture from the surface more quickly than subsurface moisture can replenish it, leaving the uppermost soil surface desiccated and susceptible to wind erosion. On the other hand, moist air can produce a moistening of the surface layer as well as a reduction in evaporation. Thus, it is reasonable to assume that relative humidity may be used as an indicator of surface soil moisture at the soil-air interface (Stout, 2001).

.

Relative Humidity (RH) data was used in this study. The data was obtained from the TCEQ website CAMS 12 station, where the Particulate Matter (PM) data was also collected. The same methodology used to obtain the PM data was used for the RH data. The data was accessed online at this link (http://www.tceq.texas.gov/cgi-bin/compliance/monops/yearly_summary.pl). A search can be done for Relative Humidity data collected on a specific day, during a particular month, or a definite year and at a specific TCEQ air monitoring site. The site displays Relative Humidity percent data from November 2001 to present. This RH data was correlated with Convective and Non-Convective dust days, visibility, PM 2.5 and PM 10.

2.1.3 Results

Graphs of PM 2.5 / PM10 concentrations of Convective and Non-Convective dust events were created and correlated with minimum visibility (<6 miles), seasonality, precipitation, relative humidity and duration of the dust events.

2.1.3.1 Particulate Matter

Figures 2.2 to 2.4 show a correlation between Particulate Matter concentrations and minimum visibility from 2001 to 2010. As seen in those figures, as the visibility goes down the PM goes up. There were a total of 418 dust events from 2001-2010. From those 418 events, 219 had a minimum visibility of 6 miles or less. Of those 219 events, 95 were Convective events and 124 were Non-Convective events.

Figure 2.5 shows a correlation of PM 2.5 and PM 10 concentrations between Convective and Non-Convective events from 2001-2010. The graph shows that there is more PM 10 during non-convective events. This occurs because the convective downburst picks up more smaller sized particles and operates over a smaller time frame (1 to 2 hours) with exponential decay setting in as soon as the downburst comes into contact with the ground (David Novlan – Personal Communication). The non convective cases start out slower with lighter winds, thus initiating the smaller particle thin haze, before gradually building to higher winds and higher concentrations of larger particles, enabling more large particles to be picked up in the atmosphere. The air is also more unstable in non convective cases, allowing a deep mixture of the larger particles to a

greater vertical depth; whereas, in convective cases, the dust is confined more in a dome of cold, stable air (cold pool) with downward and outward motion.

Figures 2.6 (a-e) shows the seasonal concentrations of PM 2.5 and PM10 for dusty days (including both convective and non-convective events) from 2001-2010. There is a solid correlation between the ratios of PM 2.5 and PM 10 in all the different seasons. As observed, the PM 2.5 drops below the PM 10. This may reflect the fact that with cooler temperatures in winter, and hence more dense air, it may be harder in the denser air to get more small particles suspended in thermals so the larger PM 10 dominates. Also earlier season storms can have a larger concentration of smaller particles; which over a single season might decrease in time, at least for the same source region, as they are depleted from the source soils observed in Figures 2.6 (b-e). Figure 2.6 (c) shows higher Particulate Matter concentrations in the spring compared to Figures 2.6 (b) (e) which showed lower PM concentrations.

Figure 2.7 shows the correlation of PM 2.5 and PM 10 concentrations between convective and non-convective dust events at the hour of minimum visibility. Again a good correlation is observed between both PM ratios measurements as explained before in Figure 2.5. Figure 2.8 draws a comparison between Convective, Non-Convective PM 2.5 and PM 10 during the duration (time) of the dust events from 2001-2010.

Table III show a correlation of the average PM 2.5 and PM 10 for non-convective and convective events and its Anova. Table IV show the Anova correlation of the average PM 2.5 and PM 10 for the hour of the 1st dust observation for the duration of the event versus the visibility.

Table III

Correlation				
	Average PM 2.5 (µg/m³) Non-C	*Average PM 10 (µg/m³) Non-C*	*Average PM 2.5 (µg/m³) C*	*Average PM 10 (µg/m³) C*
Average PM 2.5 (µg/m³) Non-C	1			
Average PM 10 (µg/m³) Non-C	0.941756	1		
Average PM 2.5 (µg/m³) C	-0.00684	0.075223	1	
Average PM 10 (µg/m³) C	0.037905	0.096469	0.903343	1

Anova: Single Factor				
SUMMARY				
Groups	*Count*	*Sum*	*Average*	*Variance*
Average PM 2.5 (µg/m³) Non-C	265	3618.8	13.65585	164.2711
Average PM 10 (µg/m³) Non-C	212	21234.44	100.1625	15193.13
Average PM 2.5 (µg/m³) C	183	2040.17	11.14847	53.32777
Average PM 10 (µg/m³) C	160	9256.01	57.85006	3023.59

ANOVA						
Source of Variation	*SS*	*df*	*MS*	*F*	*P-value*	*F crit*
Between Groups	1140882	3	380294	82.98267	7.31E-47	2.615814
Within Groups	3739575	816	4582.812			
Total	4880457	819				

Table IV

Anova: Single Factor				
SUMMARY				
Groups	*Count*	*Sum*	*Average*	*Variance*
Average PM 2.5 (µg/m³) for the hour of the 1st dust observation for the duration of the event	95	3655.664	38.48068	1258.415
Average PM 10 (µg/m³) for the hour of the 1st dust observation for the duration of the event	75	25656.04	342.0806	110529.1
VSBY (statue miles)	96	376.875	3.925781	91.78308

ANOVA						
Source of Variation	*SS*	*df*	*MS*	*F*	*P-value*	*F crit*
Between Groups	5605007	2	2802503	88.73636	3.54E-30	3.030116
Within Groups	8306160	263	31582.36			
Total	13911167	265				

2.1.3.2 Precipitation

Precipitation is another factor that can lead to the increase/decrease in the occurrence of dust storms in our area. Figure 2.9 and Figure 2.10 show the precipitation vs. number of dust events per year and precipitation vs. the hours of dust per year from 1932 to 2010. As expected during these periods, higher rainfall diminished dust events and dusty hours. In other words, more dust arose during extended dry periods. Figure 2.11 shows the correlation of dust events in 2003 versus the average precipitation three years prior to the dust events (2000-2002). The graph shows that when the precipitation averages are low the fluctuation of dust events is greater. Figures 2.12 and 2.13 show another correlation between the dust events in 2003 and the average precipitation five years prior (1997-2002) versus a 10 year precipitation average prior to the 2003 events.

Figures 2.14 -2.15 show a correlation between the numbers of dust events in 2008 versus the average precipitation 2-3 years prior to the events. During the drier months, when precipitation was low, the number of dust events was higher, and vice versa. Table V shows the correlation between the precipitation average used in Figure 2.15 and the 2008 dust events. The dust days in 2008 correlate well with the 3 year precipitation average. Figure 2.16 and 2.17 show a correlation between the number of dust events in 2010 versus the average precipitation amounts of 3 years prior (2005-2007) and 5 years prior (2005-2009) (Table VI). It is observed that the same inverse relationship mentioned previously applies here: more rain, fewer dust events.

Table V

Correlation		
	Precip. average 2005-2006-2007	*2008 dust days*
Precip. average 2005-2006-2007	1	
2008 dust days	0.881197231	1

Table VI

Correlation					
	Precip. Average 2005-2006	*Precip. Average 2005-2007*	*Precip. Average 2005-2008*	*Precip. Average 2005-2009*	*2010 Dust days*
Precip. Average 2005-2006	1				
Precip. Average 2005-2007	0.995003	1			
Precip. Average 2005-2008	0.991129	0.997744	1		
Precip. Average 2005-2009	0.819818	0.836656	0.844339	1	
2010 Dust days	0.872138	0.897584	0.894572	0.810335	1

2.1.3.3 Relative Humidity

During a typical day, relative humidity follows a daily cycle driven by diurnal temperature variations. Relatively moist conditions occur in the early morning whereas the minimum relative humidity often occurs around mid-afternoon. It is during this dry period, when relative humidity is at a minimum, that the potential for blowing dust is maximum (Stout, 2001). As seen in this research, the majority of the dust events follow the daily cycle described before. Most of them occur in the afternoon hours.

Figure 2.18 shows a correlation between the average relative humidity and precipitation per year versus the dust events frequency from 2001-2010. This graph exhibits the same inverse relation observed with the precipitation figures considered before, between the RH average and the dust frequency-more dust events with less relative humidity. The relative humidity did not vary significantly during this period.

Figures 2.19-2.20 show the PM 2.5 and PM 10 plotted as a function of the % of relative humidity. Note that the RH % varies between 5% to 40% on both Particulate Matter concentrations. Figure 2.21 shows the previous 2 figures together. Figure 2.22 shows the percentage of Relative Humidity of Convective and Non-Convective events vs. Relative Humidity averages for the hour of the first dust observation for the duration of the event. It can be noted that on Non-Convective events (red squares) the RH average conglomerated between 5 to 25 %, where in Convective events it was more scattered between 10 to 40%.

Average Relative Humidity % for the day from Convective and Non-Convective events vs. PM 2.5 and PM 10 concentrations are shown in Figures 2.23(a-b) - 2.24(a-b). On Non-Convective events (Figure 2.23 (a-b)) note that most of the events were associated with a minimum relative humidity below 35% for both PM 2.5 and PM 10 concentrations. In fact, most

PM 2.5 values above 50 μg/m^3 fell below 35% RH (Figure 2.23 (a)) and most of the PM 10 values above 500 μg/m^3 fell below 35 % too (Figure 2.23 (b)). On Convective dust events (Figure 2.24 (a-b)) most of the events were associated with a minimum relative humidity below 40%. It is also clear from the figures that it is possible to have low relative humidity without a large Particulate Matter concentration. Low relative humidity seems to be a necessary condition for a high dust PM concentration, but not a sufficient condition.

Figure 2.25 shows Visibility (<6 miles) plotted as a function of Relative Humidity for all the events from 2001-2010. This figure does not show a clear pattern, other than most of the events having a relative humidity range between 5 to 40 %, similar to previous plots. In general, all the figures showed that the drier, the higher the concentrations of PM which seems logical. This seemed a little more evident for the small (finer) PM 2.5 concentration. As seen in Figure 2.26 the wind speed and wind gust correlates very well. Table VII to IX show different correlations of relative humidity vs. PM 2.5 and PM 10. Figure 2.26 shows a plot correlating the measure wind speed and wind gust for all the events (1932-2010). This wind speed and wind gust correlation takes us to obtain the gust factor for dust storm events in El Paso, TX. The gust factor obtained is 1.2. As observed is the plot, the correlation is pretty constant.

Table VII

Correlation			
	relative humidity (RH %) average for the hour of the 1st dust observation for the duration of the event	*Average PM 10 (µg/m³) for the hour of the 1st dust observation for the duration of the event*	*Average PM 2.5 (µg/m³) for the hour of the 1st dust observation for the duration of the event*
relative humidity (RH %) average for the hour of the 1st dust observation for the duration of the event	1		
Average PM 10 (µg/m³) for the hour of the 1st dust observation for the duration of the event	-0.116594794	1	
Average PM 2.5 (µg/m³) for the hour of the 1st dust observation for the duration of the event	-0.211582566	0.894054136	1

Table VIII

Non-Convective Events				
	relative humidity (RH %) average for the hour of the 1st dust observation for the duration of the event	*RH average for the day (TCEQ)*	*Average PM 2.5 (µg/m³) for the hour of the 1st dust observation for the duration of the event*	*Average PM 10 (µg/m³) for the hour of the 1st dust observation for the duration of the event*
relative humidity (RH %) average for the hour of the 1st dust observation for the duration of the event	1			
RH average for the day (TCEQ)	0.73609637	1		
Average PM 2.5 (µg/m³) for the hour of the 1st dust observation for the duration of the event	-0.299054547	-0.179078677	1	
Average PM 10 (µg/m³) for the hour of the 1st dust observation for the duration of the event	-0.065755362	0.010378132	0.831388923	1

Table IX

Convective Events				
	relative humidity (RH %) average for the hour of the 1st dust observation for the duration of the event	*RH average for the day (TCEQ)*	*Average PM 2.5 (µg/m³) for the hour of the 1st dust observation for the duration of the event*	*Average PM 10 (µg/m³) for the hour of the 1st dust observation for the duration of the event*
relative humidity (RH %) average for the hour of the 1st dust observation for the duration of the event	1			
RH average for the day (TCEQ)	0.64864862	1		
Average PM 2.5 (µg/m³) for the hour of the 1st dust observation for the duration of the event	-0.07353306	-0.281653192	1	
Average PM 10 (µg/m³) for the hour of the 1st dust observation for the duration of the event	-0.03189756	-0.137093131	0.921025171	1

2.1.4 Summary

A synoptic climatology of significant dust event was compiled at the National Weather Service Office of El Paso, TX, based on observational data from El Paso International Airport collected since 1932. As seen in the analysis of this data, El Paso, TX dust record appears to follow a regular annual dust cycle, characterized by frequent dust events throughout the spring season and fewer during the summer and winter. This annual dust cycle results from seasonal changes in environmental conditions. The environmental factors studied here related to these seasonal changes were particulate matter, wind speed, relative humidity and precipitation. Most of the dust events studied were associated with periods of low relative humidity (<35%), no precipitation and wind speeds greater than 10 mph.

Most dust events are associated with a combination of strong winds, low land cover, and dry conditions, all of which occur most frequently during the spring season. Wind speed alone cannot be a perfect indicator of high dust levels, since other environmental factors such as surface cover and moisture can significantly reduce regional dust levels, even during high wind speeds.

The concentration of particulate matter with a size from 2.5 up to 10 micrometers in El Paso/Juarez metropolitan area on windy days is a clear proxy for blowing dust in the atmosphere. Non-Convective cases had a higher PM10 concentration and lower PM2.5 concentration, as non-convective cases can be larger in space and time and allow for a greater probability for obtaining larger particles. It was also suspected that the earlier in the season

storms would have a larger concentration of smaller particles; which over a single season might decrease in time, at least for the same source region, as they are depleted from the source soils as observed in Figures 2.6 (b-e). As seen in the PM plots, on Convective days we had more PM 2.5 (Finer particle) meaning that this type of cases can affect more the community because those smaller particles are the ones we breathe and can affect people's health, specially the kids and the elderly). Also this can raise the public's awareness of potential dust hazards and their causes in order to help residents be better prepared for action when needed.

It is known that dust storms are environmental hazards that cause air quality and visibility problems across the southwestern part of the United States. Defining and studying the environmental factor that help to produce dust events is very important because it will aid in forecasting dust storms in the El Paso, TX/Juarez, Chihuahua, MX metropolitan area, and similar studies could be followed for other dust-prone cities. In addition, an evaluation of the climatology of dust-prone cities can help the meteorological community to improve their forecasting of extreme dust events around the world.

2.1.5 References

Apodaca, K., Morris, V.R., Lozano, A.Y., Negrete, J., Fitzgerald, R.M. (2007). Interaction between dust storms, precipitation and Gulf of California moisture surges in the Paso del Norte region. Abstracts, 19th Conference on Climate Variability and Change, American Meteorological Society, no. JP2.13.

Bach, A.J., Brazel, A.J., Lancaster, N. (1996). Temporal and spatial aspects of blowing dust in the Mojave and Colorado deserts of southern California, 1973–1994. Physical Geography 17, 329-353.

Brazel, A.J., Nickling, W.G. (1987). Dust storms and their relation to moisture in the Sonoran Mojave Desert region of the Southwestern United States. Journal of Environmental Management 24, 279–291.

Brazel, A.J. & Nickling, W.G. (1986). The relationship of weather types to dust storm generation in Arizona (1965}1980). Journal of Climatology, 6: 255-275.

Brown, M.J., Krauss, R.K. & Smith, R.M. (1968). Dust deposition and weather. Weatherwise, 21:66-70.

Changery, M.J. (1983). A dust climatology of the western United States. Published by the NationalClimatic Data Center, Asheville, NC, for the Division of Health, Siting and Waste ManagementOffice, U.S. Nuclear Regulatory Commission.

Fengmei, Y. and Chongyi, E. (2010). Correlation analysis between sand-dust events and meteorological factors in Shapotou, Northern China. Environmental Earth Science, 59: 1359-1365. doi 10.1007/s12665-009-0123-4

Field, R. D., van der Werf, G. R., and Shen, S. S. P. (2009). Human amplification of drought-induced biomass burning in Indonesia since 1960, Nature Geoscience, 2, 185–188, doi:10.1038/ngeo443.

Goudie, A.S. (1983). Dust storms in space and time. Progress in Physical Geography, 7: 502-530.

Grineski, S. E., Staniswalis, J. G., Bulathsinhala, P., Peng, Y., Gill, T. E. (2011). Hospital admissions for asthma and acute bronchitis in El Paso, Texas: Do age, sex and insurance status modify the effects of dust and low wind events. Environmental Research, 111, 1148-1155.

Harvey, G. (2007). Excel 2007 Workbook for Dummies (2nd ed.). Wiley. pp. 296 ff. ISBN 0470169370.

Holcombe, T.L., Ley, T., Gillette, D.A. (1997). Effects of prior precipitation and source area characteristics on threshold wind velocities for blowing dust episodes, Sonoran Desert 1948–1978. Journal of Applied Meteorology 36, 1160–1177.

Jackson, M.L., Gillette, D.A., Danielson, E.F., Blifford, I.H., Bryson, R.A. & Syers, J.K. (1973). Global dustfall during the Quaternary as related to environments. Soil Science, 116: 135-145.

Jauregui, E. (1989). Meteorological and environmental aspects of dust storms in northern Mexico. Erdkunde, 43: 141-147.

Lancaster, N., Helm, P. (2000). A test of a climatic index of dune mobility using measurements from the southwestern United States. Earth Surface Processes and Landforms 25, 197–207.

Lee, J.A. & Tchakerian, V.P. (1995). Magnitude and frequency of blowing dust on the Southern High Plains of the United States, 1947}1989. Annals of the Association of American Geographers,**85**: 684-693.

Lee, J.A., Allen, B.L., Peterson, R.E., Gregory, J.M. & Moffett, K.E. (1994). Environmental controls on blowing dust direction at Lubbock, Texas, U.S.A. Earth Surface Processes and Landforms, 19: 437-449.

Littmann, T.J. (1991). Dust storm frequency in Asia: climatic control and variability. International Journal of Climatology 11, 393–412.

Mahowald, N. M., Ballantine, J. A., Feddema, J., and Ramankutty, N. (2007). Global trends in visibility: implications for dust sources, Atmos. Chem. Phys., 7, 3309–3339, doi:10.5194/acp-7-3309-2007.

Middleton, N.J. (1984). Dust storms in Australia: frequency, distribution and seasonality. Search, 15: 46-47.

Nicole Pauly, H. (2009). Impaired visibility: the air pollution people see, Atmos. Environ., 43, 182–195, doi:10.1016/j.atmosenv.2008.09.067.

Novlan, D. J., Hardiman, M., and Gill, T. E., (2007). A synoptic climatology of blowing dust events in El Paso, Texas from 1932-2005. Preprints, 16th Conference on Applied Climatology, American Meteorological Society, J3.12, 13 pp.

Okin, G. S., Bullard, J. E., Reynolds, R. L., Ballantine, J-A. C., Schepanski, K., Todd, M. C., Benalp, J., Baddock, M. C., Gill, T.E. and Miller, M. E. (2011). Dust emission: small-scale processes with global-scale consequences. EOS-Transactions of American Geophysical Union.

Okin, G., Reheis, M. (2002). An ENSO predictor of desertification in the southwestern United States. Geophysical Research Letters 29, doi: 10.1029/2001GL014494

Orgill, M.M. & Sehmel, G.A. (1976). Frequency and diurnal variation of dust storms in the contiguous U.S.A. Atmospheric Environment, 10: 813-825.

Pecille, J.A. (1973). Wind and dust study for Lubbock, Texas. NOAA Technical Memorandum NWS SR-70, US Department of Commerce.

Pelletier, J. D. (2006). Sensitivity of playa windblown-dust emissions to climatic and anthropogenic change. Journal of Arid Environment, 66, 62-75.

Pollard, M.C. 1977. An Investigation of dust storm generation in the Southern Great Plains. M.Sc. thesis, Texas A&M, College Station. 75 pp.

Rivera Rivera, N. I., Gill, T. E., Gebhart, K. A., Hand, J. L., Bleiweiss, M. P., Fitzgerald, R. M. (2009). Wind Modeling of Chihuahuan Desert dust outbreaks. Atmospheric Environment, 43, 347-354.

Rivera Rivera, N.I.(2006). Detection and characterization of dust source areas in the Chihuahuan Desert, southwestern North America. M.S. Thesis, University of Texas at El Paso, United States.

Samet, J.M., Dominici, F., Curriero, F.C., Cousac, I., Zeger, S.L. (2000). Fine particulate air pollution and mortality in 20 US cities, 1987–1994. New England Journal of Medicine 343, 1742–1749.

Smith, R.M., Twiss, P.C., Kraus, R.K. & Brown, M.J. (1970). Dust deposition in relation to site, season and climatic variables. Soil Science Society of America Proceedings, 34: 112-117.

Stout, J. E. (2001). Dust and Environment in the Southern High Plains of North America. Journal of Arid Environment, 47:425-441.

TCEQ-CAMS website

http://www.tceq.state.tx.us/compliance/monitoring/air/monops/hourly_data.html.

Vedal, S. (1997). Ambient particles and health: lines that divide. Journal of the Air & Waste ManagementAssociation 47, 551–581.

Vautard, R., Yiou, P., and van Oldenborgh, G. J. (2009). Decline of fog, mist and haze in Europe over the past 30 years, Nature Geosci., 2, 115–119, doi:10.1038/ngeo414.

Wang, K. C., Dickinson, R. E., Su, L., Trenberth, K. E. (2012). Contrasting trend of mass and optical properties of aerosols over the Northern Hemisphere from 1992 to 2011. Atmos.Chem,. Phys., 12, 9387-9398. Doi:10.5194/acp-12-9387-2012.

Wang, K., Dickinson, R. E., and Liang, S. (2009). Clear sky visibility has decreased over land globally from 1973 to 2007, Science, 323, 1468–1470, doi:10.1126/science.1167549.

Warn, G.F. & Cox, W.H. (1951). A sedimentary study of dust storms in the vicinity of Lubbock, Texas. American Journal of Science, 249: 553-568.

Watson, J. G. (2002). Visibility: science and regulation, J. Air & Waste Manage. Assoc., 52, 628–628.

Watson, J. G., J. C. Chow, D. Dubois, M. Green, N. Frank, and Pitchford M. (1997). Guidance for Network Design and Optimum Site Exposure for PM 2.5 and PM 10 . Prepared for the Office of Air Quality Planning and Standards, United State Environmental Protection Agency, Research Triangle Park, NC 27711.

Yu, B., Hesse, P.P., Neil, D.T. (1993). The relationship between antecedent regional rainfall conditions and the occurrence of dust events at Mildura, Australia. Journal of Arid Environments 24, 109–124.

Wigner, K.A. & Peterson, R.E. (1987). Synoptic climatology of blowing dust on the Texas South Plains, 1947}84. Journal of Arid Environments, 13: 199-209.

Zobeck, T.M., and Van Pelt, R.S. (2005). Erosion: Wind-induced. In: Hillel, D., editor. Encyclopedia of Soils in the Environment. Oxford, UK, Elsevier, Ltd., pp. 470-478.

Figures

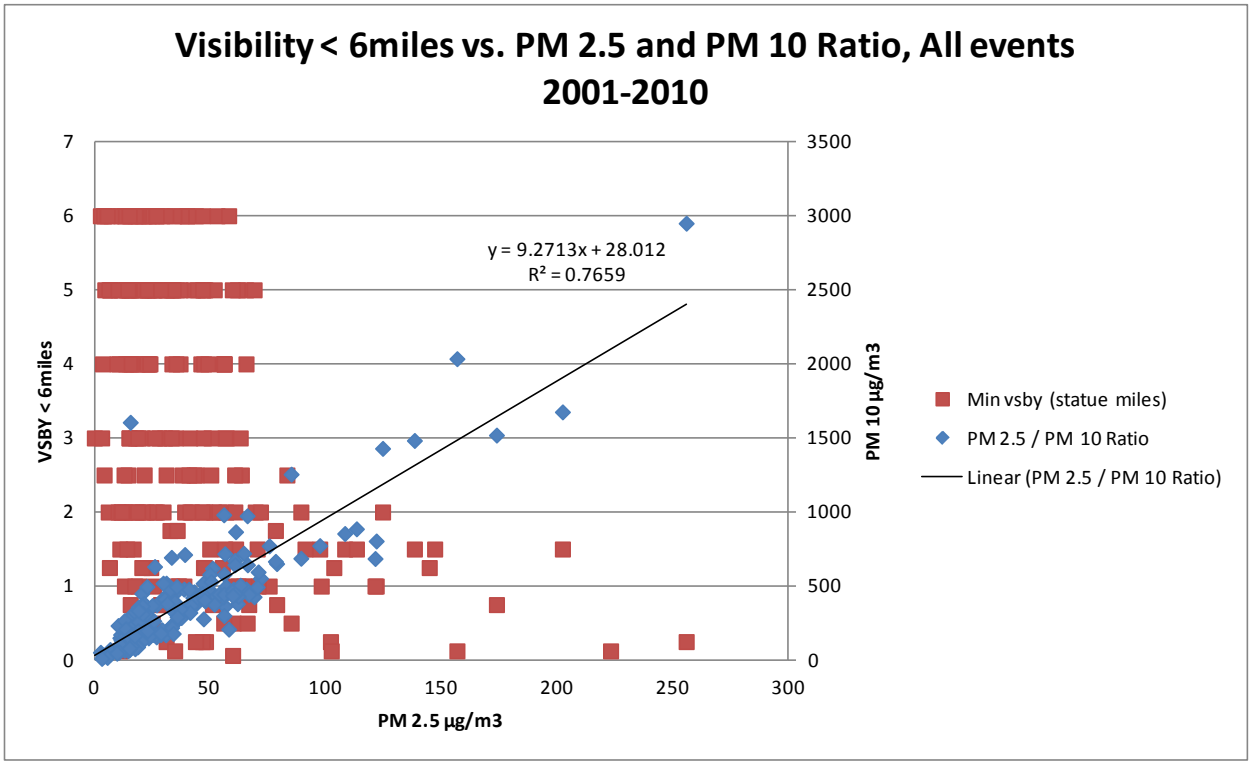

Figure 2.2

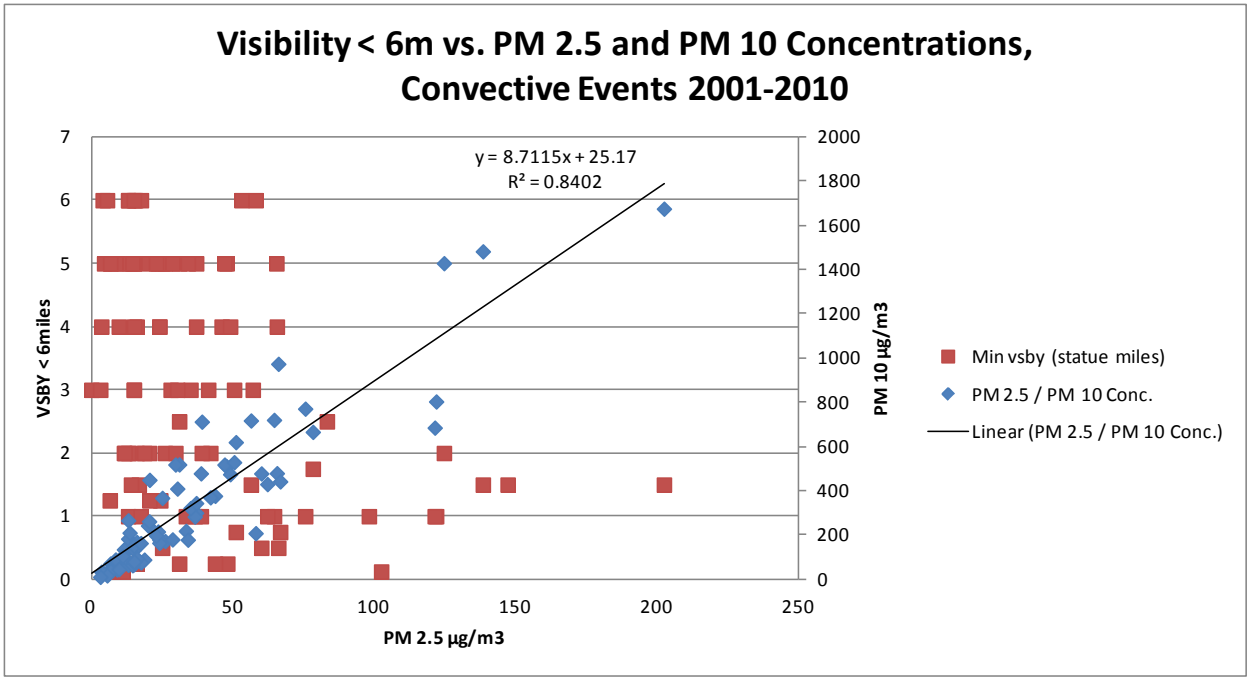
Visibility < 6m vs. PM 2.5 and PM 10 Concentrations, Convective Events 2001-2010
y = 8.7115x + 25.17
R² = 0.8402
VSBY < 6miles
PM 10 µg/m3
PM 2.5 µg/m3
0
1
2
3
4
5
6
7
0
200
400
600
800
1000
1200
1400
1600
1800
2000
0
50
100
150
200
250
Min vsby (statue miles)
PM 2.5 / PM 10 Conc.
Linear (PM 2.5 / PM 10 Conc.)

Figure 2.3

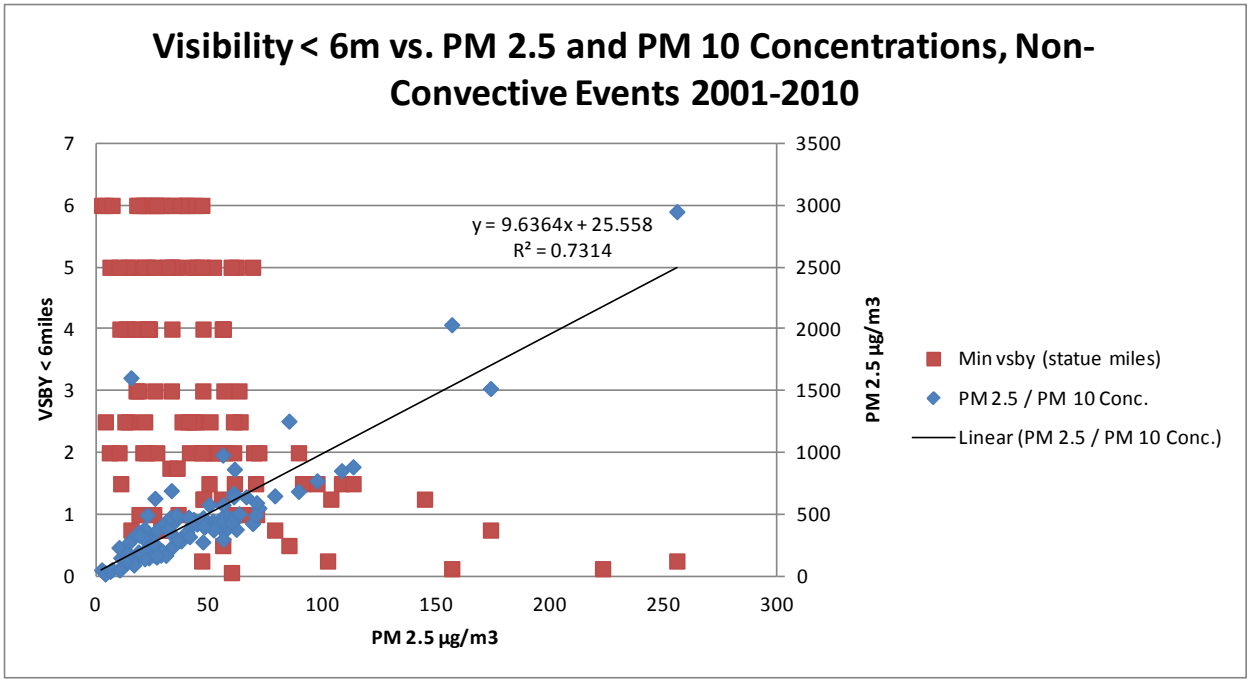
Visibility < 6m vs. PM 2.5 and PM 10 Concentrations, Non-Convective Events 2001-2010
y = 9.6364x + 25.558
R² = 0.7314
VSBY < 6miles
PM 2.5 µg/m3
PM 2.5 µg/m3
0
1
2
3
4
5
6
7
0
500
1000
1500
2000
2500
3000
3500
0
50
100
150
200
250
300
Min vsby (statue miles)
PM 2.5 / PM 10 Conc.
Linear (PM 2.5 / PM 10 Conc.)

Figure 2.4

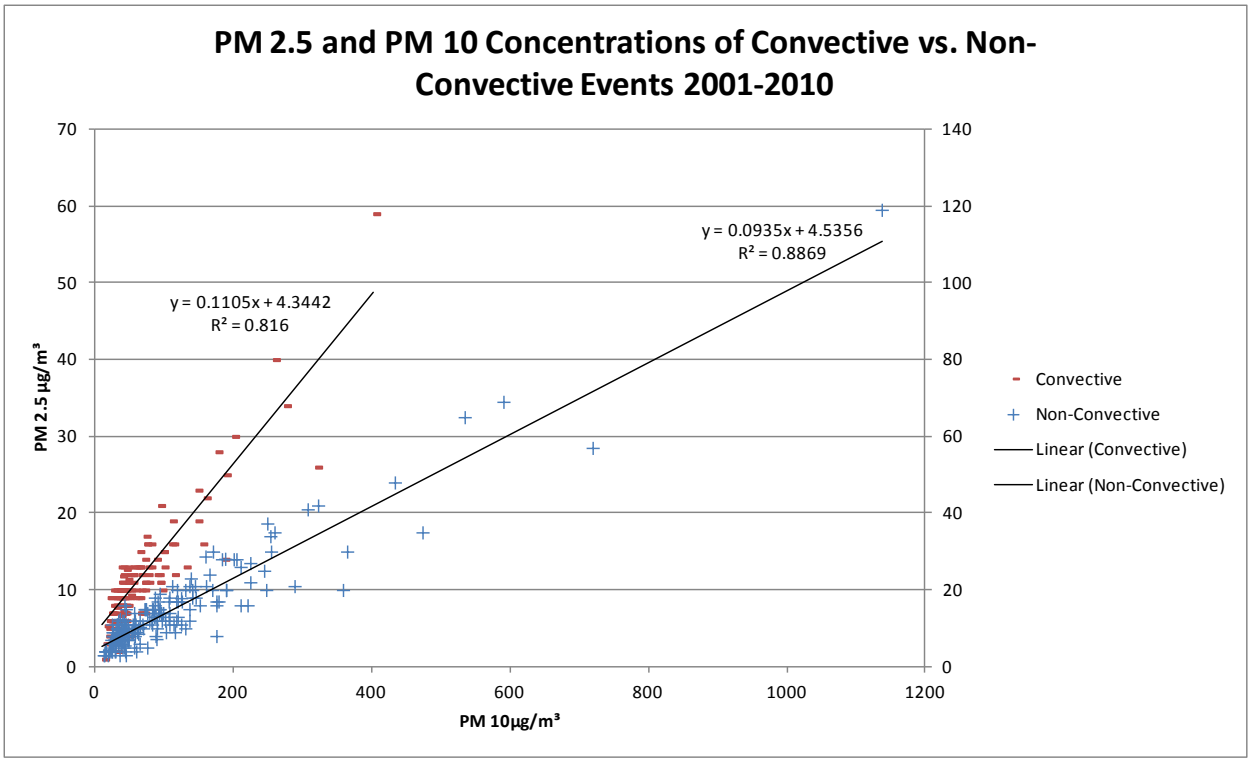
PM 2.5 and PM 10 Concentrations of Convective vs. Non-Convective Events 2001-2010
y = 0.1105x + 4.3442
R² = 0.816
y = 0.0935x + 4.5356
R² = 0.8869
PM 2.5 µg/m³
PM 10µg/m³
0
10
20
30
40
50
60
70
0
20
40
60
80
100
120
140
0
200
400
600
800
1000
1200
Convective
Non-Convective
Linear (Convective)
Linear (Non-Convective)

Figure 2.5

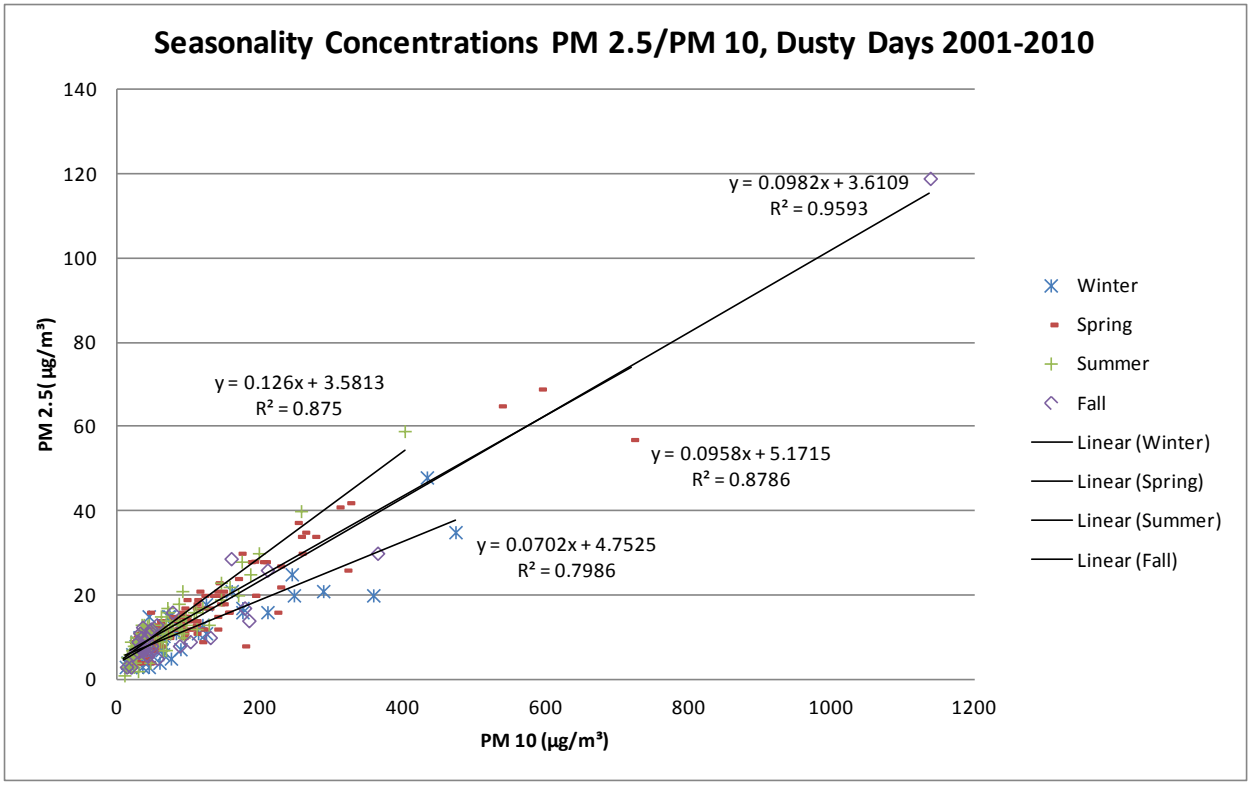
Seasonality Concentrations PM 2.5/PM 10, Dusty Days 2001-2010
PM 2.5 (µg/m³)
PM 10 (µg/m³)
0
20
40
60
80
100
120
140
0
200
400
600
800
1000
1200
y = 0.0982x + 3.6109
R² = 0.9593
y = 0.126x + 3.5813
R² = 0.875
y = 0.0958x + 5.1715
R² = 0.8786
y = 0.0702x + 4.7525
R² = 0.7986
Winter
Spring
Summer
Fall
Linear (Winter)
Linear (Spring)
Linear (Summer)
Linear (Fall)

Figure 2.6(a)

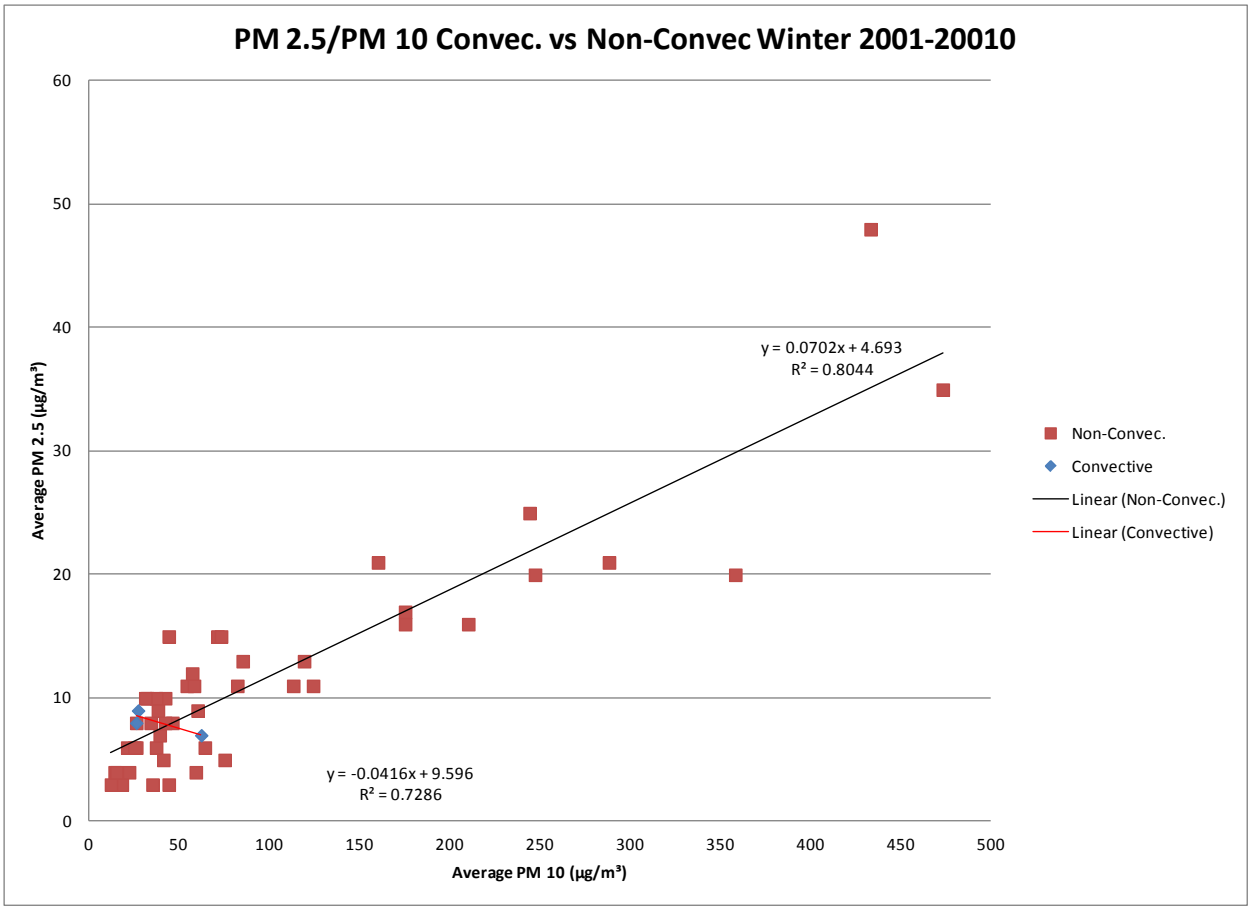
PM 2.5/PM 10 Convec. vs Non-Convec Winter 2001-20010
Average PM 2.5 (µg/m³)
Average PM 10 (µg/m³)
y = 0.0702x + 4.693
R² = 0.8044
y = -0.0416x + 9.596
R² = 0.7286
Non-Convec.
Convective
Linear (Non-Convec.)
Linear (Convective)
0
10
20
30
40
50
60
0
50
100
150
200
250
300
350
400
450
500

Figure 2.6(b)

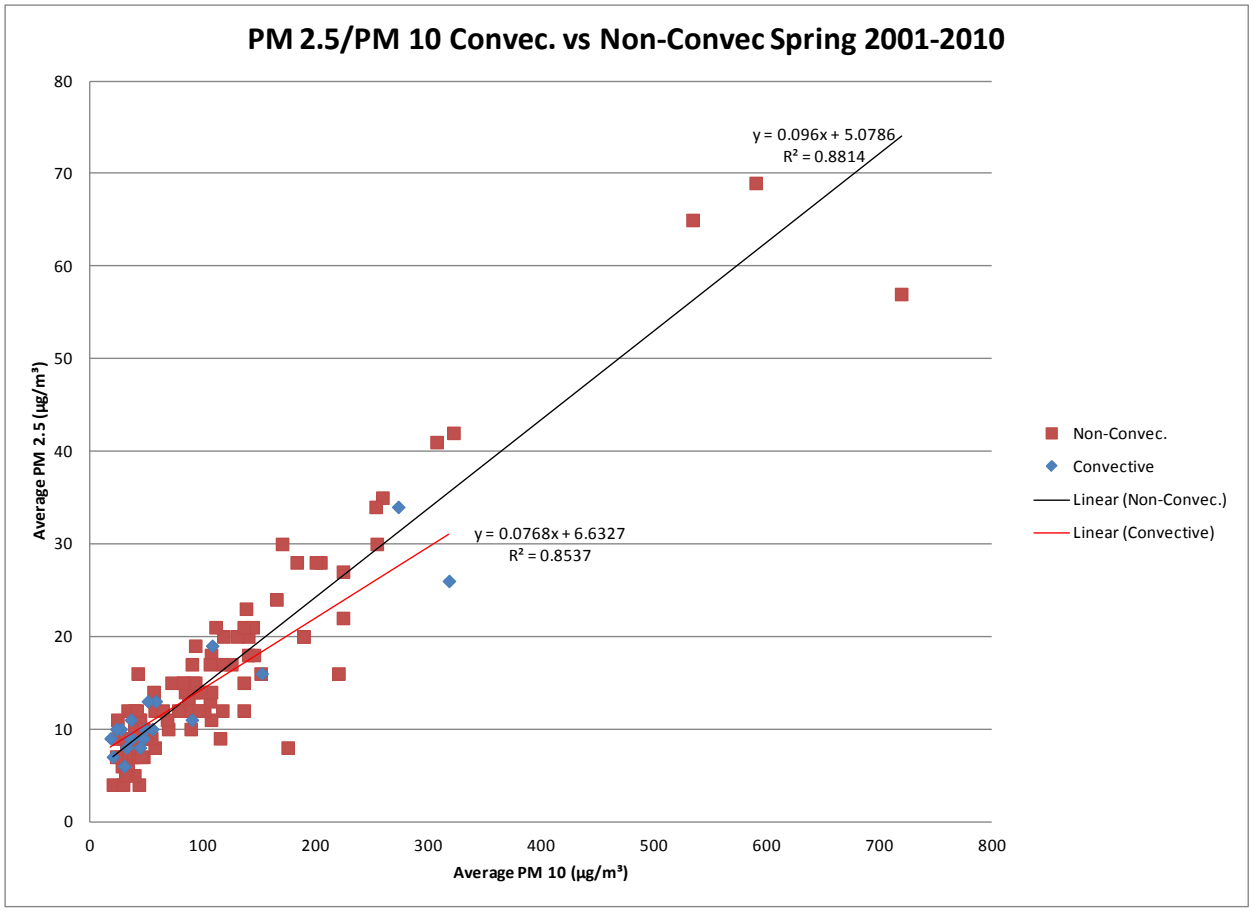
PM 2.5/PM 10 Convec. vs Non-Convec Spring 2001-2010
y = 0.096x + 5.0786
R² = 0.8814
y = 0.0768x + 6.6327
R² = 0.8537
Average PM 2.5 (µg/m³)
Average PM 10 (µg/m³)
0
10
20
30
40
50
60
70
80
0
100
200
300
400
500
600
700
800
Non-Convec.
Convective
Linear (Non-Convec.)
Linear (Convective)

Figure 2.6(c)

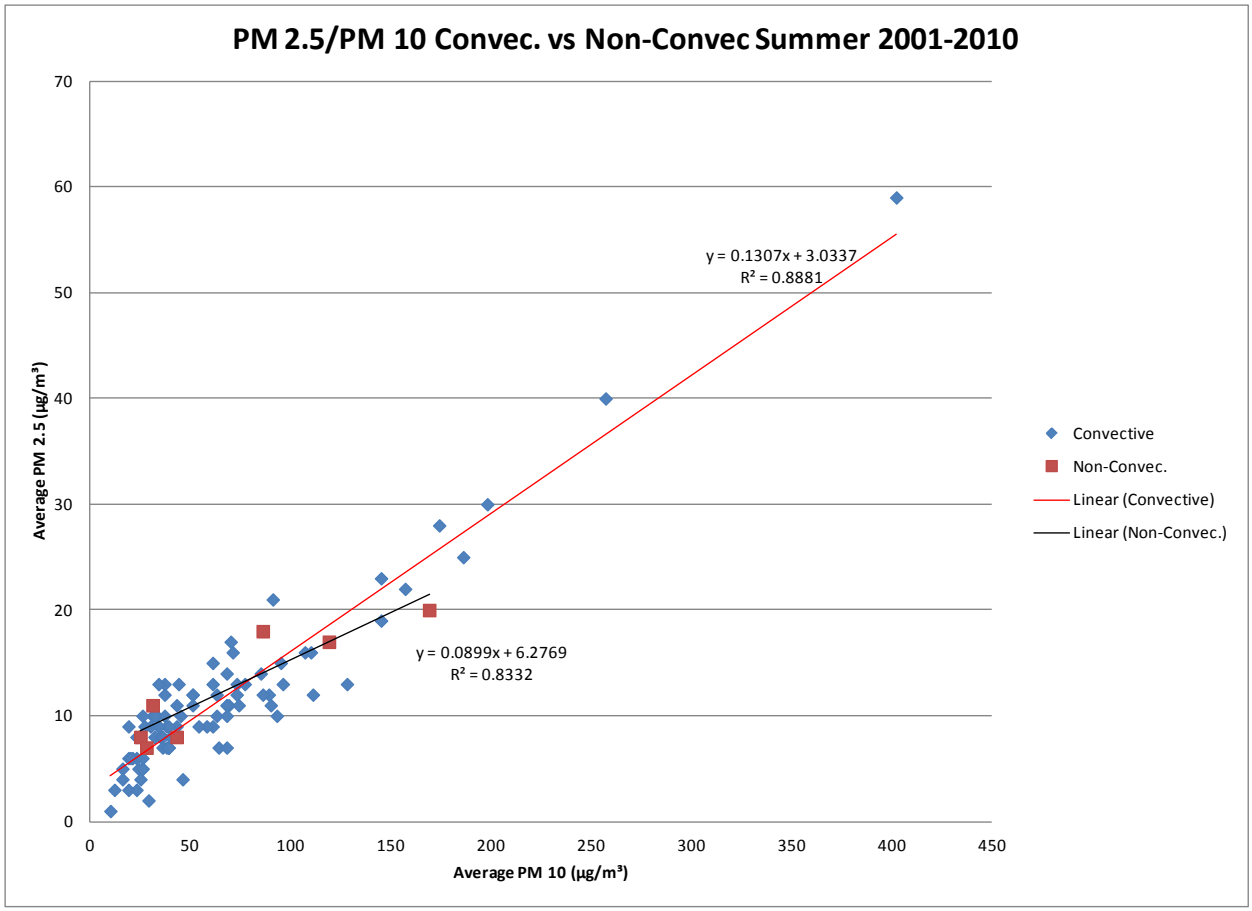
PM 2.5/PM 10 Convec. vs Non-Convec Summer 2001-2010
Average PM 2.5 (µg/m³)
Average PM 10 (µg/m³)
y = 0.1307x + 3.0337
R² = 0.8881
y = 0.0899x + 6.2769
R² = 0.8332
Convective
Non-Convec.
Linear (Convective)
Linear (Non-Convec.)

Figure 2.6(d)

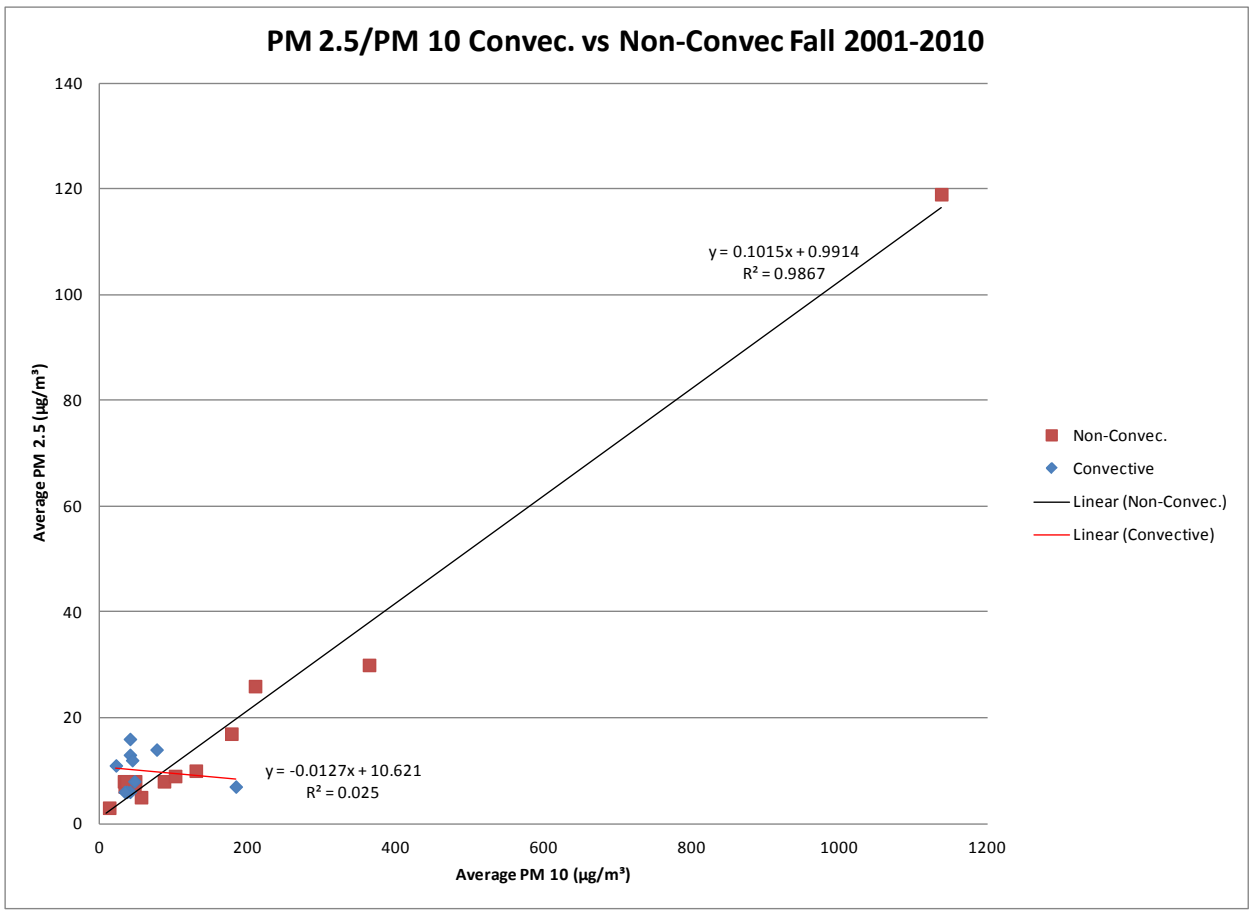
PM 2.5/PM 10 Convec. vs Non-Convec Fall 2001-2010
Average PM 2.5 (µg/m³)
Average PM 10 (µg/m³)
y = 0.1015x + 0.9914
R² = 0.9867
y = -0.0127x + 10.621
R² = 0.025
Non-Convec.
Convective
Linear (Non-Convec.)
Linear (Convective)
0
20
40
60
80
100
120
140
0
200
400
600
800
1000
1200

Figure 2.6(e)

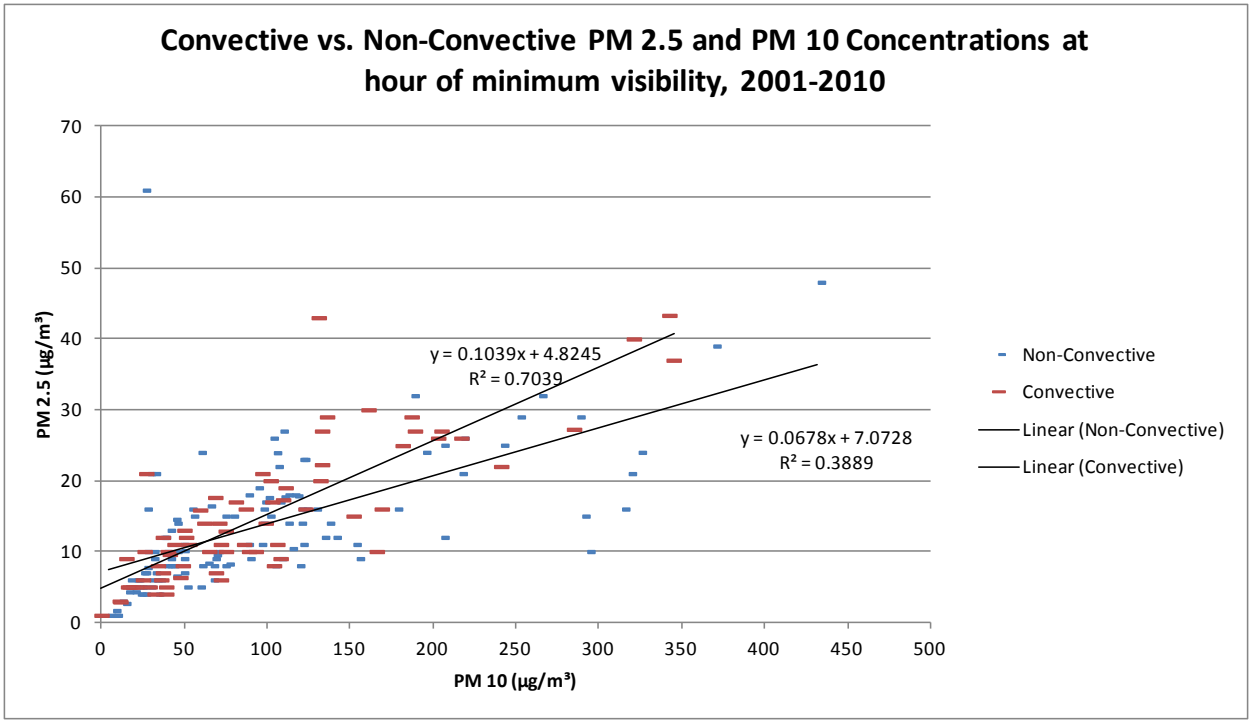
Convective vs. Non-Convective PM 2.5 and PM 10 Concentrations at hour of minimum visibility, 2001-2010
PM 2.5 (µg/m³)
PM 10 (µg/m³)
y = 0.1039x + 4.8245
R² = 0.7039
y = 0.0678x + 7.0728
R² = 0.3889
Non-Convective
Convective
Linear (Non-Convective)
Linear (Convective)

Figure 2.7

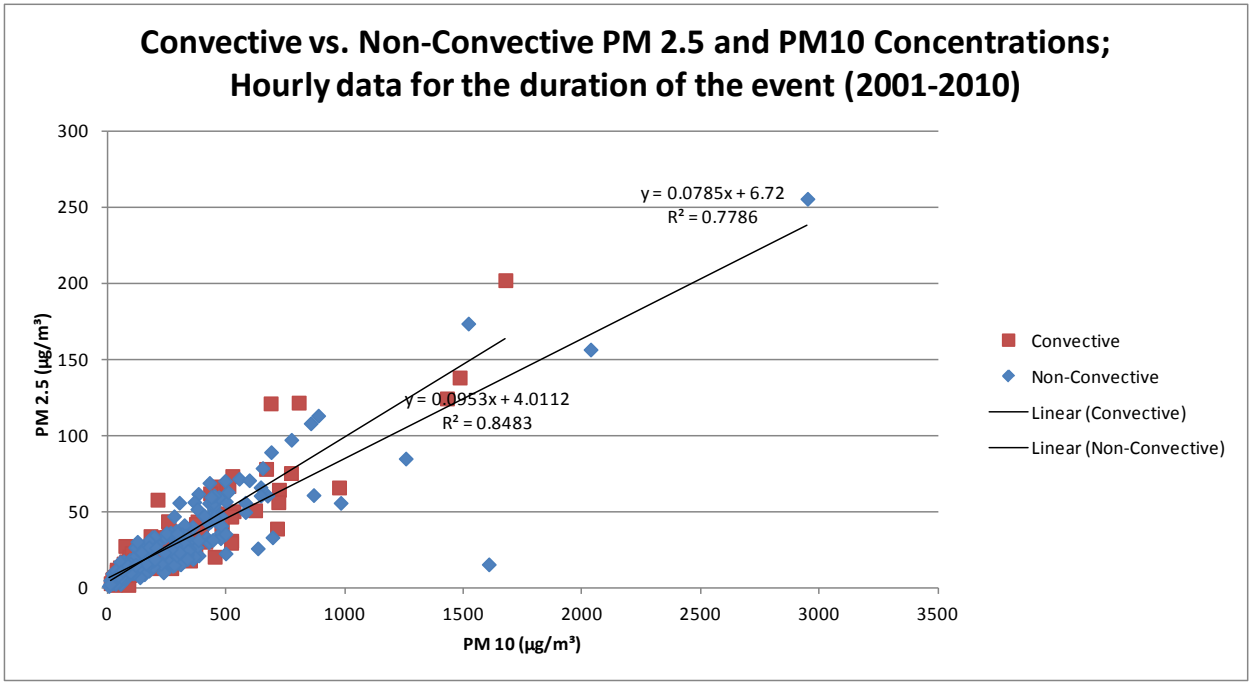
Convective vs. Non-Convective PM 2.5 and PM10 Concentrations; Hourly data for the duration of the event (2001-2010)
PM 2.5 (µg/m³)
PM 10 (µg/m³)
y = 0.0785x + 6.72
R² = 0.7786
y = 0.0953x + 4.0112
R² = 0.8483
Convective
Non-Convective
Linear (Convective)
Linear (Non-Convective)
0
50
100
150
200
250
300
0
500
1000
1500
2000
2500
3000
3500

Figure 2.8

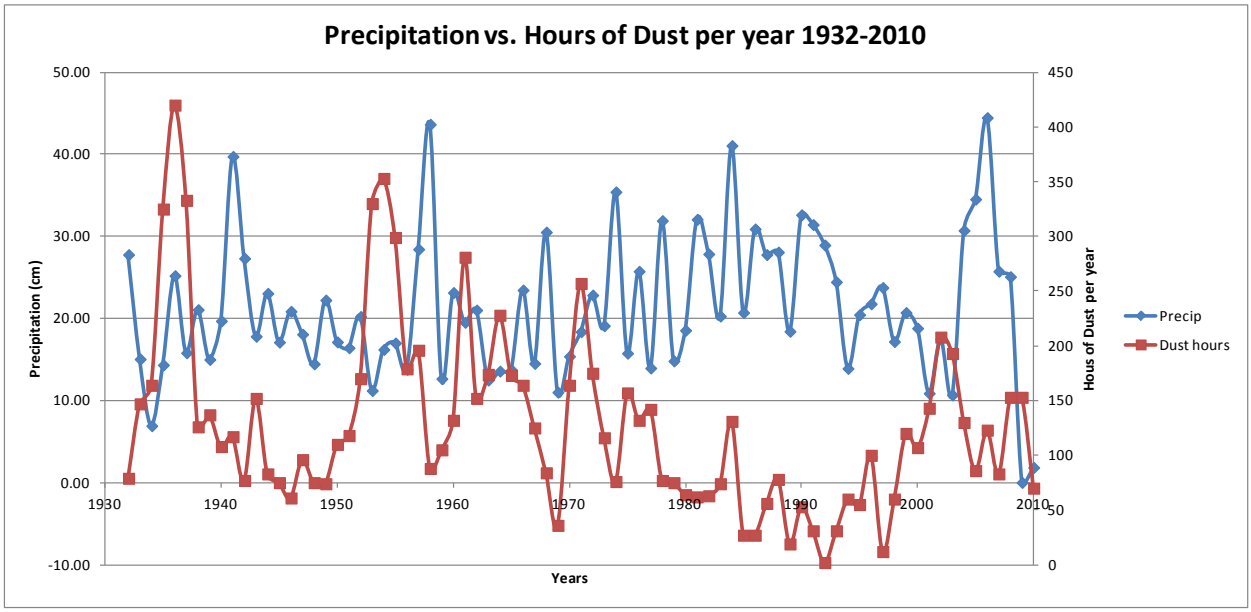
Precipitation vs. Hours of Dust per year 1932-2010
Precipitation (cm)
Hous of Dust per year
Years
Precip
Dust hours
50.00
40.00
30.00
20.00
10.00
0.00
-10.00
450
400
350
300
250
200
150
100
50
0
1930
1940
1950
1960
1970
1980
1990
2000
2010

Figure 2.9

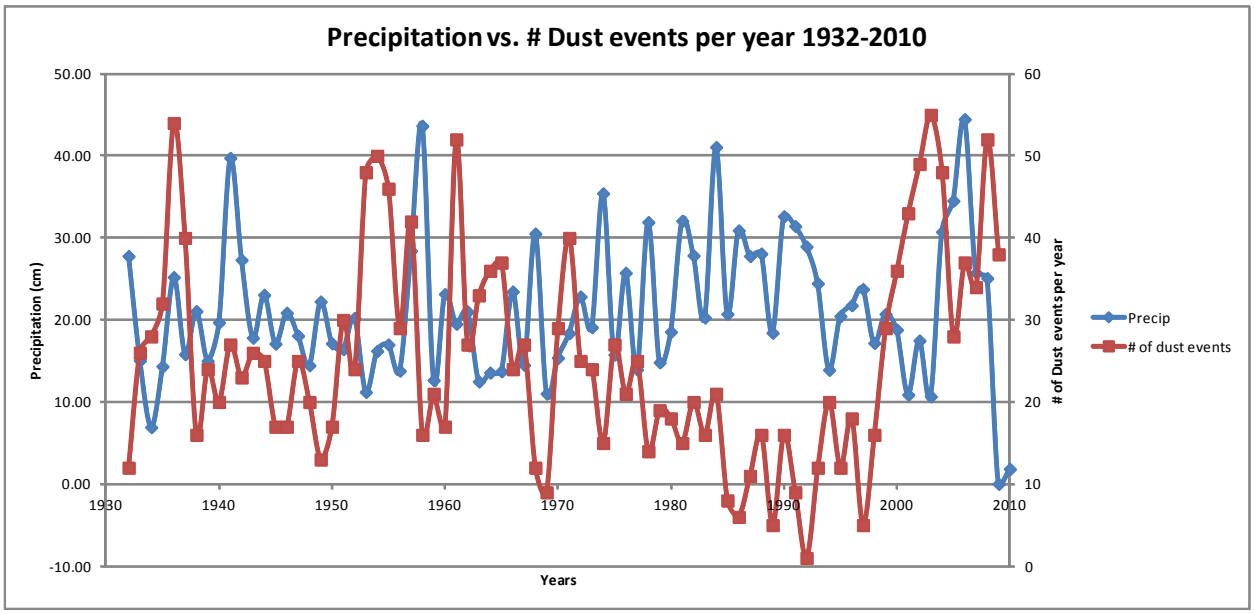
Precipitation vs. # Dust events per year 1932-2010
50.00
40.00
30.00
20.00
10.00
0.00
-10.00
Precipitation (cm)
60
50
40
30
20
10
0
# of Dust events per year
1930
1940
1950
1960
1970
1980
1990
2000
2010
Years
Precip
# of dust events

Figure 2.10

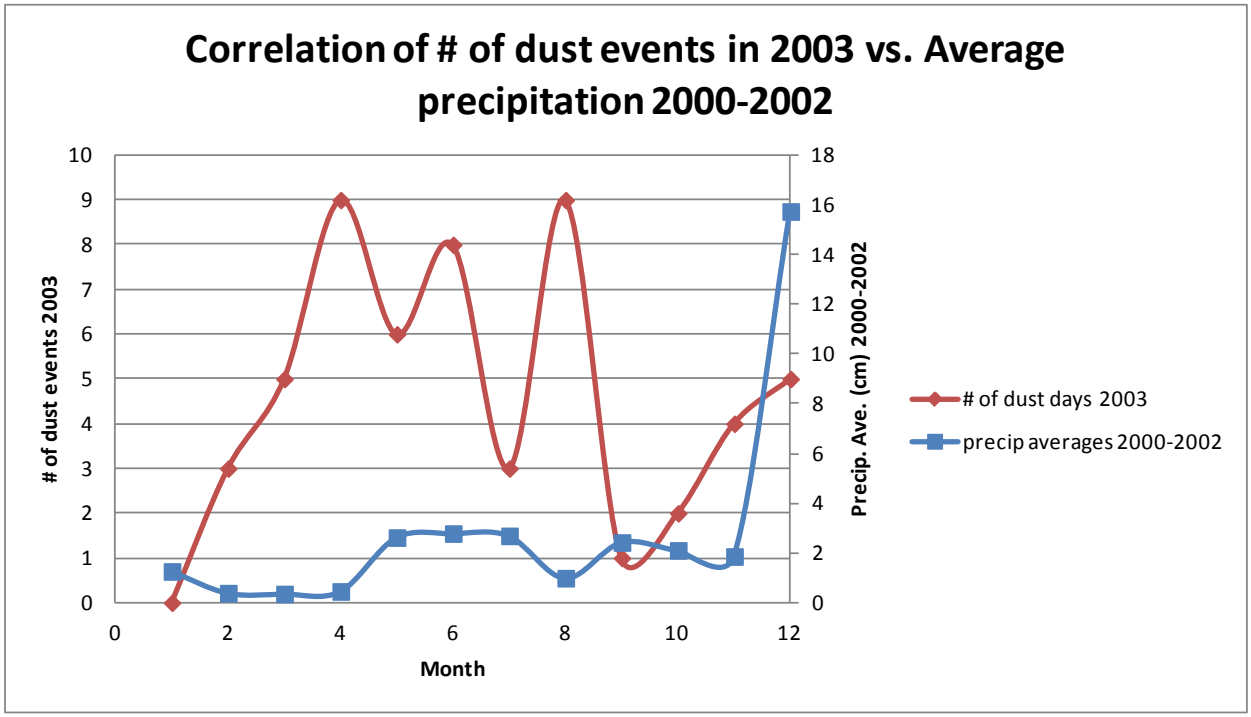
Correlation of # of dust events in 2003 vs. Average precipitation 2000-2002
# of dust events 2003
Precip. Ave. (cm) 2000-2002
Month
0
1
2
3
4
5
6
7
8
9
10
0
2
4
6
8
10
12
14
16
18
0
2
4
6
8
10
12
# of dust days 2003
precip averages 2000-2002

Figure 2.11

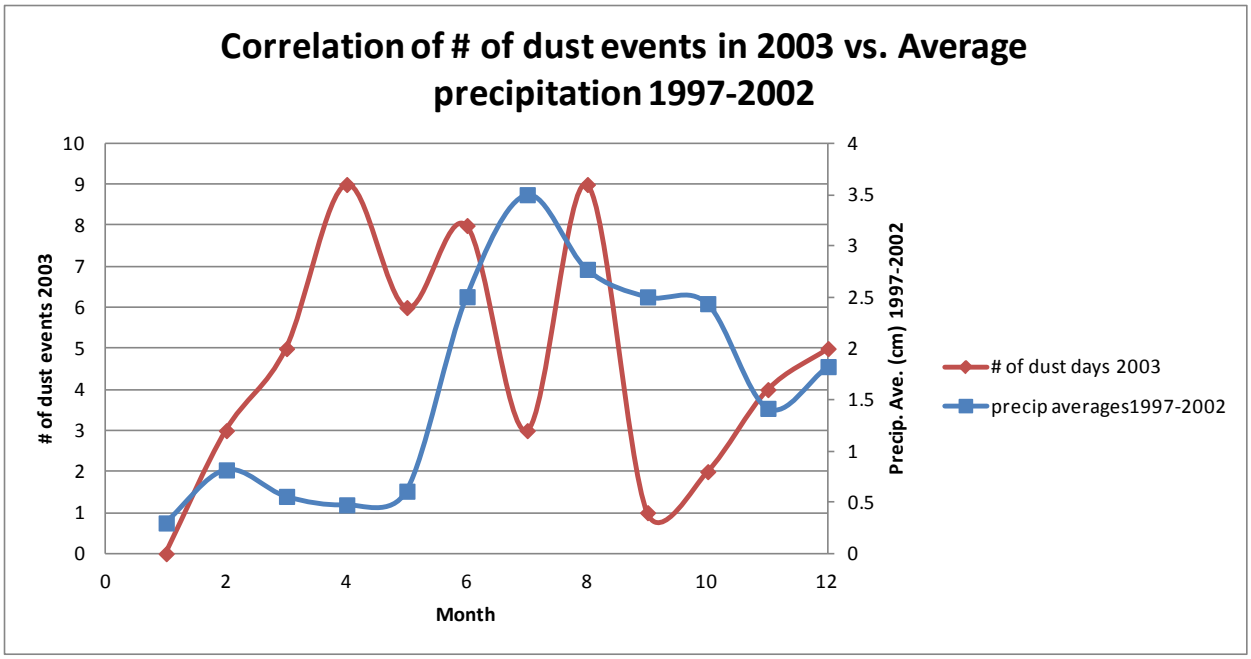
Correlation of # of dust events in 2003 vs. Average precipitation 1997-2002
# of dust events 2003
Precip. Ave. (cm) 1997-2002
Month
0
1
2
3
4
5
6
7
8
9
10
0
0.5
1
1.5
2
2.5
3
3.5
4
0
2
4
6
8
10
12
# of dust days 2003
precip averages1997-2002

Figure 2.12

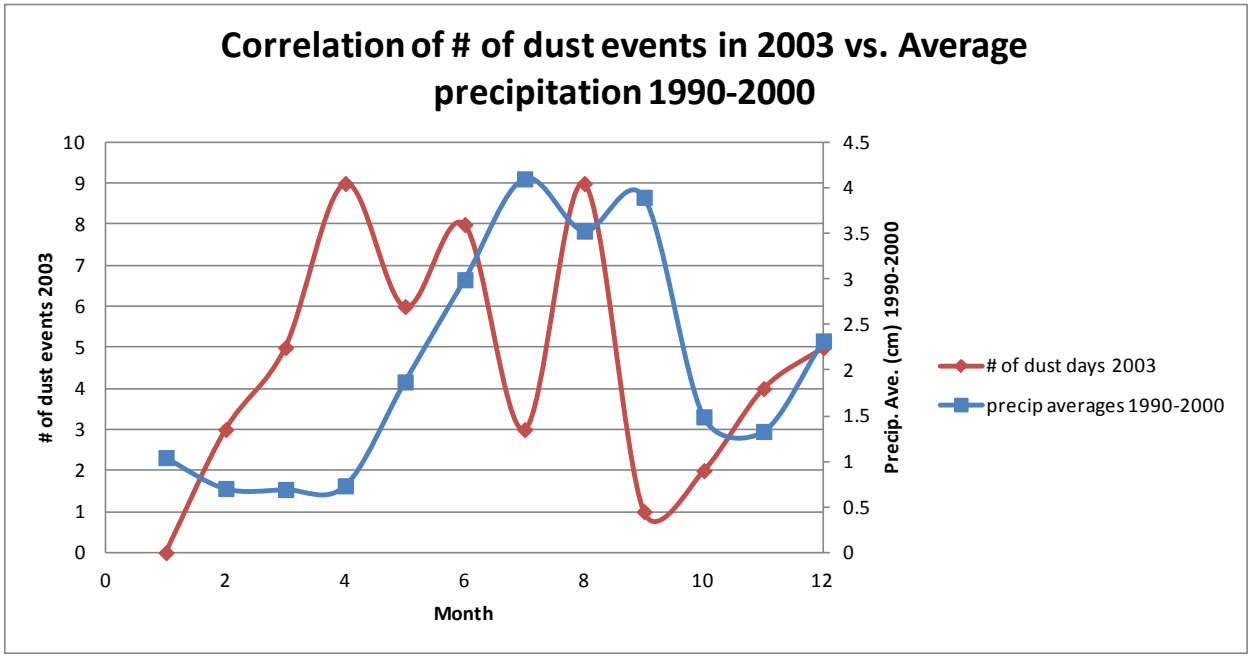
Correlation of # of dust events in 2003 vs. Average precipitation 1990-2000
# of dust events 2003
Precip. Ave. (cm) 1990-2000
Month
# of dust days 2003
precip averages 1990-2000

Figure 2.13

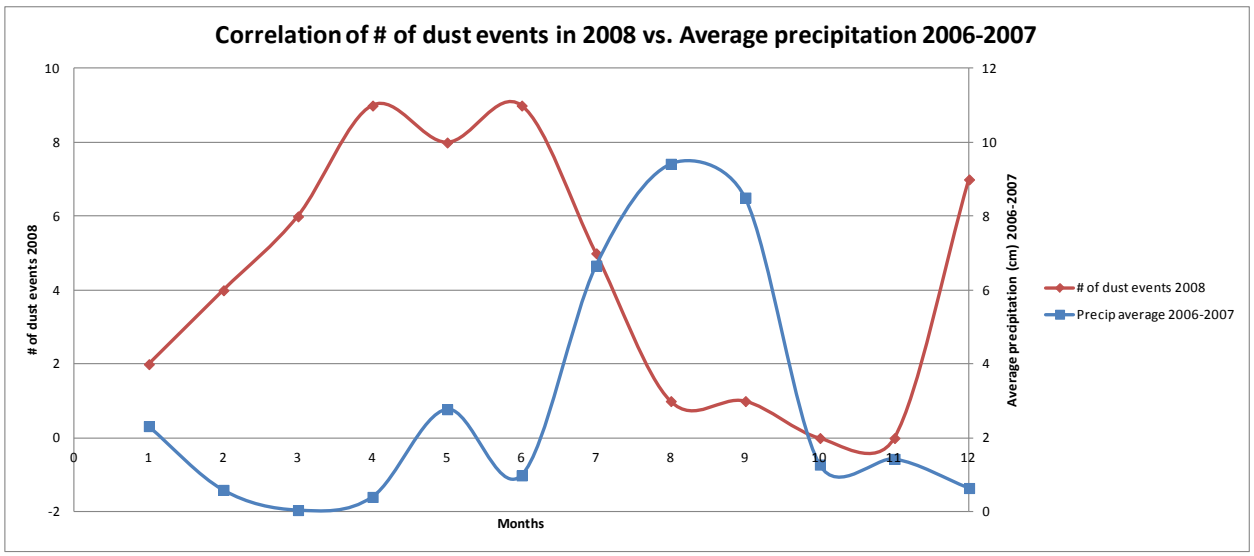
Correlation of # of dust events in 2008 vs. Average precipitation 2006-2007
# of dust events 2008
Average precipitation (cm) 2006-2007
Months
# of dust events 2008
Precip average 2006-2007

Figure 2.14

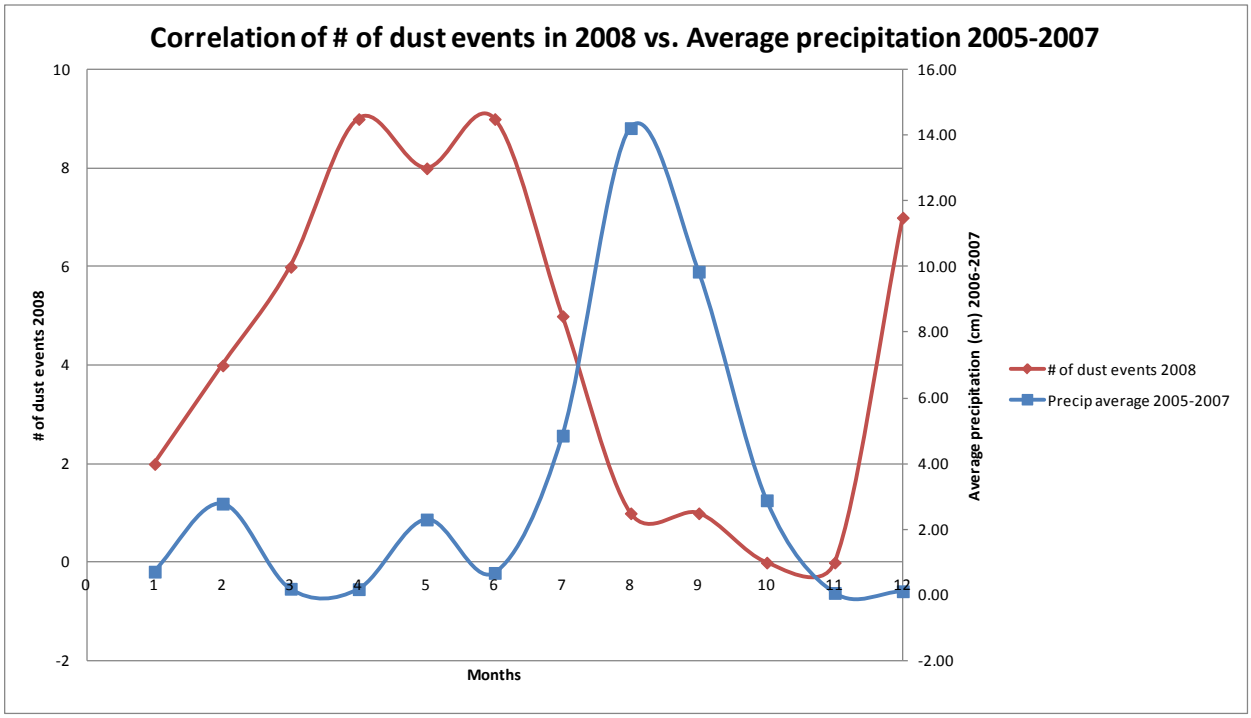
Correlation of # of dust events in 2008 vs. Average precipitation 2005-2007
# of dust events 2008
Average precipitation (cm) 2006-2007
Months
# of dust events 2008
Precip average 2005-2007

Figure 2.15

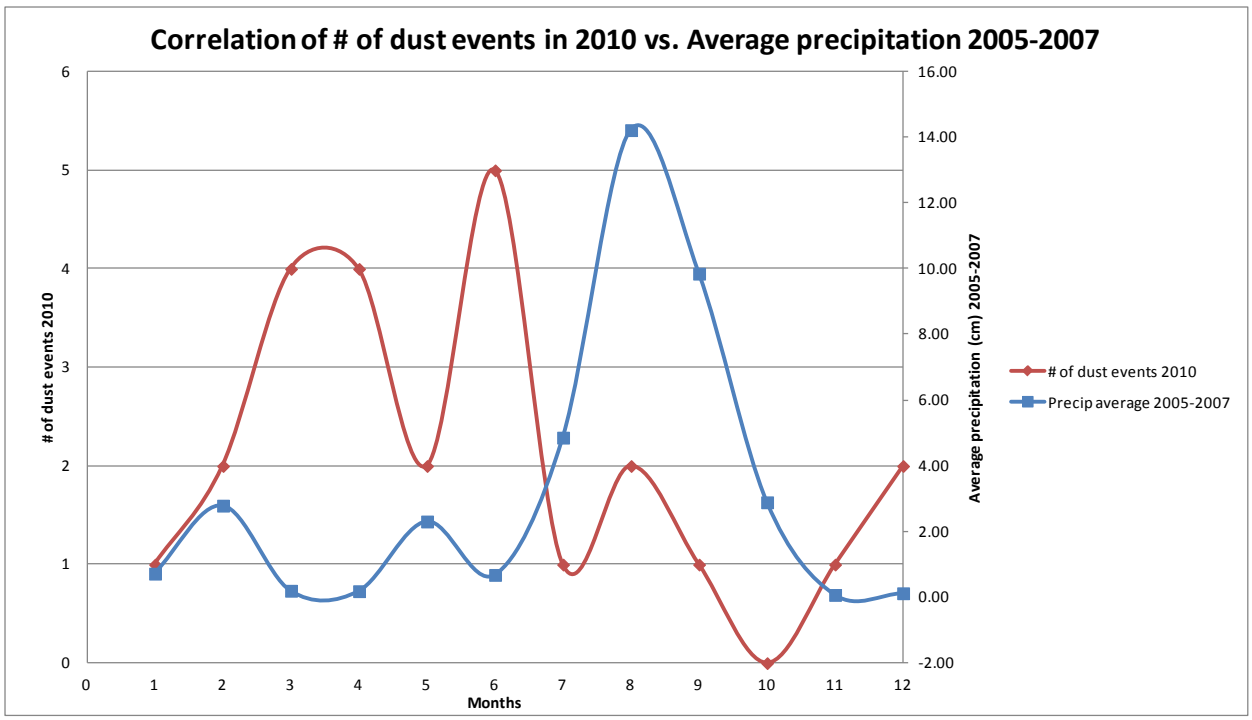
Correlation of # of dust events in 2010 vs. Average precipitation 2005-2007
# of dust events 2010
Average precipitation (cm) 2005-2007
Months
# of dust events 2010
Precip average 2005-2007
0
1
2
3
4
5
6
-2.00
0.00
2.00
4.00
6.00
8.00
10.00
12.00
14.00
16.00
0
1
2
3
4
5
6
7
8
9
10
11
12

Figure 2.16

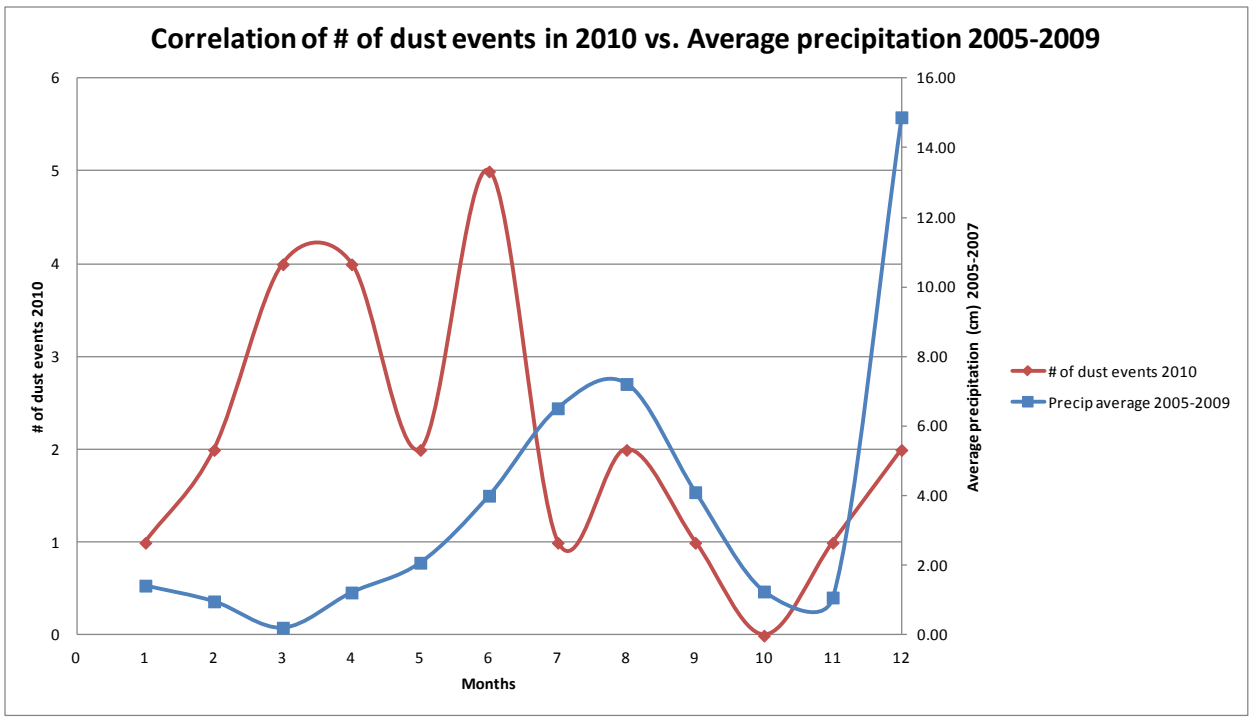
Correlation of # of dust events in 2010 vs. Average precipitation 2005-2009
# of dust events 2010
Average precipitation (cm) 2005-2007
Months
# of dust events 2010
Precip average 2005-2009
0
1
2
3
4
5
6
0.00
2.00
4.00
6.00
8.00
10.00
12.00
14.00
16.00
0
1
2
3
4
5
6
7
8
9
10
11
12

Figure 2.17

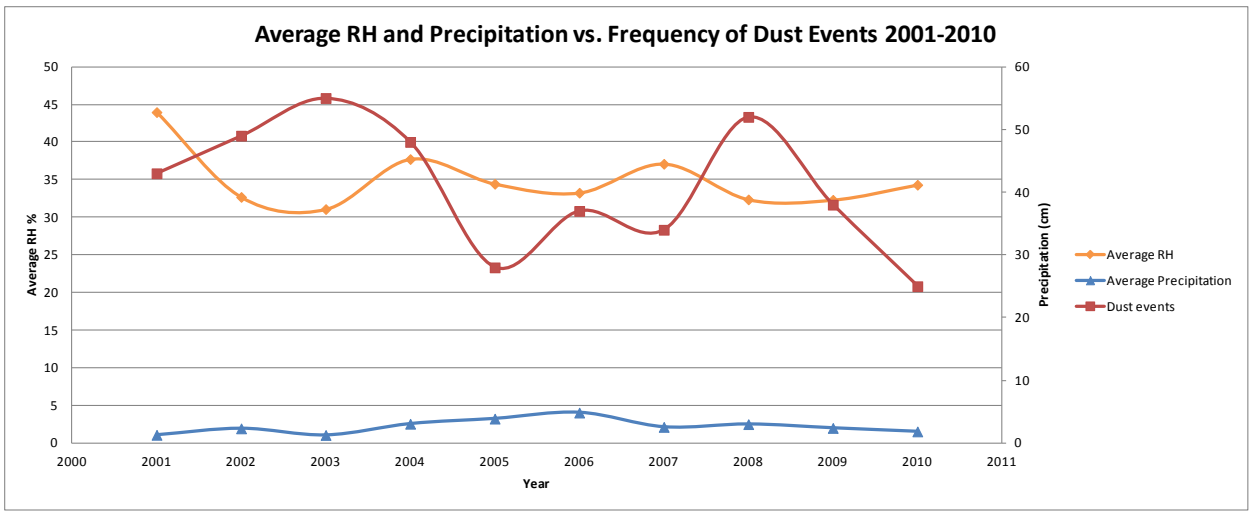
Average RH and Precipitation vs. Frequency of Dust Events 2001-2010
Average RH %
Precipitation (cm)
Year
Average RH
Average Precipitation
Dust events

Figure 2.18

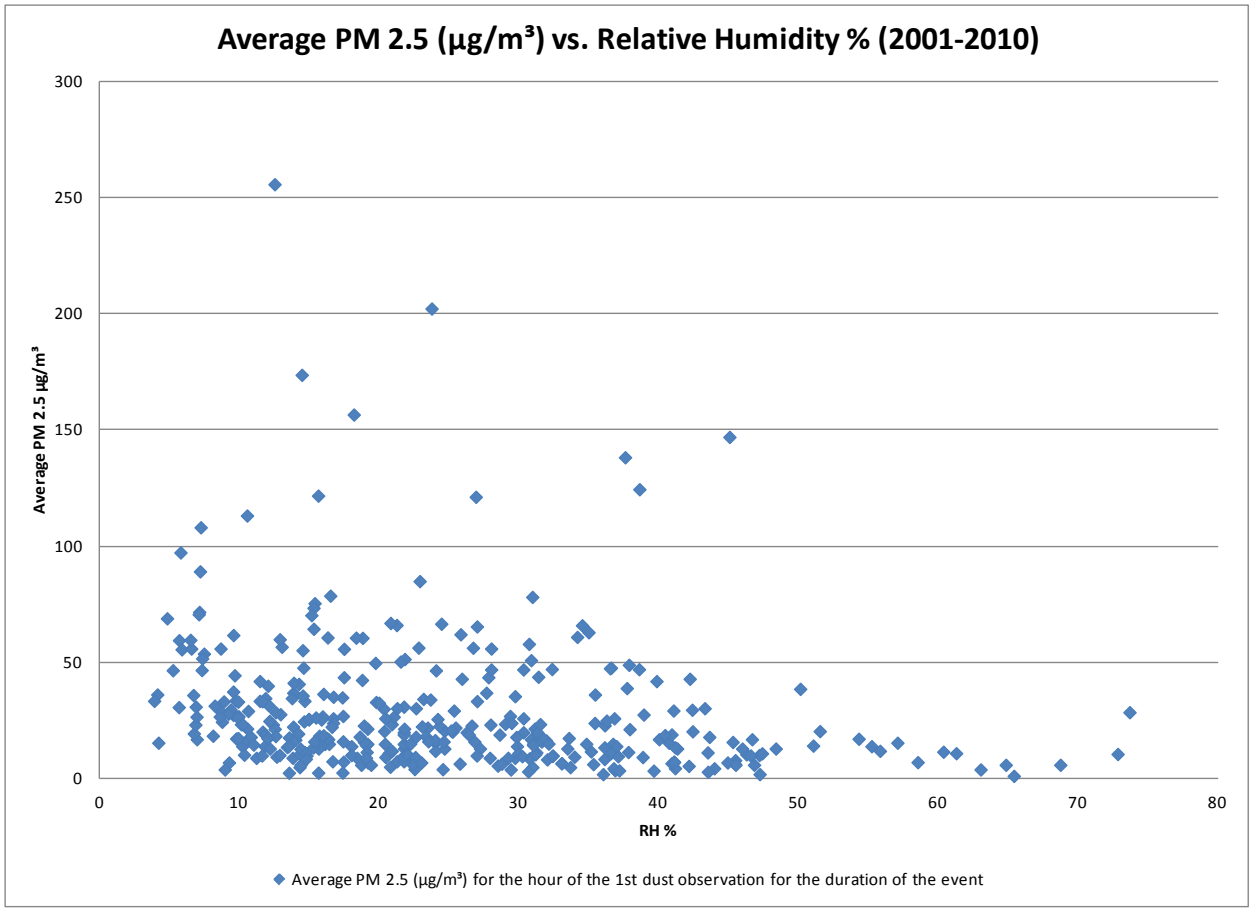
Average PM 2.5 (µg/m³) vs. Relative Humidity % (2001-2010)
Average PM 2.5 µg/m³
RH %
0
50
100
150
200
250
300
0
10
20
30
40
50
60
70
80
Average PM 2.5 (µg/m³) for the hour of the 1st dust observation for the duration of the event

Figure 2.19

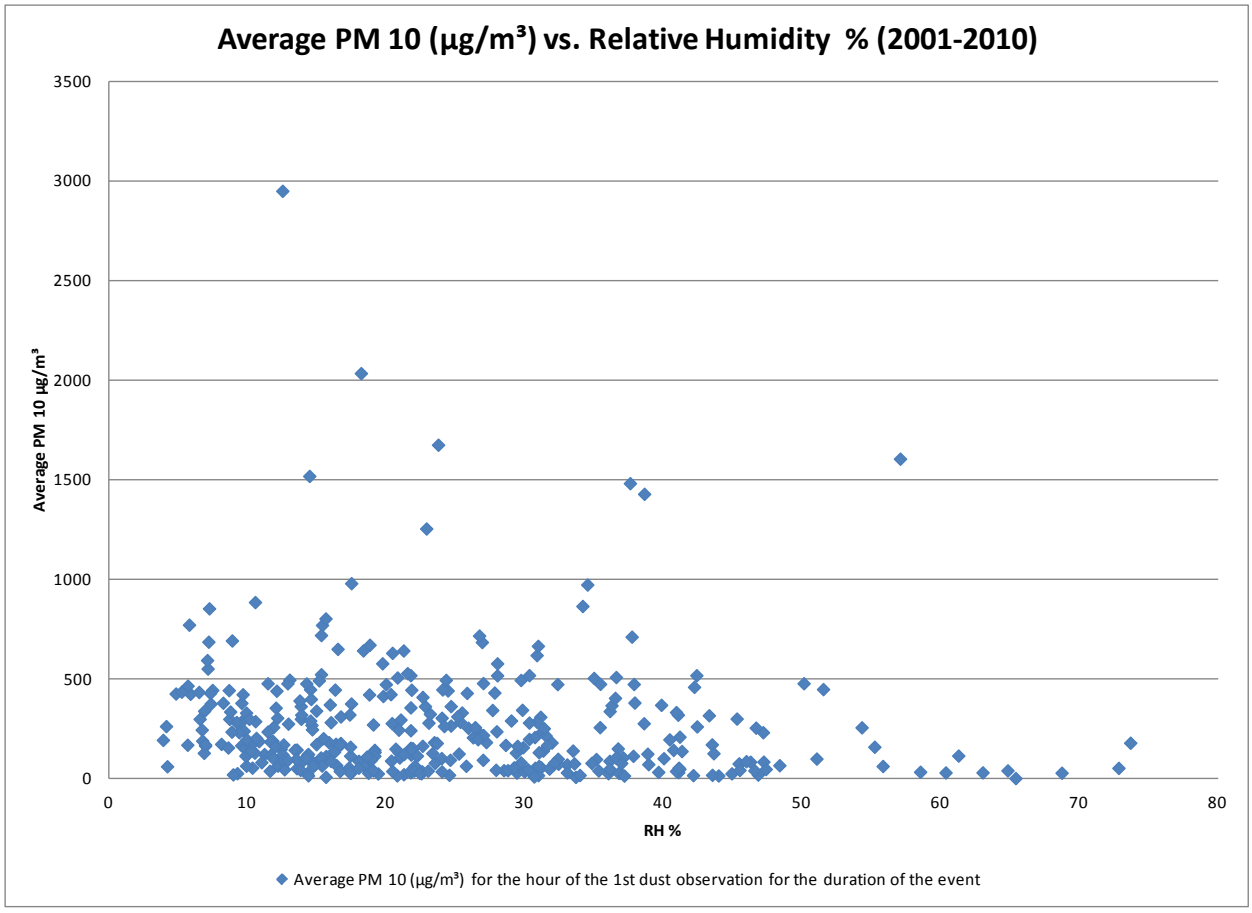
Average PM 10 (µg/m³) vs. Relative Humidity % (2001-2010)
Average PM 10 µg/m³
3500
3000
2500
2000
1500
1000
500
0
0
10
20
30
40
50
60
70
80
RH %
Average PM 10 (µg/m³) for the hour of the 1st dust observation for the duration of the event

Figure 2.20

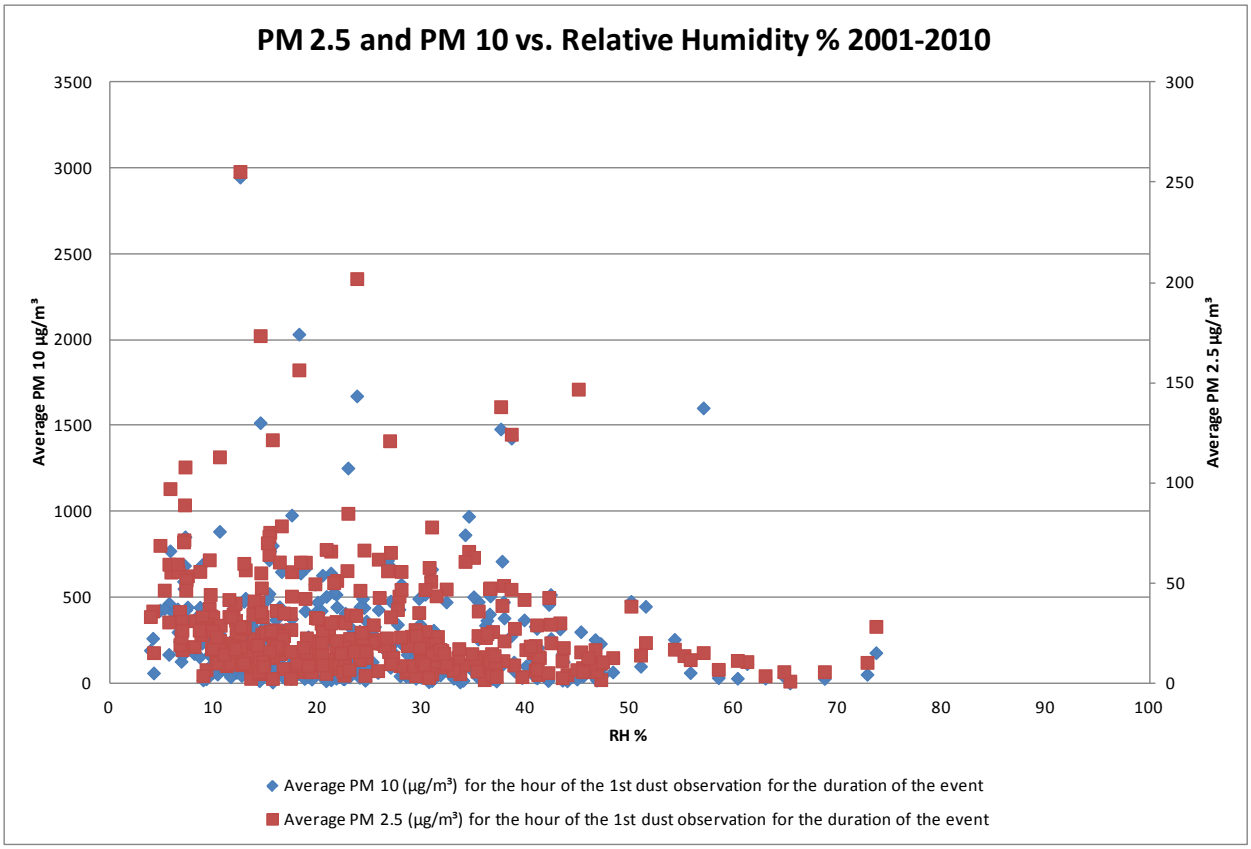
PM 2.5 and PM 10 vs. Relative Humidity % 2001-2010
Average PM 10 µg/m³
Average PM 2.5 µg/m³
RH %
0
500
1000
1500
2000
2500
3000
3500
0
50
100
150
200
250
300
0
10
20
30
40
50
60
70
80
90
100
Average PM 10 (µg/m³) for the hour of the 1st dust observation for the duration of the event
Average PM 2.5 (µg/m³) for the hour of the 1st dust observation for the duration of the event

Figure 2.21

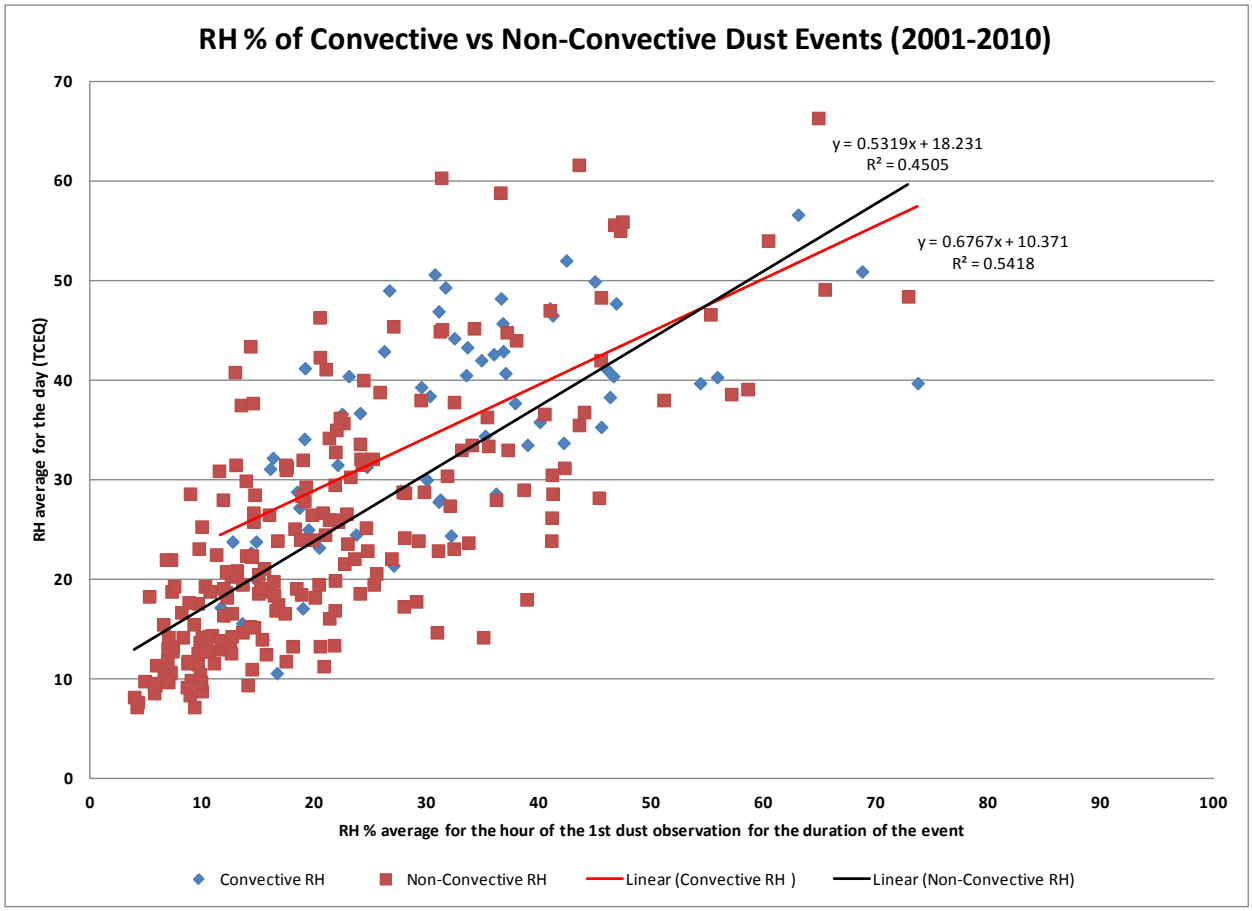
RH % of Convective vs Non-Convective Dust Events (2001-2010)
y = 0.5319x + 18.231
R² = 0.4505
y = 0.6767x + 10.371
R² = 0.5418
RH average for the day (TCEQ)
RH % average for the hour of the 1st dust observation for the duration of the event
Convective RH
Non-Convective RH
Linear (Convective RH)
Linear (Non-Convective RH)

Figure 2.22

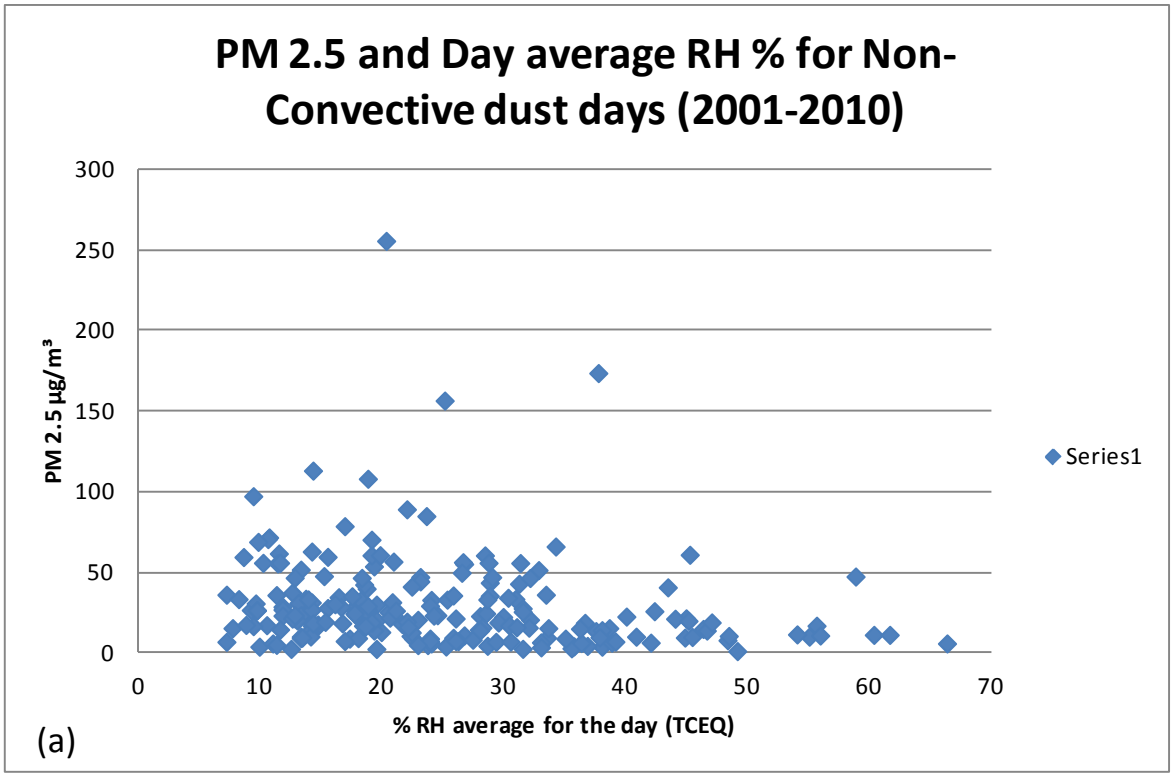
PM 2.5 and Day average RH % for Non-Convective dust days (2001-2010)
PM 2.5 µg/m³
% RH average for the day (TCEQ)
Series1
(a)

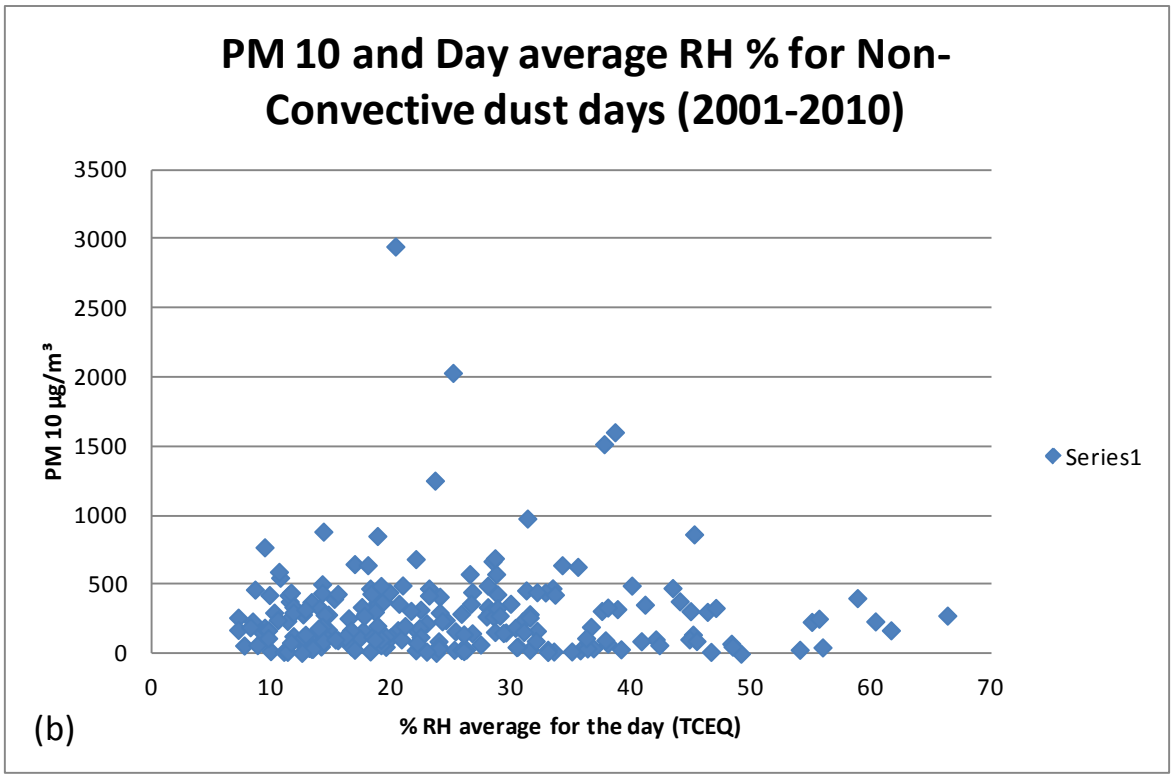
PM 10 and Day average RH % for Non-Convective dust days (2001-2010)
PM 10 µg/m³
% RH average for the day (TCEQ)
Series1
(b)

Figure 2.23

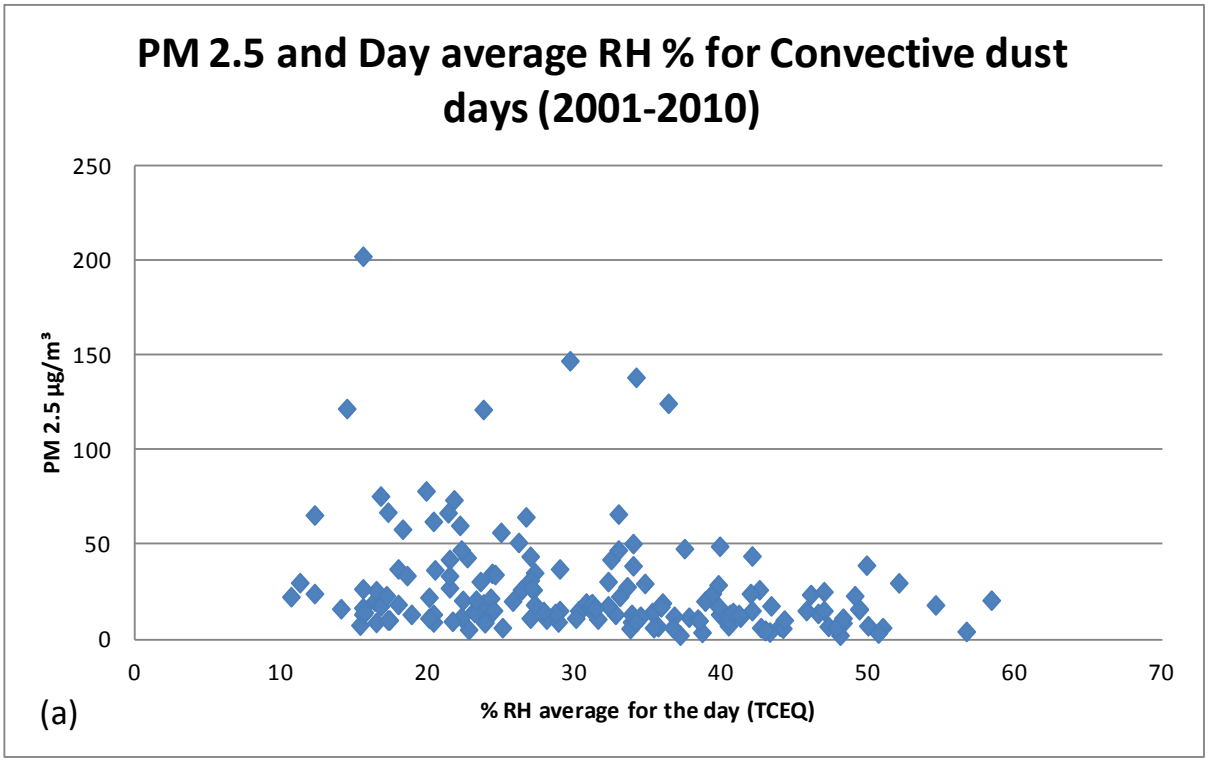
PM 2.5 and Day average RH % for Convective dust days (2001-2010)
PM 2.5 µg/m³
250
200
150
100
50
0
0
10
20
30
40
50
60
70
% RH average for the day (TCEQ)
(a)

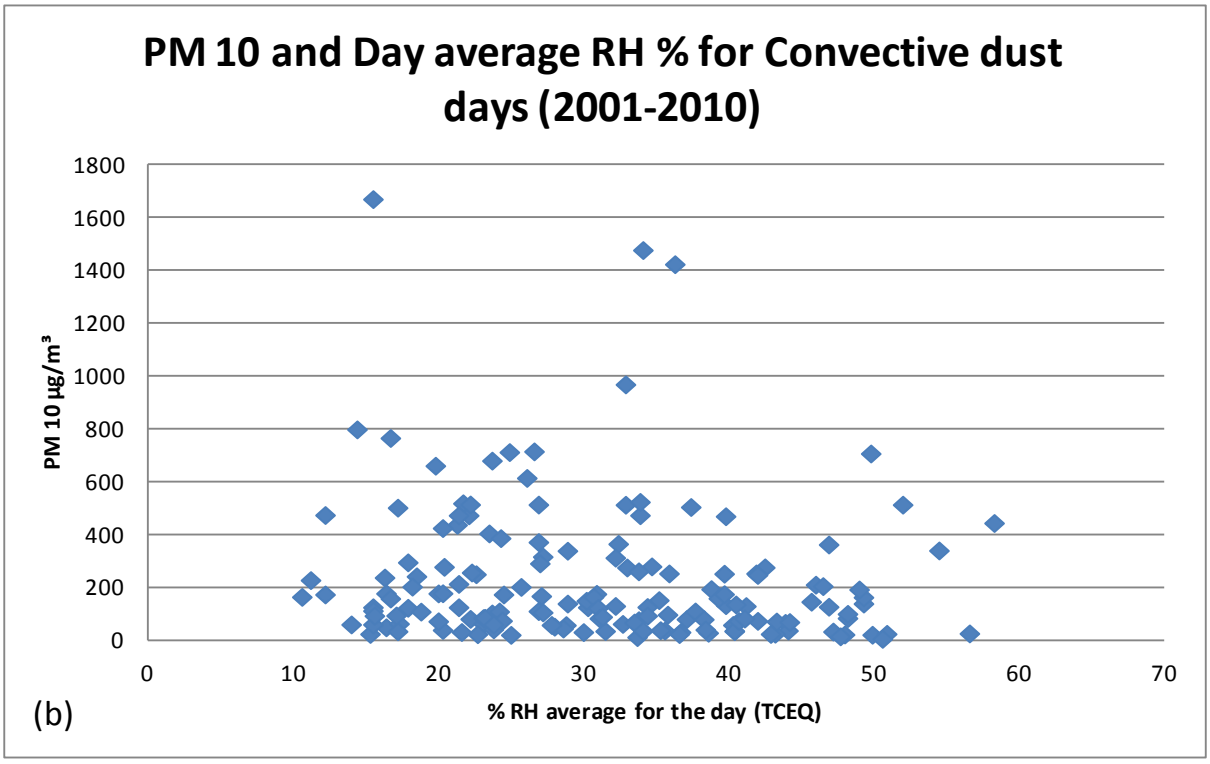
PM 10 and Day average RH % for Convective dust days (2001-2010)
PM 10 µg/m³
1800
1600
1400
1200
1000
800
600
400
200
0
0
10
20
30
40
50
60
70
% RH average for the day (TCEQ)
(b)

Figure 2.24

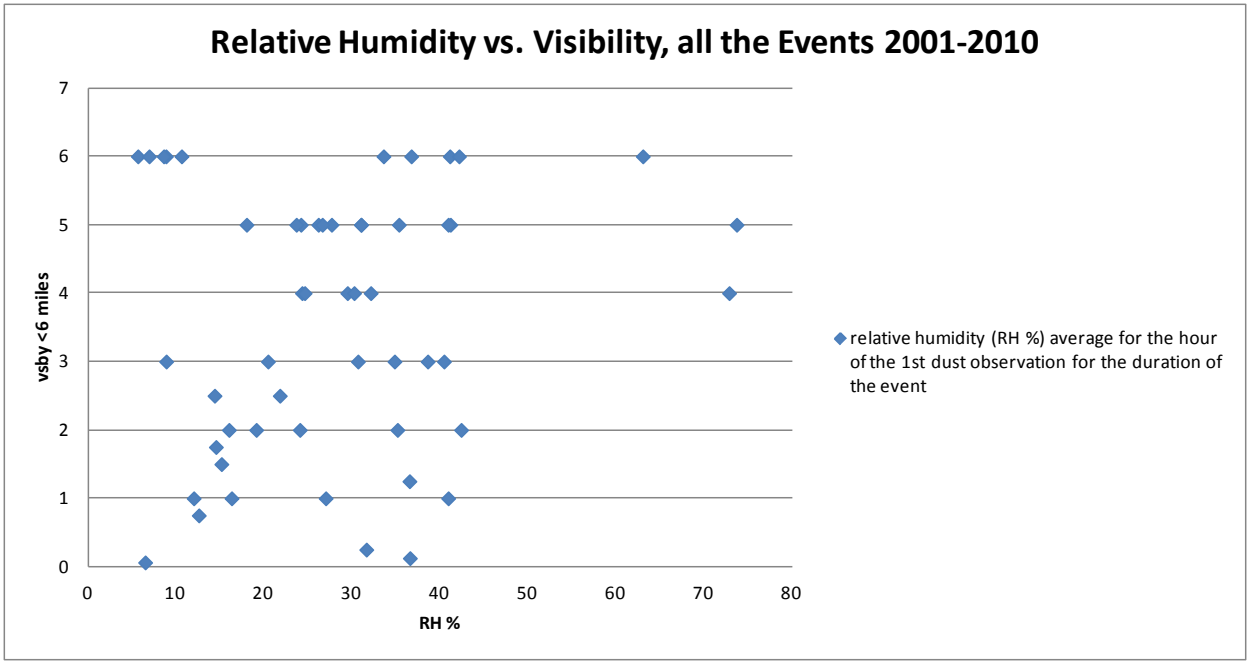
Relative Humidity vs. Visibility, all the Events 2001-2010
vsby <6 miles
RH %
0
1
2
3
4
5
6
7
0
10
20
30
40
50
60
70
80
relative humidity (RH %) average for the hour of the 1st dust observation for the duration of the event

Figure 2.25

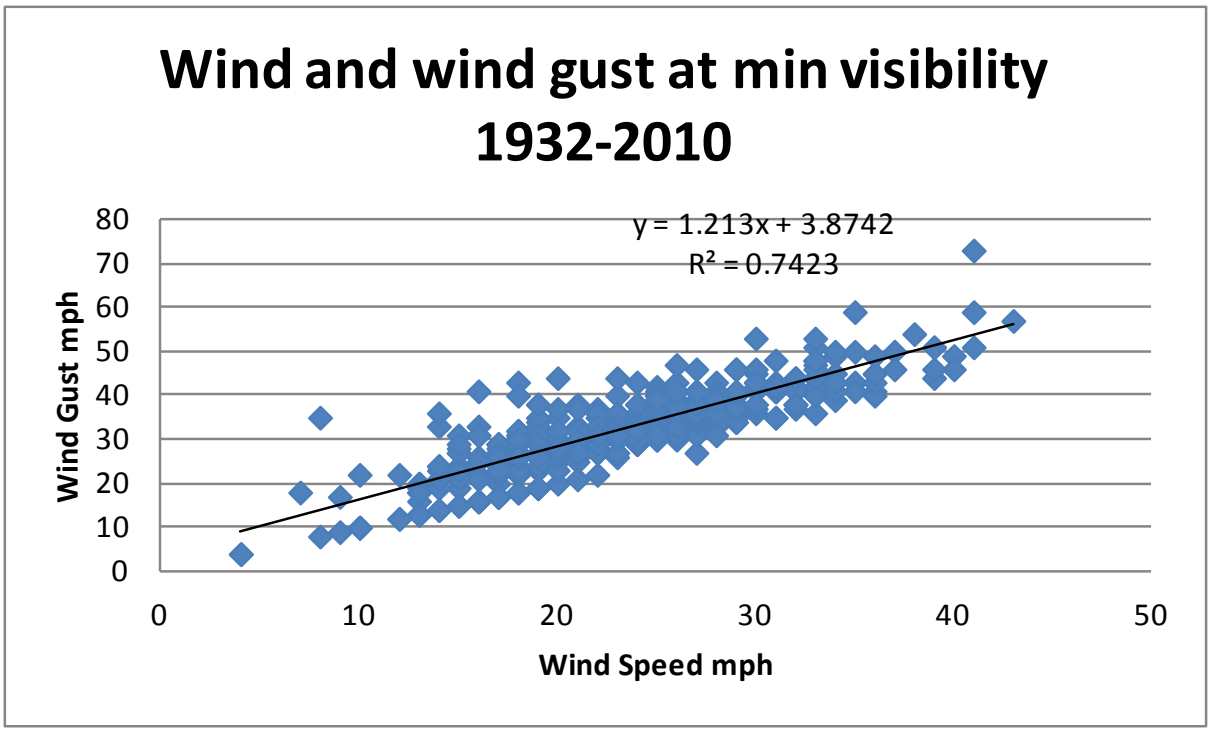
Wind and wind gust at min visibility
1932-2010
y = 1.213x + 3.8742
R² = 0.7423
Wind Gust mph
Wind Speed mph
0
10
20
30
40
50
60
70
80
0
10
20
30
40
50

Figure 2.26

Chapter 3

3.1 Back Trajectory analysis of air transport patterns that bring dust storms to El Paso, TX

3.1.1 Introduction

The Chihuahuan Desert of North America has been described as a critical climatic boundary region between the subtropics and the middle latitudes (Castiglia and Fawcett, 2006). The area receives most of its annual precipitation in the summer (MacMahon and Wagner, 1985) through the monsoon circulation off the Gulf of Mexico (Schmidt, 1986; Warner, 2004), while the other months of the year are generally much drier. El Paso, Texas, USA and Ciudad Juarez, Chihuahua, Mexico (collectively the "Paso del Norte" metropolitan area) comprise the largest metropolitan area in the Chihuahuan Desert, with a population of over 2 million. In this area, dust storms are one of the principal hazardous weather phenomena, causing significant airborne particle pollution in the region (Novlan *et al*., 2007; Rivera Rivera *et al*., 2009, 2010; Yin *et al*., 2007). From 1932 through 2005, aeolian transport of particulate matter sufficient to restrict visibility (classified as "blowing dust," "dust storm," "dust haze," "dust" "blowing sand," or "sandstorm": hereinafter referred to as "dust events") and lasting at least 2 hours were recorded at the El Paso International Airport (ELP) at an average of 15 days per year (Novlan *et al.*, 2007). This dust has effects on the local economy and infrastructure, and may adversely affect the health of the Paso del Norte's residents (Peng *et al.*, 2010).

Novlan *et al*. (2007) describe three monsoon regimes (in the sense of prevailing wind change) in the El Paso area, with a dominant northerly wind flow in the cooler seasons of

October through February, a shift to west-southwest in the spring or peak dust season of March into early June, and another distinct shift to prevailing southeast winds in the classic North American Monsoon (rainy) season of July through mid September. The development of dust storms depends on many causal factors encompassing meteorological and land surface conditions. Favored conditions include strong wind, turbulent air currents, small soil particles and loose topsoil texture (Gillette, 1999; Xia *et al,* 1996; Xiao and Chang, 2008).

Dust events are most common in the Chihuahuan Desert lowland areas during the dry season (roughly November through May), during which dust can be raised and/or transported throughout the region primarily by synoptic-scale weather systems (non-convective dust events) (Lee *et al*., 2009; Rivera Rivera *et al*., 2009). These events usually start with the formation of a cold front and its associated surface low pressure center over the Pacific Ocean west of the. Pacific Northwest of the USA. The front moves southeastward and sweeps through the southwestern USA and northern Mexico, with a strong pressure gradient associated with a developing cyclone crossing north of the Chihuahuan Desert (Warner, 2004), creating high wind speeds that cause widespread wind erosion (Alfaro *et al*., 1997; Doggett *et al.*, 2002; Rivera Rivera *et al*., 2009, 2010; Yin *et al*., 2007).

During the summer monsoon, thunderstorms entrain and transport dust (convective dust events) (Idso *et al*., 1972) over more localized areas than synoptic-scale dust events do (Table I). Convective dust events are less frequent in the El Paso area than synoptic events. They can originate from thunderstorm outflow boundaries (haboobs), dry or wet microbursts, or some combination (Novlan *et al.,* 2007). The idealized synoptic patterns of the North American

monsoon (Adams and Comrie, 1997) which drive convectively-spawned dust events in Arizona (Brazel and Nickling, 1986) can also help to explain the formation of convective dust events in the Chihuahuan Desert. Individual thunderstorm cells and merged Mesoscale Convective Systems (MCS's) typically form initially over the higher terrain, and move out of the mountains towards the desert lowlands via discrete propagation; haboobs are created when gust fronts from mature thunderstorms advance across erodible desert soils. Table I shows the factors that affect both non-convective and convective events.

Table I: Factors that affect convective and non-convective dust events in El Paso, Texas.

Factors	**Synoptic-Scale Dust Events**	**Convective Dust Events**
Speed of onset	• Recognizable weather patterns predictable 24 to 36 hours in advance • Specific plume locations not precisely identifiable in advance	• Recognizable weather patterns predictable 24 to 36 hours in advance • Individual thunderstorms predictable over an area 0 to 3 hours in advance • Specific locations identifiable minutes in advance
Spatial Coverage	Multiple plumes of dust spreading downwind from 'hotspot' point sources and sometimes coalescing, individual plumes covering an area of ~500-5000 km²	Individual thunderstorm cells or complexes, on the order of 1 km² (microburst)-1500 km² (mesoscale convective system)
Duration	Ranges from 3 to 4 hours up to 2 to 3 days, usually with nocturnal lulls	• Microbursts – range from minutes to possibly an hour • Haboobs – 1 to 3 hours • Organized convective systems 2 to 4 hours
Timing	• Occur mainly during the late winter and early spring when pressure gradients are extreme, soils are dry and vegetation cover at minimum	Occur mainly in association with late afternoon or evening thunderstorms, generally during the summer North American Monsoon, but can occur at any

	• Conditions worsen during late morning and are most intense during late afternoon	time if convective storms with sufficiently dry antecedent conditions

The analysis of a large number of back trajectories of air masses arriving at a receptor site is a valuable tool for investigating the sources and origins of particulate matter arriving at the site, allowing the identification of geographical areas associated with extreme values of particulate matter or its components, and identifying the source regions and air flow regimes associated with regional pollution transport (Salvador *et al*., 2010). In this work, we investigate and statistically analyze air transport pathways into El Paso during days with convective and non-convective dust events, as well as days in which dust was not reported, in order to aid forecasting of dust storms (Makra *et al.*, 2010; Wong *et al.*, 2012).

3.1.2 Data and Methology

3.1.2.1 Dust events data extraction

Daily weather records for El Paso, TX from the NWSO were examined for the period 2001 though 2005 to determine the days in which blowing dust was present in at least one hourly observation at ELP. During that period of time dust events were observed at ELP on 219 days. Fifty five percent of the events were synoptically driven while forty five percent were convectively-driven. Figure 3.1 shows the monthly distribution of these events, illustrating the different seasonality of convectively-driven and synoptically-driven dust. This graphic demonstrates the two distinct monsoonal flow regimes in El Paso separated by four months; namely, the dry monsoon with southwest prevailing winds and the wet monsoon of summer with southeast prevailing winds. The wet monsoon can produce a nearly identical dust distribution to

the dry season, again demonstrating the complexity of dust producing mechanism in the Chihuahuan Desert.

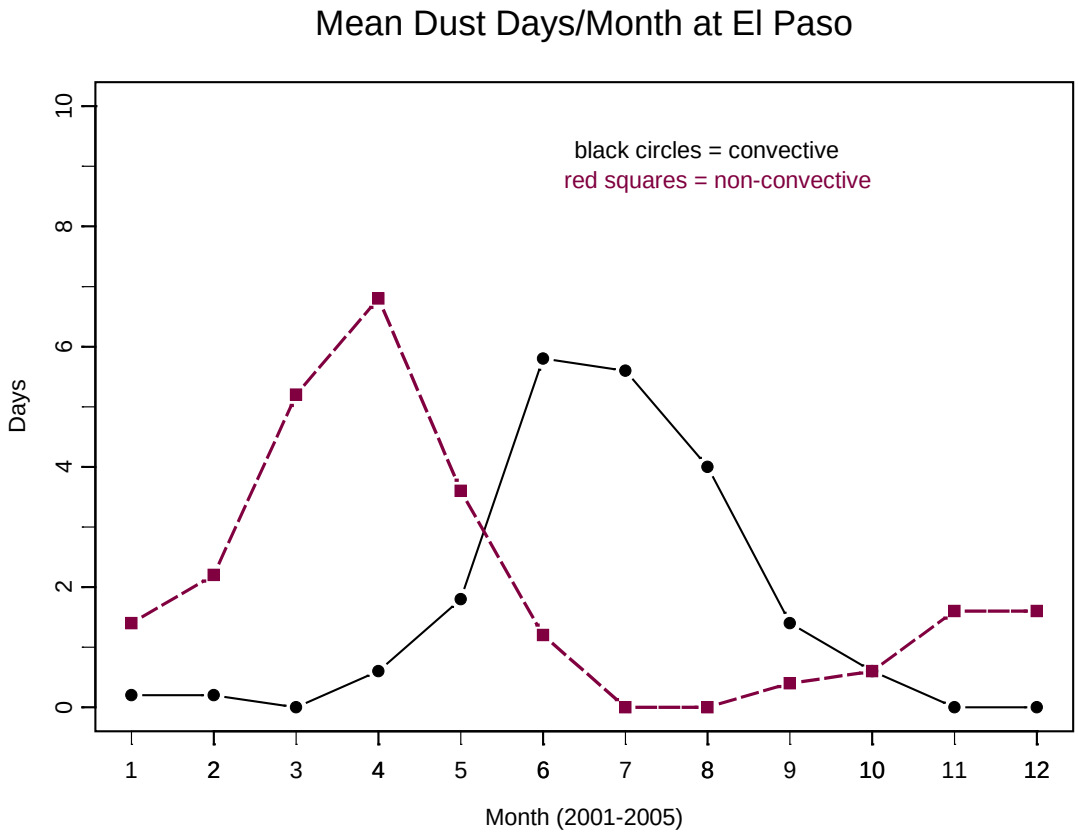

Figure 3.1: Monthly frequency of dust days at El Paso during 2001- 2005, convective and non-convective.

3.1.2.2 Back Trajectories

The NOAA Air Resources Laboratory's HYbrid Single-Particle Lagrangian Integrated Trajectory (HYSPLIT) model is a complete system for computing both simple air parcel trajectories and complex dispersion and deposition simulations (Draxler and Rolph, 2003). As stated in the model summary guide (http://www.arl.noaa.gov/documents/Summaries/HYSPLIT_FINAL.pdf), the model calculation

method is a hybrid between the Lagrangian approach, which uses a moving frame of reference as the air parcels move from their initial location, and the Eulerian approach, which uses a fixed three-dimensional grid as a frame of reference. In HYSPLIT, advection and diffusion calculations are made in a Lagrangian framework following the transport of the air parcel, while pollutant concentrations are calculated on a fixed grid. HYSPLIT supports a wide range of simulations related to the atmospheric transport and dispersion of pollutants and hazardous materials including dust, as well as the deposition of these materials to the Earth's surface (Draxler and Hess, 2004; Draxler *et al*., 2001).

The data used to create the back trajectories were gridded meteorological data from either analyses or short-term forecasts from routine numerical weather prediction models from NOAA Air Resources Laboratory. Each trajectory was started from the receptor site (El Paso TX, 31.86° N, -106.44° W). Start heights of 100m, 200m, and 500m above ground level at the receptor site were combined, and hourly air parcel positions, referred to as endpoints, were calculated back in time for 24 hours. The source areas of visibility-degrading dust advecting into El Paso (Gill *et al.*, 2008; Rivera Rivera *et al*., 2010; Baddock *et a.*, 2011) lie well within these trajectories.

Back trajectories were created with the HYSPLIT model for each day in the 2001-2005 period; they were grouped on days with dust events, convective dust events and no dust events occurred. Back trajectories' contour plots for all days with at least one dust event observation were compared to those days in which dust was never observed. To investigate the presence of large scale transport patterns into El Paso associated with dust event days and days

without dust, residence time, probability and source contribution function analyses of the trajectories were performed (see figures 8-16). For a detailed explanation of how this was computed, see Rivera Rivera *et. al* 2009.

3.1.2.3 Statistical Analysis

To investigate large- scale air transport patterns into El Paso associated with dust event days (synoptically-forced and/or convective) and days without dust, we performed residence time, probability, and source contribution function analyses of the trajectories. The residence time probability (*Pi,j*) is defined as the number of back trajectory endpoints in a given grid cell (in this case, 0.25 deg latitude by 0.25 deg longitude) over a specified time interval:

$$P_{i,j} = \frac{1}{N} \sum_{t=1}^{T} n_{i,j,t}$$

where $n_{i,j,t}$ is the number of endpoints falling in a grid cell at longitude *i* and latitude *j* before the trajectory arrived at the receptor during measurement period *t*, *T* is the total number of time periods, and *N* is the total number of endpoints throughout the domain for all time periods (Ashbaugh *et al*., 1985; Rivera Rivera *et al*., 2009). Residence times can also be generated for groups of days meeting selected criteria, in this case, days with or without dust events. These are referred to as high concentration and low concentration residence times respectively, while those generated for all days are the overall residence times. Differential and conditional residence time probabilities (Poirot *et al.,* 2001; Schichtel *et al.,* 2006) were also computed. Differential probability is the difference between two residence times, in this case being overall residence time probability subtracted from a high concentration (dust event) residence time probability. Similarly, conditional probability is the ratio of two residence times- in this case, the ratio of high concentration (dust event) residence time to overall residence time. With regards to the

areas through which air moves during dust events, the higher the differential probability, the greater the probability of dust at the receptor as compared to a day with typical transport. Conditional probability is the probability that an air mass would arrive during a dust day if the air mass traveled through the area and eventually arrived at the receptor. Conditional probability does not reveal the frequency of transport, only the probability of the condition (dust) for days when there was transport from a given area. Residence time and differential probability are higher when the transport from the area is both more frequent and meets dust criteria.

A dimensionless source contribution function (Si,j) was computed by normalizing Pi,j by a hypothetical probability function of air parcels arriving at the receptor site from all directions equally (Ashbaugh *et al*., 1985). The source contribution function is proportional to residence time multiplied by the distance, and serves to remove the otherwise-unavoidable probability peak at the receptor site. A source contribution function with a value greater than one corresponds to a transport pattern that is more likely than if air masses arrived from all directions with equal probability, and may be considered statistically significant.

Probabilities and source contribution functions were determined for all days, all days with dust, all days with convective dust events, and all days with no dust observed. Positive probability values show those areas from which air masses were proportionally more likely to arrive during a given condition (dust, no dust, convectively-driven dust). Contour plots of the source contribution function and probabilities during days with different types of dust events, compared to those for all days and/or non-dusty days, illustrate airflow patterns associated with dust being observed at El Paso. Higher residence time, source contribution function and

probability values over certain regions in the contour plots correspond to a higher likelihood of air parcels arriving from those regions during a certain class of events.

3.1.3 Results

Contour plots of the HYSPLIT trajectory endpoints and residence time, source contribution function, incremental probability, and conditional probability showed different airflow patterns during all dusty days and with convectively-raised dust, as compared to overall and dust-free day trajectories into El Paso during 2001- 2005.

3.1.3.1 Overall Data for El Paso, 2001- 2005

The pattern of air mass trajectories arriving in El Paso on all days over the five-year period was shown to be more or less relatively symmetrically distributed around the receptor site, with maxima to the west and east of the city (Figures 3.2 and 3.3).

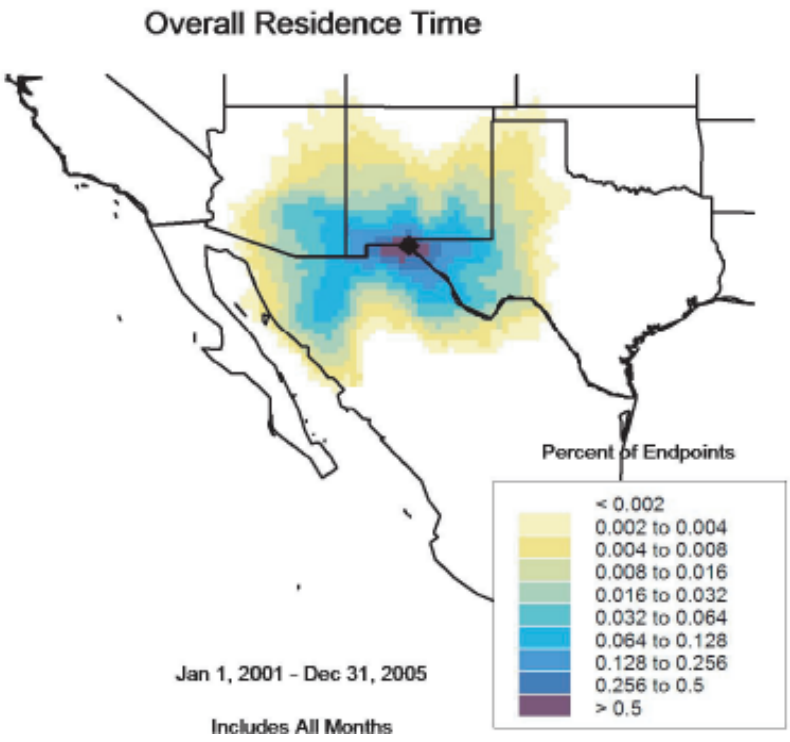

Figure 3.2: Contour plot of overall residence times for 2001- 2005.

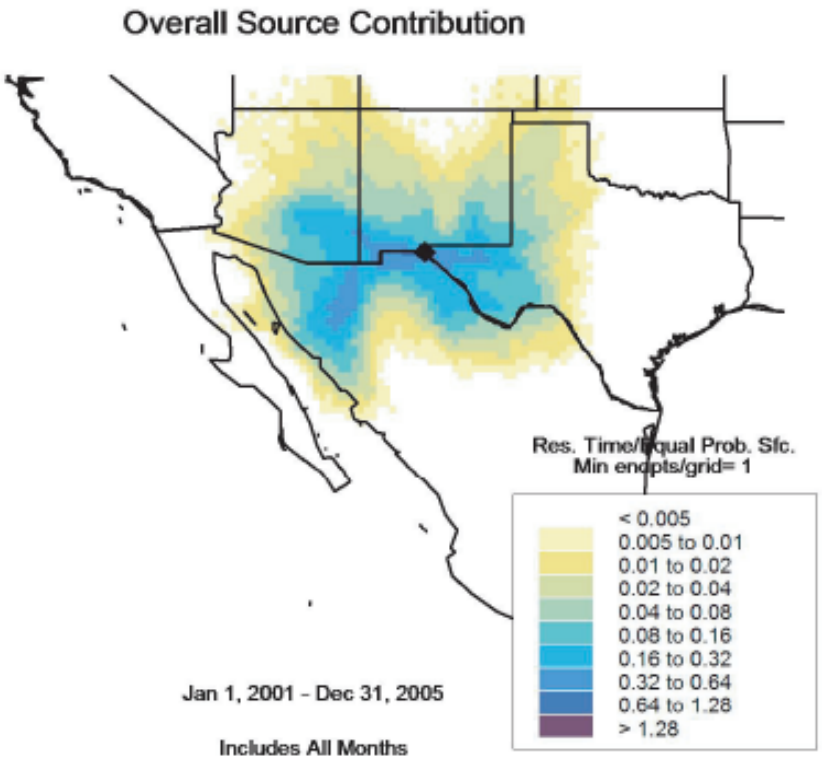

Figure 3.3: Contour plot of overall source contributions for 2001- 2005.

Overall residence times were skewed to the southwest (210° to 280°; primarily synoptic events) and skewed to the southeast (100° to 170°; primarily convective events) during high concentration (dust observed) days (Figure 3.4) but not during low concentration (no dust observed) days (Figure 3.5).

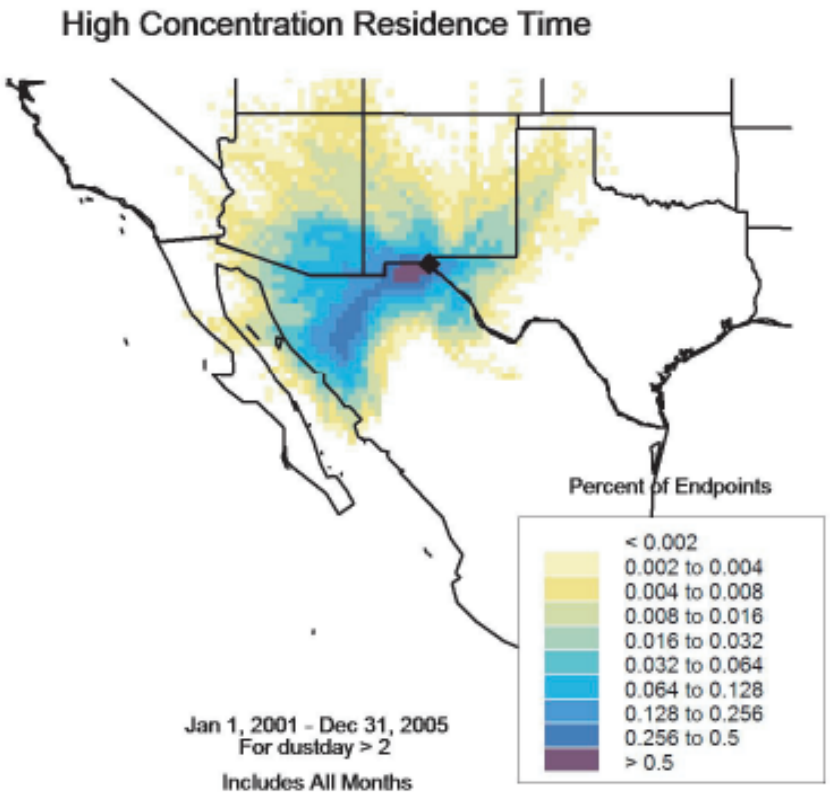

Figure 3.4: Contour plot of residence times for all days during which dust was observed for 2001- 2005.

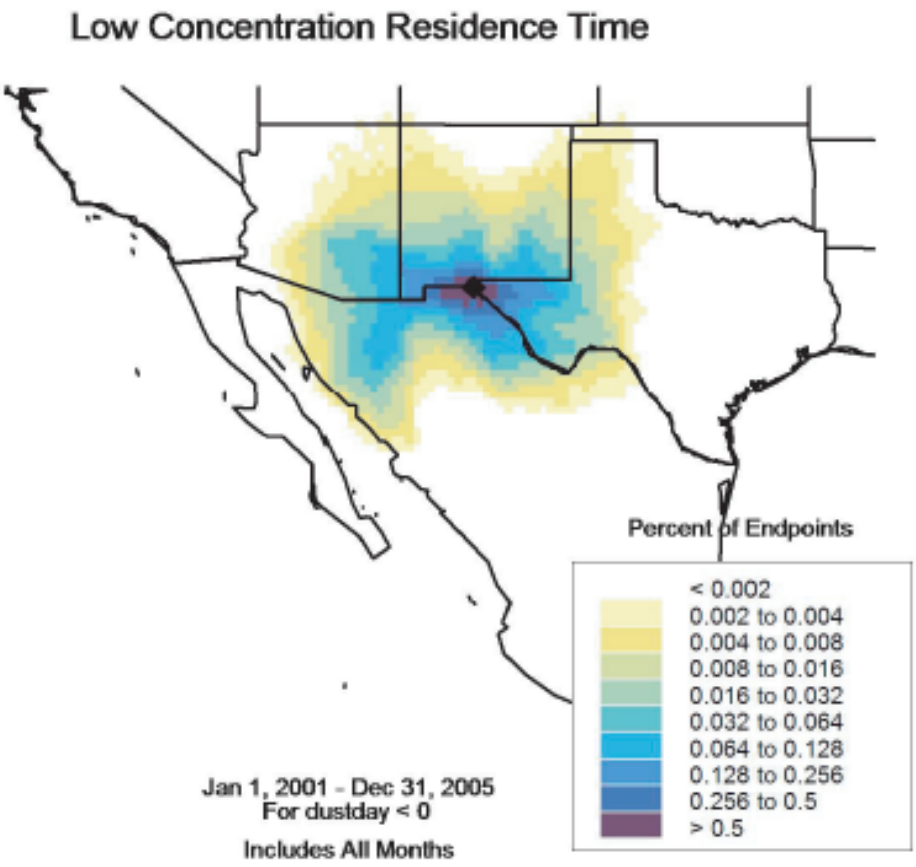

Figure 3.5: Contour plot of residence times for all days during which dust was not observed for 2001- 2005.

Source contributions for high concentration days (Figure 3.6) were skewed to the west and southwest of El Paso. An area with source contribution function >1 (significant) can be seen in northwest Chihuahua, Mexico east of the Sierra Madre Occidental mountain range. This is an area of dry lakes (playas), braided desert streams, and anthropogenically-disturbed agricultural soils which has been identified as a "hotspot" of wind erosion in the Chihuahuan Desert (Baddock et al., 2011; Bullard et al., 2011; Dominguez, 2009; Gill *et al*., 2008; Lee *et al*., 2009; Prospero *et al.*, 2002; Rivera Rivera *et al*., 2010) and during the period of study was also experiencing the most severe drought conditions in Mexico in the early 21st century (Seager and

Heim, 2009). Dust from these "hotspots" is advected up to several hundred kilometers into the Paso del Norte, and occasionally far beyond (Doggett *et al*., 2002; Lee *et al*., 2009; Park *et al*., 2007). A slight secondary swath can be seen extending to the northeast into the Texas Panhandle: this trajectory is associated with so-called "backdoor" cold fronts which regularly advect into El Paso and occasionally bring dust generated in the North American Great Plains during the winter and spring (Wigner and Peterson, 1987). Source contributions for low concentration days (not shown) were similar to overall source contributions (Figure 3.3).

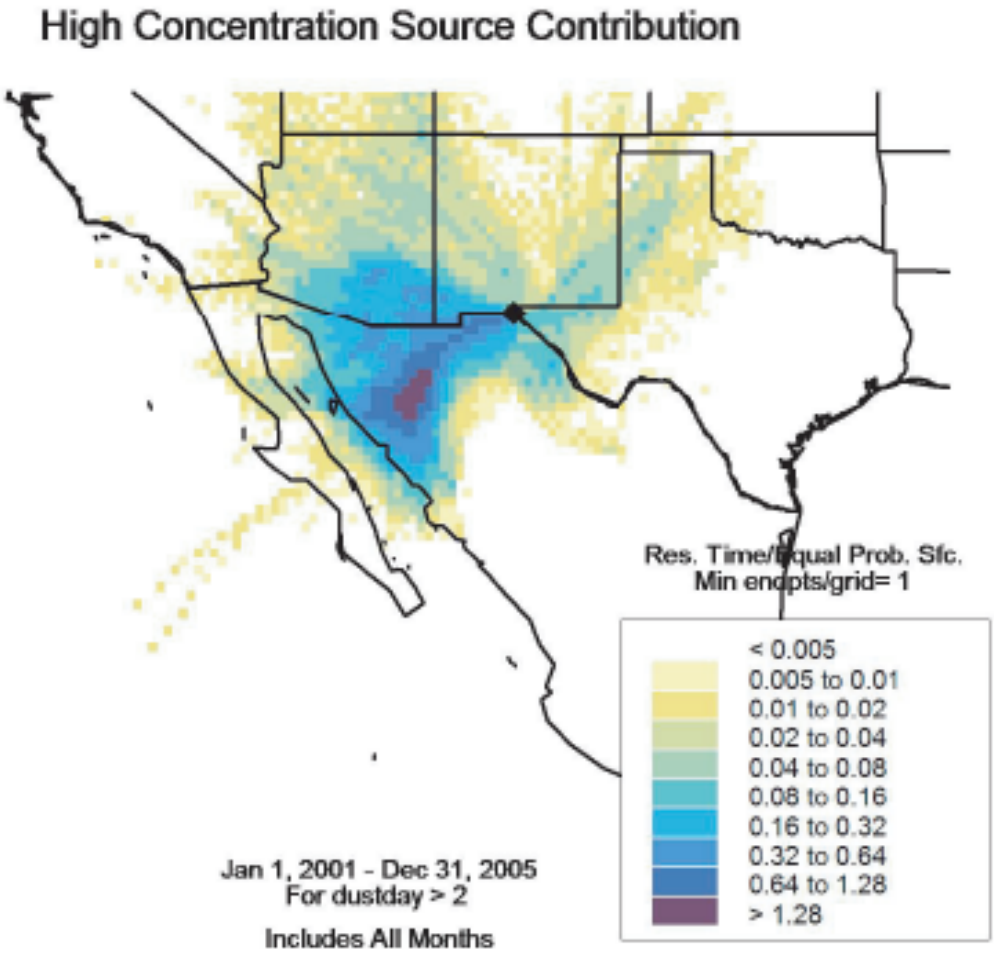

Figure 3.6: Contour plot of source contributions for all days during which dust was observed for 2001- 2005.

Differential probability contour plots are shown in Figures 3.7 and 3.8. The differential probability for high-concentration days (Figure 3.7) was again strongly positively correlated with the known dust source region southwest of El Paso: note the negative correlation with all the other immediately surrounding areas. The differential probability for low-concentration days (Figure 3.8) also was most anti-correlated with trajectories arriving from the southwest.

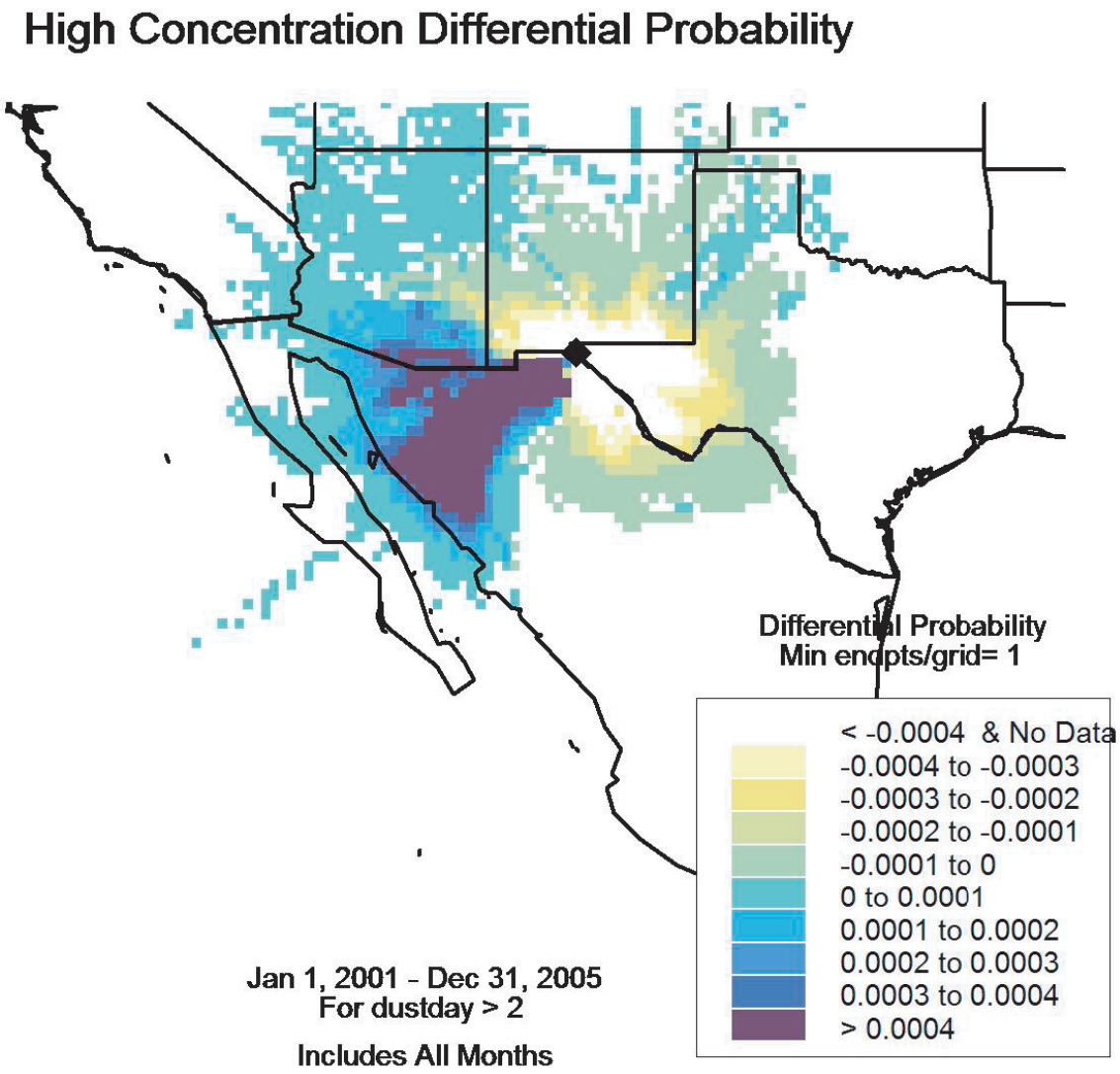

Figure 3.7: Contour plot of differential probability for all days during which dust was observed for 2001- 2005.

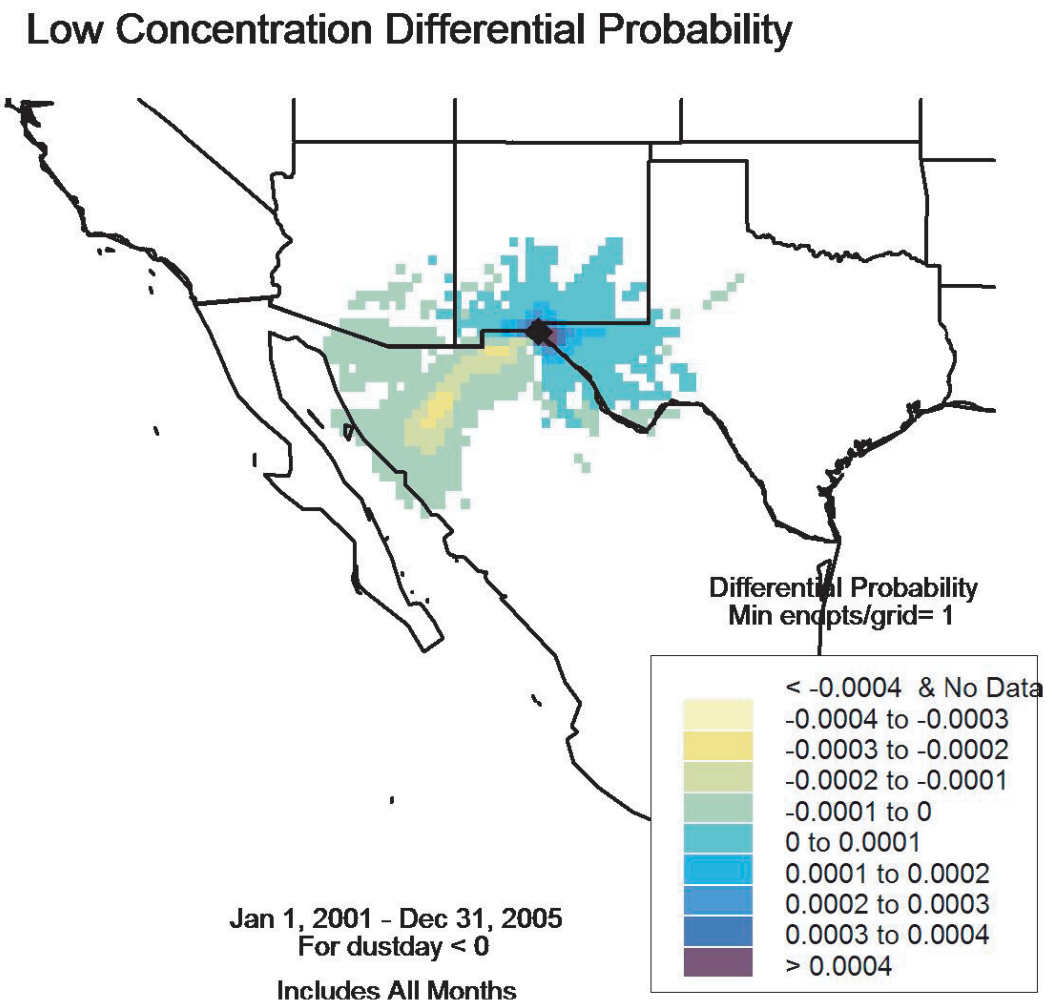

Figure3.8: Contour plot of differential probability for all dust-free days in 2001- 2005.

The trajectories for high concentration events (Figures 3.6 and 3.7) come from the Pacific Ocean across Baja California, consistent with deep troughs bearing high-momentum air entering the Chihuahuan Desert from the southwest. Some of these trajectories moved more than 600 km into El Paso from the southwest over a 24-hour period. These fastest-moving (farthest-distance) trajectories bringing dust to El Paso would be consistent with air parcels moving toward cyclones crossing and/or developing northeast of the region. The most intense synoptic-scale dust events

in El Paso are associated with lee cyclones deepening over New Mexico and the Texas Panhandle (Doggett *et al.*, 2002; Rivera Rivera *et al.*, 2009; Lee *et al.*, 2009).

3.1.3.2 Convectively-Driven Dust Events

Differential and conditional probabilities for days in which convectively-driven dust events were observed are shown in Figures 3.9 and 3.10.

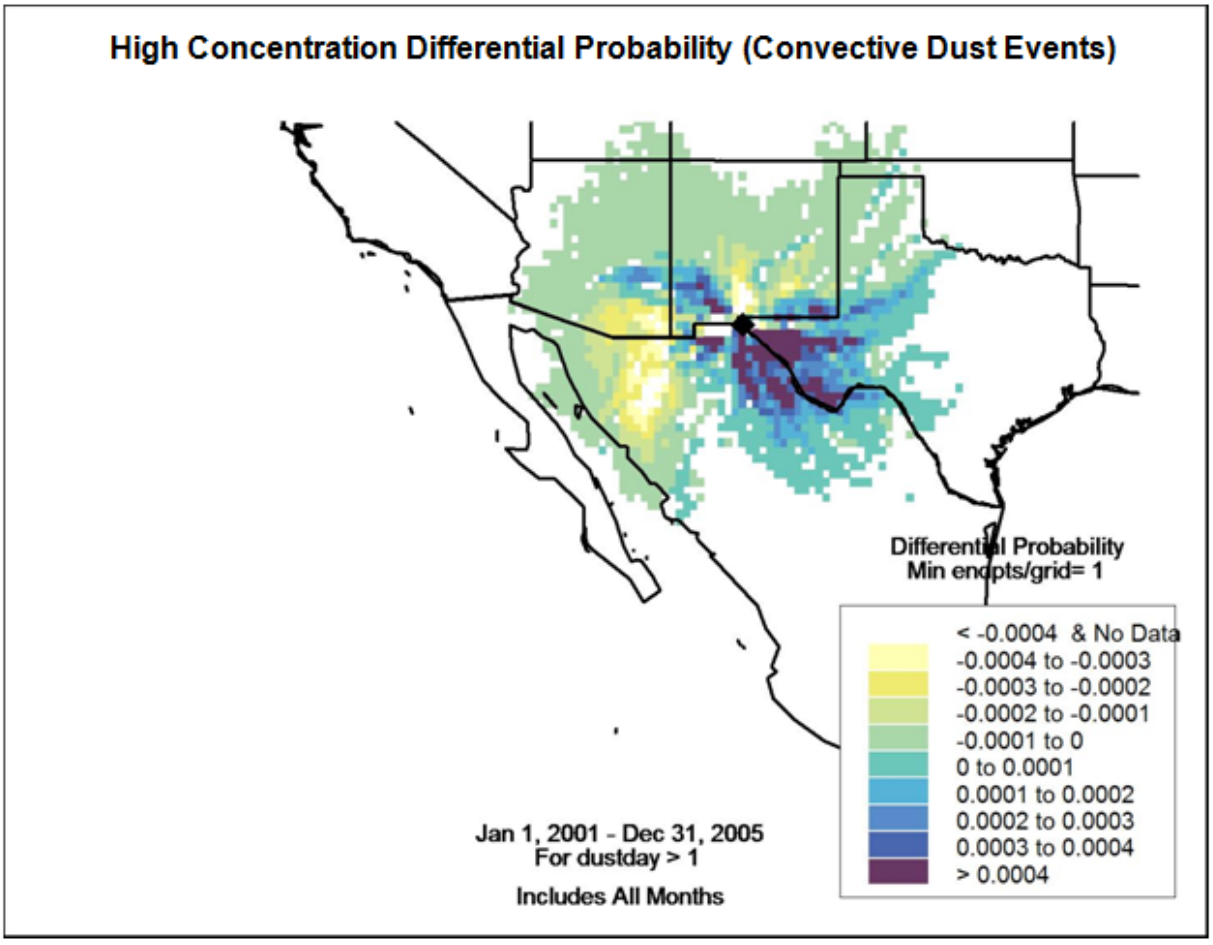

Figure 3.9: Contour plot of differential probability for all days during which convectively-driven dust was observed for 2001- 2005.

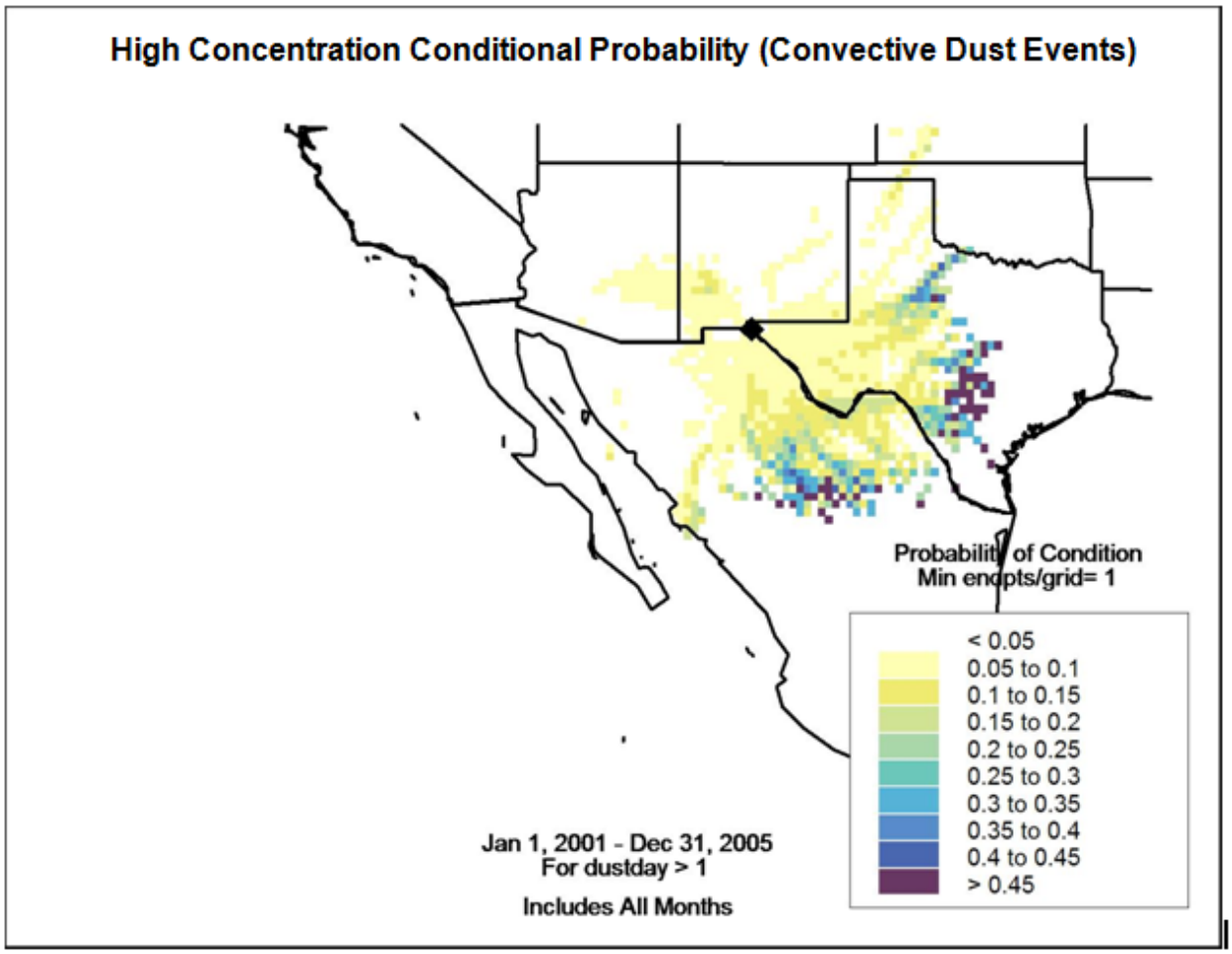

Figure 3.10: Contour plot of conditional probability for all days during which convectively-driven dust was observed for 2001- 2005.

Note that convectively-driven dust events (occurring primarily during the wet, summertime North American Monsoon) are most associated with airflow from the southeast- from the Gulf of Mexico and up the Rio Grande Valley- as opposed to air flow from the southwest across northwestern Mexico (note the area of negative differential probability in Figure 3.9). Conditional probabilities for convective dust days (Figure 3.10) are most positively associated with 24-hour trajectory endpoints >600 km south and east of El Paso. These fastest-

moving (farthest-distance) trajectories bringing convectively-driven dust to El Paso would be consistent with maritime tropical air mass surges from the direction of the Gulf of Mexico.

Heavy summer convective precipitation in the Chihuahuan Desert is often associated with moisture surges advecting from the Gulf of California region (Stensrud *et al*., 1997) south and southwest of El Paso. However, thunderstorms associated with Gulf of California moisture surges are less likely to generate dusty outflows than thunderstorms associated with air masses arriving from the southeast. Indeed, other analyses have shown an anti-correlation between particulate matter concentrations and moisture levels in El Paso (Wise and Comrie, 2005) and an explicit anti-correlation between dust concentrations in El Paso and precipitation from Gulf of California monsoon moisture surges during 1998- 2006 (Lozano *et al.*, 2007).

3.1.4 Summary

Although 24-hour air mass back trajectories into El Paso, Texas during 2001- 2005 were overall relatively symmetrically distributed around the city, for days in which dust was observed during this drought period (about 12% of all days) the trajectories were most associated with southwesterly flow from an area of known dust sources in the Chihuahuan Desert. An area with source contribution function >1 (more likely than random upwind location for air residence) during dust days existed in northwest Chihuahua, Mexico near the eastern slope of the Sierra Madre Occidental.

Convectively-driven dust events, most frequent in El Paso during the summer North American Monsoon, were most prevalent with airflow from the south and east, as opposed to Gulf of California moisture surges which bring heavy precipitation and convection that is less dusty. The fastest- moving trajectories during days with dust in El Paso advected a distance of >600 km in 24-hours (7 m/sec), consistent with air parcels moving toward intensifying lee cyclones over the southwestern Great Plains or (for convectively-driven dust events) moisture surges from the Gulf of Mexico region.

This type of modeling and analysis has high utility in dust weather forecasting. When meteorological and land-surface conditions are conducive to dust storm generation, then a mean wind vector can be generated from the surface (around 880 mb at El Paso) to the forecast mixing height which usually is around 700-600 mb. If this vector is within a high source contribution area identified here, then the meteorologist can have increased confidence of a potential dust event, which would have implications for air quality, aviation, and health and safety through high particulate concentration and visibility reduction. The recognition of these characteristic air mass trajectories will aid in forecasting dust storms in the Paso del Norte metropolitan area, and similar methodologies could be followed for other dust-prone cities.

3.1.5 References

Adams, D.K., and Comrie, A.C. (1997). The North American Monsoon. Bull. Amer. Met. Soc. 78: 2197- 2213.

Alfaro, S.C., Gaudichet, A., Gomes, L., and Maille, M. (1997). Modeling the size distribution of a soil aerosol produced by sandblasting. J. Geophys. Res., 102 (D10), 11239– 11249.

Ashbaugh, L.L., Malm, W.C., and Sadeh, W.Z. (1985). A residence time probability analysis of sulfur concentrations at Grand Canyon National Park. Atmos. Environ., 19, 1263- 1270.

Brazel, A.J. and Nickling, W.G. (1986). The relationship of weather types to dust storm generation in Arizona (1965-1980). J. Climatol., 6, 255-275.

Baddock, M. C., Gill, T. E. Bullard, J. E., Dominguez-Acosta, M., Rivera Rivera, N. I. (2011). Geomorphology of the Chihuahuan Desert on potential dust emissions. Journal of Maps, 249-259.

Bullard, J.E., Harrison, S.P., Baddock, M.C., Drake, N., Gill, T.E., McTainsh, G. and Sun Y. (2011). Preferential dust sources: A geomorphological classification designed for use in global dust-cycle models. Journal of Geophysical Research. Earth Surface 116, F04034, doi:10.1029/2011JF002061

Castiglia, P. J., and Fawcett, P. J. (2006). Large Holocene lakes and climate change in the Chihuahuan desert. Geology, 34, 113- 116.

Doggett, A.L., Gill, T.E., Peterson, R.E., Bory, A.J.M., and Biscaye, P.E. (2002). Meteorological characteristics of a severe wind and dust emissions event: southwestern USA, 6-7 April 2001. Preprints, 21st Conference on Severe Local Storms, August 2002, San Antonio, TX, published by American Meteorological Society, Boston, pp. 78-80.

Dominguez, M.A. (2009). The Pluvial Lake Palomas- Samalayuca Dunes system. Ph.D. dissertation (Geology), University of Texas at El Paso.

Draxler, R.R., and Rolph, G.D. (2003). HYSPLIT (HYbrid Single-Particle Lagrangian Integrated Trajectory). Model accessed via NOAA ARL READY Website (http://www.arl.noaa.gov/ready/hysplit4.html). NOAA Air Resources Laboratory, Silver Spring, MD.

Draxler, R.R., and Hess, G.D. (2004). Description of the HYSPLIT_4 modeling system. NOAA Tech. Memo. ERL ARL-224, 1- 28.

Draxler, R.R., Gillette, D.A., Kirkpatrick, J.S., and Heller, J. (2001). Estimating PM10 air concentrations from dust storms in Iraq, Kuwait and Saudi Arabia. Atmos. Environ., 35, 4315-4330.

Gill, T.E., Dominguez Acosta, M., and Rivera Rivera, N.I. (2008). The Lake Palomas basin: dust engine of the Chihuahuan Desert. Geol. Soc. Amer. Abst. Prog., 40(6), 78.

Gillette, D.A. (1999). A qualitative geophysical explanation for “Hot Spot” dust emitting source regions. Cont. Atmos. Phys., 72, 67 - 77.

Idso, S., Ingram, R.S., and Pritchard, J.M. (1972). An American haboob. Bull. Amer. Meteor. Soc., 53, 930–935.

Lee, J.A., and Tchakerian, V.P. (1995). Magnitude and frequency of blowing dust on the Southern High Plains of the United States, 1947-1989. Ann. Assoc. Am. Geogr., 85, 684– 693.

Lee, J.A., Gill, T.E., Mulligan, K.R., Dominguez Acosta, M., and Perez, A.E. (2009). Land use/land cover and point sources of the 15 December 2003 dust storm in southwestern North America. Geomorphology, 105, 18- 27.

Lozano, A.Y., Negrete, J., Fitzgerald, R.M., Apodaca, K., and Morris, V.R. (2007). Correlation between precipitation, dust storms and Gulf of California moisture surges in the Paso del Norte region during the North American Monsoon. Abstracts, 21st Conference on Hydrology, American Meteorological Society, P2.11.

MacMahon, J.A., and Wagner, F.H. (1985). The Mojave, Sonoran and Chihuahuan Deserts of North America. In: Evenari, M., Noy-Meir, I., and Goodall, D.W. (Eds.), Hot Deserts and Arid Shrublands. Ecosystems of the World Series, Elsevier, 12A: 105- 202.

Makra, L., Sánta, T., Matyasovszky, I., Damialis, A., Karatzas, K., Bergmann, K-C. and Vokou, D. (2010). Airborne pollen in three European cities: Detection of atmospheric circulation pathways by applying three-dimensional clustering of backward trajectories. Journal of Geophysical Research, 111, D24220, doi:10.1029/2010JD014743.

Novlan, D. J., Hardiman, M., and Gill, T. E. (2007). A synoptic climatology of blowing dust events in El Paso, Texas from 1932-2005. Preprints, 16th Conference on Applied Climatology, American Meteorological Society, J3.12, 13 pp.

Park, S. H., Gong, S.L., Zhao, T.L., Vet, R.J., Bouchet, V.S., Gong, W., Makar, P.A., Moran, M.D., Stroud, C., Zhang, J. (2007). Simulation of entrainment and transport of dust particles within North America in April 2001 ("Red Dust Episode"). J. Geophys. Res., 112, D20209, doi:10.1029/2007JD008443.

Peng, Yanlei, Staniswalis, J.G., Grineski, S.E., and Gill, T.E. (2010). A retrospective analysis of the association of dust storms and respiratory hospitalizations in El Paso, Texas, using a case-crossover study design. Abstracts, 1st Environment and Health Symposium, American Meteorological Society, J20.7.

Poirot, R.L., Wishinski, P.R., Hopke, P.K., and Polissar, A.V. (2001). Comparative application of multiple receptor methods to identify aerosol sources in northern Vermont. Env. Sci. Tech, 35, 4622- 4636.

Prospero, J.M., Ginoux, P., Torres, O., Nicholson, S.E., Gill, T.E. (2002). Environmental characterization of global sources of atmospheric soil dust identified with the Nimbus 7 Total Ozone Mapping Spectrometer (TOMS) absorbing aerosol product. Rev. Geophys., 40, 1002, doi:10.1029/ 2000RG000095.

Rivera Rivera, N.I., Gill, T.E., Gebhart, K.A., Hand, J.L., Bleiweiss, M.P., and Fitzgerald, R.M. (2009). Wind modeling of Chihuahuan Desert dust outbreaks. Atmos. Environ., 43, 347- 354.

Rivera Rivera, N.I., Gill, T.E., Bleiweiss, M.P., and Hand, J.L. (2010). Source identification of hazardous Chihuahuan Desert dust outbreaks. Atmos. Environ., 44, doi:10.1016/j.atmosenv.2010.03.019

Salvador, P., Artinaño, B., Pio, C., Alfonso, J., Legrand, M., Puxbaum, H., and Hammer, S. (2010). Evaluation of aerosol sources at European high altitude background sites with trajectory statistical methods. Atmospheric Environment, 44, doi:10.1016/j.atmosenv.2010.03.042

Schichtel, B.A., Gebhart, K.A., Barna, M.G., and Malm, W.C. (2006). Association of airmass transport patterns and particulate sulfur concentrations at Big Bend National Park, Texas. Atmospheric Environment , 40, 992- 1006.

Schmidt, R.H. (1986). Chihuahuan Climate. Proceedings, 2nd Symposium on Resources of the Chihuahuan Desert, Chihuahuan Desert Research Institute, Alpine, Texas, pp. 40- 63.

Seager, R., and Heim, R.R. (2009). Early 21st-century drought in Mexico. Eos- Trans. AGU 90 (11), 89 – 90.

Stensrud, D.J., Gall, R.L., and Nordquist, M.K. (1997). Surges over the Gulf of California during the Mexican Monsoon. Mon. Wea. Rev., 125, 417– 437.

Warner, T.T. (2004). Desert Meteorology. Cambridge University Press, Cambridge, UK, p. 112.

Wigner, K. A., and Peterson, R. E. (1987). Synoptic climatology of blowing dust on the Texas South Plains, 1947-84. J. Arid Environ., 13, 199-209.

Wise, E.K., and Comrie, A.C. (2005). Meteorologically adjusted urban air quality trends in the Southwestern United States. Atmos. Environ., 39, 2969- 2980.

Wong, M. S., Nichol, J. E. and Lee, K. H. (2012). Estimation of aerosol sources and aerosol transport pathways using AERONET clustering and backward trajectories: a case study of Hong Kong, International Journal of Remote Sensing, 34:3, 938-955

Xia, X.C., and Yang, G.S. (1996). Dust storms and its control in Northwest China. Chinese Environmental Press, Beijing, 128 pp.

Xiao J., and Chang, C. (2008). Dust storm's characters and correlation with meteorological data. 2008 International Workshop and Education Technology and Training & 2008 International Workshop on Geoscience and Remote Sensing. IEEE Computer Society, vol. 1, pp. 563- 566, doi:10.1109/ETTandGRS.2008.188 .

Yin, D., Nickovic, S., and Sprigg, W.A. (2007). The impact of using different land cover data on wind-blown desert dust modeling results in the southwestern United States. Atmospheric Environment. 41, 10, 2214-2224.

Chapter 4

4.1 Modeling analysis of El Paso dust storm meteorological data using the Weather Research and Forecast (WRF) model coupled with Chemistry (WRF-Chem)

4.1.1 Introduction

Modeling and forecasting of air quality involves meteorological factors such as wind speed, wind direction, precipitation, emission (source regions) contributions, and chemical processes, *e.g*, deposition and transformation. In the atmosphere, the chemical and physical processes are coupled; the chemistry can also affect the meteorology and vice versa (Grell *et al*., 2005). The separation of the meteorology and chemistry can cause a loss of important information about atmospheric processes that quite often have a time scale of much less than the output time of the meteorological model (Grell *et al*., 2005). In addition, the modeling of atmospheric aerosols requires appropriate representations of aerosol size distribution and microphysics in three-dimensional air quality models.

Many models have been developed to study dust storms and their effects (Xie *et al*., 2009). Some of these models include: the Community Aerosol and Radiation Model for the Atmosphere (CARMA) (Barnum *et al*., 2004), Navy Operational Global Atmospheric Prediction System (NOGAPS) (Rosmond *et al*., 2002); SKIRON, a weather model with dust forecast based on the Eta model (Nickovic *et al*., 1997); Global Forecast System (GFS) (Raman and Arellano, 2011), among others. Over the past years, several research institutes have collaborated in the

development of a new state-of-the-art meteorological model, the Weather Research and Forecasting (WRF) model (Grell 2005). All these dust models mentioned are developed by coupling dust simulation modules to weather forecasting models, and high performance computers are needed in order to run them (Xie *et al*., 2009).

4.1.2 WRF and WRF-Chem model description

The Weather Research and Forecasting (WRF) Model (WRF, 2009) is a next-generation mesoscale numerical weather prediction system designed to serve both operational forecasting and atmospheric research needs. It features multiple dynamical cores, a 3-dimensional variational (3DVAR) data assimilation system, and a software architecture allowing for computational parallelism and system extensibility. WRF is suitable for a broad spectrum of applications across scales ranging from meters to thousands of kilometers (WRF, 2009). WRF allows researchers the ability to conduct simulations reflecting either real data or idealized configurations. WRF provides operational forecasting a model that is flexible and efficient computationally while offering the advances in physics, numerics, and data assimilation contributed by the research community (WRF, 2009).

The principal components of the WRF system are shown in Figure 4.1. The WRF Software Framework (WSF) provides the infrastructure that accommodates the dynamics solvers and chemical packages that interface with the solvers, to obtain the air quality model, WRF-Chem. There are two dynamics solvers in the WSR: the Advanced Research WRF (ARW) solver (originally referred to as the Eulerian mass or “em” solver) developed primarily at the

National Center for Atmospheric Research (NCAR), and the NMM (Nonhydrostatic Mesoscale Model) solver developed at the National Center for Environmental Prediction (NCEP). Community support for the former is provided by the MMM Division of NCAR and that for the latter is provided by the Developmental Testbed Center (DTC).

WRF-Chem is an air quality model that uses WRF as a meteorological driver and which also simultaneously simulates the emission, turbulent mixing, transport, transformation, and fate of trace gases and aerosols (PNNL, 2009). Some of the objectives of this model are to:

- Integrate WRF-Chem simulations and a wide range of field campaign measurements to develop a better understanding of local and regional-scale evolution of particulates and aerosol radiative forcing that are sub-grid scale processes for global climate models.
- Employ the modeling framework of WRF-Chem to develop new treatments of aerosol processes for global climate models.
- Perform process studies investigating aerosol aging, aerosol-cloud interactions, and aerosol radiative forcing.
- Explore the feasibility of using a version of WRF-Chem as a regional climate model.

Version 3.0 of WRF-Chem was released on 4 April 2008. Its Chemistry Package consists of the following components (WRF/Chem version 3.1, 2009):

- Dry deposition, coupled with the soil/vegetation scheme.
- Aqueous phase chemistry coupled to some of the microphysics and aerosol schemes.
- Four choices for biogenic emissions:

- No biogenic emissions.
- Online calculation of biogenic emissions (as in Simpson *et al*., 1995 and Guenther *et al*., 1994) which includes emissions of isoprene, monoterpenes, and nitrogen emissions by soil.
- Online modification of user specified biogenic emissions - such as the EPA Biogenic Emissions Inventory System (BEIS) version 3.13. The user must provide the emissions data for their own domain in the proper WRF data file format.
- Online calculation of biogenic emissions using the MEGAN v2.04 biogenic emissions routine.

- Two choices for anthropogenic emissions:
  - No anthropogenic emissions.
  - User specified anthropogenic emissions - such as those available from the EPA NEI-99 data inventory. The user must provide the emissions data for their own domain in the proper WRF data file format.

- Two choices for gas-phase chemical reaction calculations.
  - The RADM2 chemical mechanism.
  - The CBM-Z mechanism.

- Several choices for gas-phase chemical reaction calculations through the use of the Kinetic Pre-Processor, or KPP.
- Three choices for Photolysis schemes:

- Madronich scheme coupled with hydrometeors, aerosols and convective parameterizations.
- Fast-J Photolysis scheme coupled with hydrometeors, aerosols and convective parameterizations.
- FTUV scheme coupled with hydrometeors, aerosols and convective parameterizations.

- Three choices for aerosol schemes:
  - The Modal Aerosol Dynamics Model for Europe - MADE/SORGAM.
  - The Model for Simulating Aerosol Interactions and Chemistry (MOSAIC - 4 or 8 bins) sectional model aerosol parameterization.
  - The GOCART aerosol model (experimental) aerosol parameterization.

The Georgia Tech/Goddard Global Ozone Chemistry Aerosol Radiation and Transport (GOCART) model (Ginoux *et al*., 2001) simulates the global distribution of aerosols. The GOCART model is driven by the assimilated meteorological fields from the Goddard Earth Observing System Data Assimilation System (GEOS DAS) which facilitates direct comparison with observations. The model includes seven size classes of mineral dust ranging from 0.1-6 /µm radius. The model has been evaluated by comparing simulation results with ground-based measurements and satellite data. The evaluation has been performed by comparing surface concentrations, vertical distributions, deposition rates, optical thickness, and size distributions. The comparisons show that the model results generally agree with the observations (Ginoux *et al*., 2001).

- There is a tracer transport option in which the chemical mechanism, deposition, etc. has been turned off. The user must provide the emissions data for their own domain in the proper WRF data file format for this option.

In WRF version 3.0 chemistry, the MOSAIC aerosol scheme is coupled to the NASA Goddard atmospheric radiation scheme.

Possible applications of the current modeling system include:

- Prediction and simulation of weather using WRF, or regional or local climate.
- Coupled weather prediction/dispersion model to simulate release and transport of constituents.
- Coupled weather/dispersion/air quality model with full interaction of chemical species with prediction of O_3 and UV radiation, as well as PM.

For a more detailed explanation of the WRF-Chem see Grell *et al*., 2005.

4.1.3 Modeling Research – Case study

In this part of the research, the WRF-Chem model was run for a case study that was selected from a database of dust events in El Paso, Texas maintained by the El Paso, Texas National Weather Service Forecast Office. The selected case study was a dust event that occurred on February 4, 2008. Very strong gusty winds across much of northern Mexico, eastern New Mexico and Northwest Texas generated widespread dense blowing dust in the afternoon on that day. Gusty winds of about 59 miles per hour were reported at Fort Bliss in El Paso (Texas Commission on Environmental Quality (TCEQ) website). The PM 2.5 and PM 10 measures on that day were catalogued as Moderate based on the U.S. Environmental Protection Agency (EPA)'s Air Quality Index (AQI). The highest measured daily average PM10 concentration in El Paso County was 107 micrograms per cubic meter ($\mu g/m^3$) at the UTEP Continuous Ambient Monitoring Station (CAMS) 12. The average PM 10 for the hours of the event at CAMS 12 was 448 $\mu g/m^3$. The highest measured PM10 hourly average was 791 $\mu g/m^3$ at Socorro CAMS 49 for the hour from 5:00 p.m. to 6:00 p.m. Mountain Standard Time (MST). The visibility measured at Chamizal CAMS 41 dropped as low as 1.4 miles at 4:35 p.m. MST. The visibility measured at Guadalupe Mountains CAMS 5018 dropped as low as 3.8 miles at 8:40 p.m. Central Standard Time CST, indicating that the blowing dust reached as far east as the Guadalupe Mountains (TCEQ webpage). This case study was the only one selected because of the computer power and running time required the WRF-Chem model. Figure 4.2 is a satellite image that shows the dust event on February 4, 2008.

The WRF-Chem model was run for the day of February 4, 2008 from a 4km radius from the latitude 31.86° N Longitude 106.44° W more or less at a surface height of 2 meters. The data obtained as result of the model run was: Planetary Boundary Layer Height (PBLH), Temperature in degrees Kelvin at 2 meters above the ground (T2(K)), Relative Humidity at 2 meter above the ground (RH(2)), Horizontal wind speed (meter per second) at the respective pressure levels (3D Winds), Pressure at our elevation reduced to sea level pressure (SLP) and surface wind speed (meters per second) (Wdspd) (see Tables I-VI). All the data outputs times were Coordinated Universal Time (UTC) which was then changed to local time. PBLH, also known as Atmospheric Boundary Layer (ABL) is the lowest part of the troposphere and its behavior is directly influenced by its contact with a planetary surface. The PBL is thermally induced during the day, influenced by the presence of the Earth's surface, responding to forces and processes such as frictional drag, solar heating, and evapotranspiration. Each of these forces generates turbulence of various-sized eddies, which can be as deep as the boundary layer itself, lying on top of each other. The ABL depth is variable in time and space, ranging from tens of meters in strongly statistically stable situations, to several kilometers in convective conditions over deserts (Stull, 1988). Figures 4.3-4.4 show a schematic example of the PBLH and its interaction with the Earth surface forces and processes.

The data results from the WRF-Chem model run were plotted and different graphs were created using the Excel program (see Figures 4.5-4.10). Data obtained from the TCEQ for wind speed, relative humidity, temperature and Particulate matter data from most of TCEQ's Continuous Air Monitoring Stations (CAMS) located at El Paso, TX were obtained to compare them with the WRF-Chem model results (see Figures 4.11-4.15).

The TCEQ's Continuous Ambient Monitoring Stations (CAMS) document air and water parameters via instruments measuring as explained in Chapter 2. This data is accessed online at http://www.tceq.state.tx.us/compliance/monitoring/air/monops/hourly_data.html. A search was done for specific data such as relative humidity, wind speed, temperature and Particulate Matter collected on Februrary 4, 2008. Data were obtained from these CAMS stations:

- **CAMS 12**, located at 250 Rim Rd. El Paso, TX (UTEP station) near The University of Texas at El Paso (UTEP) at latitude 31° 46' 05" North and longitude 106° 30' 04" West.
- **CAMS 40**, located at 700 San Francisco Ave. El Paso, TX (Sun Metro station) at latitude 31° 45' 30.00" North and longitude 106° 30' 3.00" West;
- **CAMS 41**, located at 800 S. San Marcial Street, El Paso, TX (Chamizal station) at latitude 31° 45' 56.00" North and longitude 106° 27' 18.00" West;
- **CAMS 49** located at 201 South Nevarez Rd. El Paso, TX (Socorro station) at latitude 31° 39' 43.00" North and longitude 106° 18' 11.00" West;
- **CAMS 72**, 5050 A. Yvette El Paso, TX (Skyline Park station) at latitude 31° 53' 38.00" North and longitude 106° 25' 32.00" West;
- **CAMS 324**, Haan Road Bldg 1780 Sewage Pump Station, El Paso, TX (Fort Bliss station) at latitude 31° 48' 7.00" North and longitude 106° 25' 14.00" West.

- These stations had the measuremed data corresponding to the model outputs used in this study. Some stations had the measurements of all the parameters, while some of them had only one or two parameters.

4.1.4 Results

4.1.4.1 WRF-Chem Model

Tables I to VI are the results obtained from the WRF-Chem model run for the day of February 4, 2008. Different graphs of the data were created using the Excel program. Figure 4.5 shows the surface wind speed (4km) obtained from the WRF-Chem. It illustrates a sudden increase in wind speed from 10 mph to 26 mph from 11:00 to 16:00 local time. Figure 4.6 shows the surface wind speed modeled at 4 different pressure levels. You can see that the wind speed is higher at lower pressure levels. Figure 4.7 shows the height of the PBLH through the day modeled at 4km. It can be seen that the PBL height starts rising after 9:00 (local time) and starts decreasing at about 14:00 (local time).

The relative humidity graph (Figure 4.8) shows that about 8:00 (local time) the relative humidity started, reaching as low as about 60% at 14:00 and then rising back up to a steady 100% at about 19:00 (local time). Figure 4.9 shows the modeled to sea level pressure (SLP) at 4km. A drop in pressure can be observed at about 12:00 to 15:00 (local time). The surface temperature plot (Figure 3.10) shows that the temperature was continuously increasing, reaching its highest point at 14:00 (local time). In most of the plots the sharp changes occurred more or less from 12:00 to 16:00 (local time), matching more of less the real time where the event started to happen about 14:00 local time.

4.1.4.2 TCEQ Continuous Air Monitoring Stations (CAMS) data

Tables V to X are the results obtained from the different TCEQ Continuous Air Monitoring Stations for the February 4, 2008 day. Different graphs of the data were created using the Excel program. Wind speed (mph), temperature (k), relative humidity (%) and particulate matter (PM) data were obtained. These data are shown to compare the WRF-Chem model output data with ground stations' data to see how well or not the model performed. Figure 4.11 shows a wind speed (mph) comparison between the output data from the WRF-Chem model and the data measurements from the TCEQ CAMS sites. As observed in the figure, the model output at 4 km is similar with most of TCEQ stations wind speed measurements. The wind speed predicted by the model at 12 km is of the early morning hours compared to the ground measurements.

Figure 4.12 shows the Temperature (k) measurements obtained by the TCEQ stations in comparison to the predicted temperature from the WRF-Chem model. In this case the model prediction and the stations' measurements where mostly similar. Relative Humidity (RH) was compared in Figure 4.13. As observed in the plot, the RH predicted by the model was higher than that measured by the ground stations. On Figure 4.14 and 4.15 the PM 2.5 and PM10 measurements are shown. These measurements were obtained from some of the TCEQ stations (CAMS 12, 40, 41, 49). In both plots an increment in the PM that starts about 1 pm until 6pm with the highest peak from 4 to 5 pm.

4.1.5 Summary

My focus in this chapter was not to obtain PM results using an Air Quality Model, since it is well known that Air Quality Models don't perform well under extreme circumstances, such as those exhibited during a dust storm. Instead, my concentration was to examine the meteorological conditions predicted in a model conducive of a dust storm and compare them to measurements obtained by the ground stations and see how well or bad the model performed. As seen in the previous graphs (Figures 4.11 and Figure 4.12), the model did well predicting the wind speeds and temperature when compared to the TCEQ stations' data. When looking at the Relative humidity data, there is a large discrepancy between the model and the ground data. This discrepancy could be because the model used an RH average from all the stations around and not one station in particular.

4.1.6 References

Ginoux, P., Chin, M., Tegen, I., Prospero, J.M., Holben, B.N., Dubovik, O., and Lin, S.J. (2001). Sources and distribution of dust aerosols with the GOCART model. Journal of Geophysical Research 106: 20255-20273.

Grell, G. A., Peckham, S. E., Schmitz, R., McKeen, S. A., Frost, G., Skamarock, W. C., and Eder, B. (2005). Fully coupled "online" chemistry within the WRF model. Atmospheric Environment, 39, 6957-6975.

Guenther, A., Zimmerman, P., Wildermuth, M. (1994). Natural volatile organic compound emission rate estimates for US woodland landscapes. Atmos. Environ., 28, 1197–1210.

National Weather Service (NWS) Glossary (2010).

http://www.weather.gov/glossary/

Nichovic, S., Kallos, G., Kakaliagou, O., and Jovic, D. (1997). Aerosol production/transport/deposition processes in the Eta model: Desert cycle simulations. In Proceedings of the Symposium on Regional Weather Prediction on Parallel Computer Environments . Athens, Greece (pp. 137–145) [Preprints].

Raman, A. and Arellano, A. F. (2011). Modeling and Data Analysis of 2011 Phoenix Dust Storm. 15th Conference on Atmospheric Chemistry. 93 AMS Annual Meeting, Paper 5.5. Austin, TX.

Rosmond, T. E., Teixeira, J., Peng, M., Hogan, T. F., and Pauley, R. (2002). Navy Operational Global Atmospheric Prediction System (NOGAPS): Forcing for ocean models. Oceanography, 15(1), 99–108.

Simpson, D., Guenther, A., Hewitt, C. N., Steinbrecher, R. (1995). Biogenic emissions in Europe. Estimates and uncertainties. J. Geophys. Res., 100D, 22875–22890.

Skamarock, W. C., Klemp, J. B., Dudhia, J., Gill, D. O., Barker, D. M., Duda, M. G., Huang, X-Yu., Wang, W. and Powers, J. G. (2008). A Description of the Advanced Research WRF Version 3. NCAR Technical Note. Mesoscale and Microscale Meteorology Division National Center for Atmospheric Research. Boulder, Colorado, USA

Stull, R. B. (1988). An Introduction to Boundary Layer Meteorology, Kluwer Academic Publisher, 666 p.

WRF – The Weather and Research Forecasting Model. (2009). Retrieved from:

http://wrf-model.org/index.php

WRF-chem. (2009). Pacific Northwest National Laboratory (PNNL). Retrieved from:

http://www.pnl.gov/atmospheric/research/wrf-chem/

Xie, J., Yang, C., Zhou, B. and Huang, Q. (2009). High-performance computing for the simulation of dust storms. Computer, Environment and Urban System. doi:10.1016/j.compenvurbsys.2009.08.002

Figures

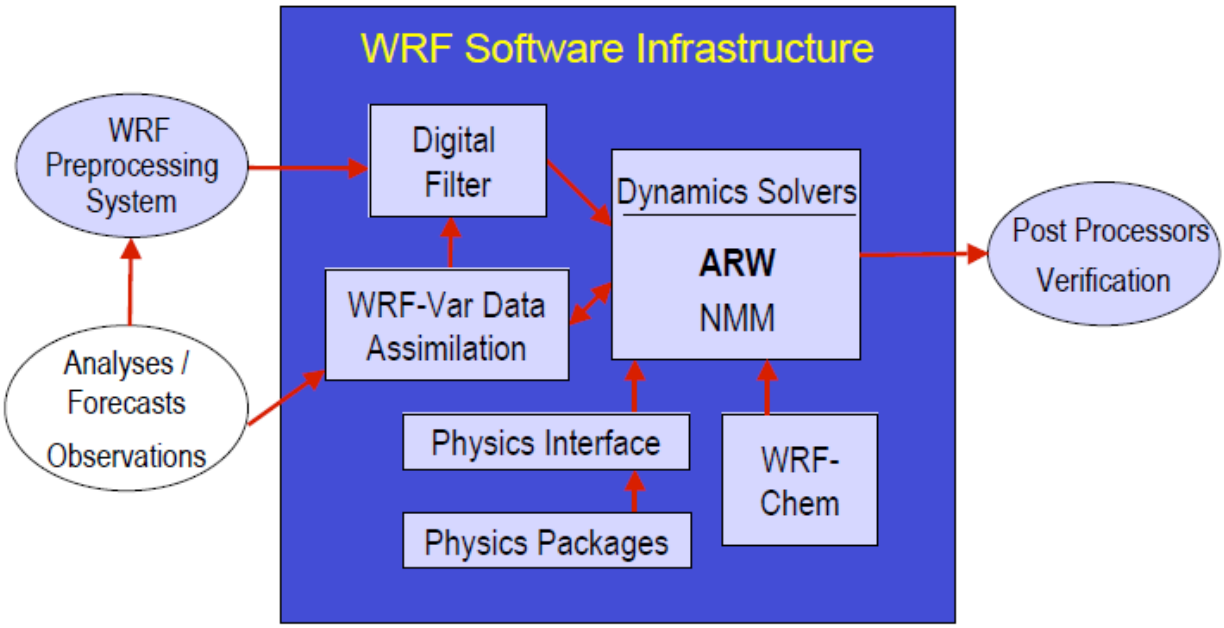

Figure 4.1

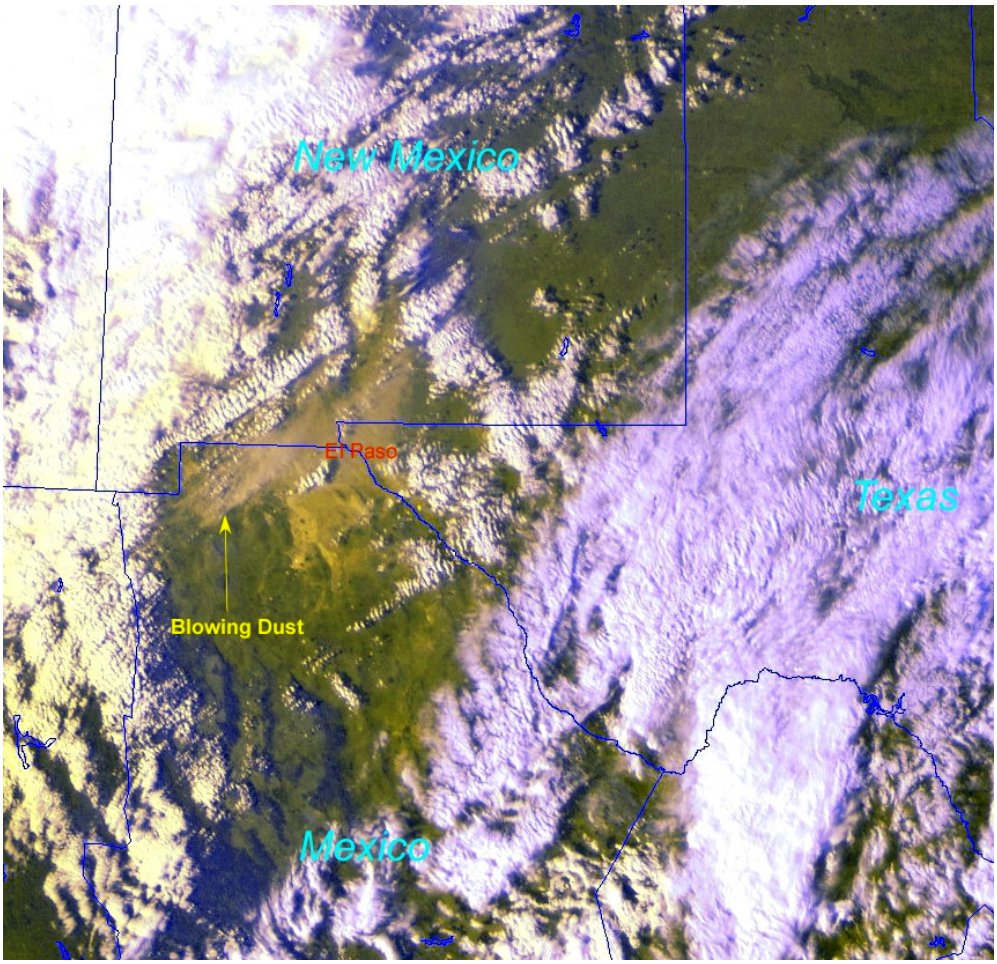

Figure 4.2

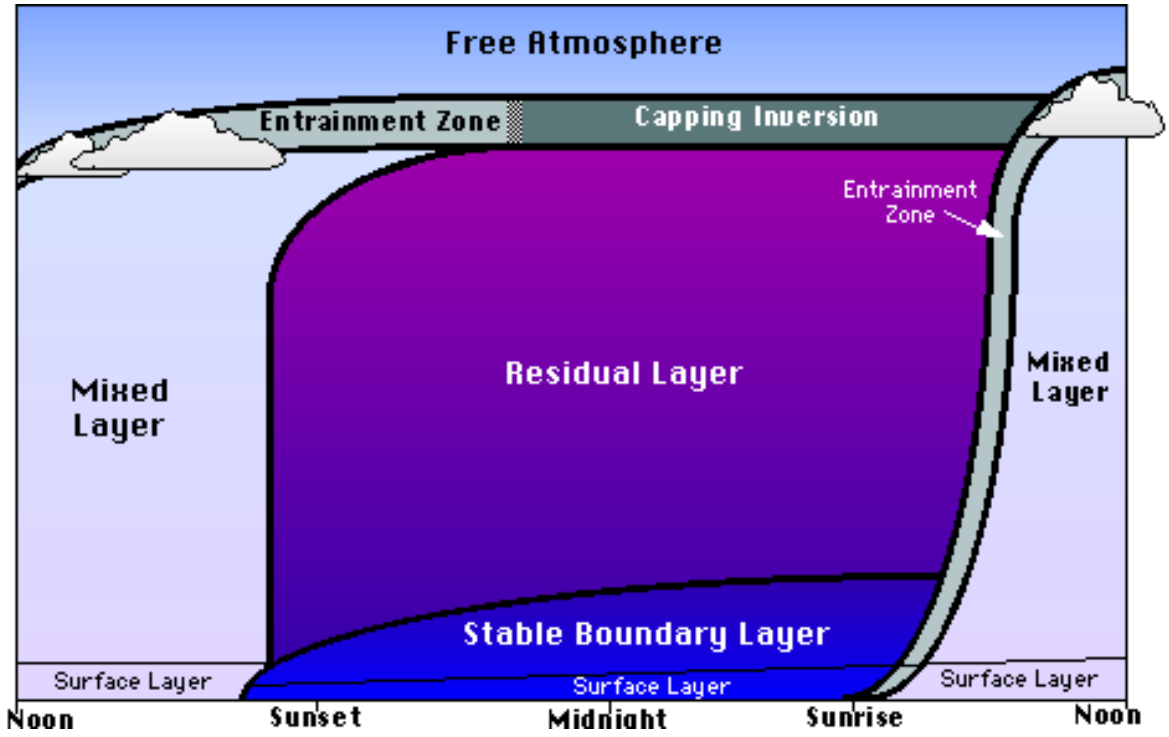
Free Atmosphere
Entrainment Zone
Capping Inversion
Entrainment Zone
Mixed Layer
Residual Layer
Mixed Layer
Stable Boundary Layer
Surface Layer
Surface Layer
Surface Layer
Noon
Sunset
Midnight
Sunrise
Noon

Figure 4.3

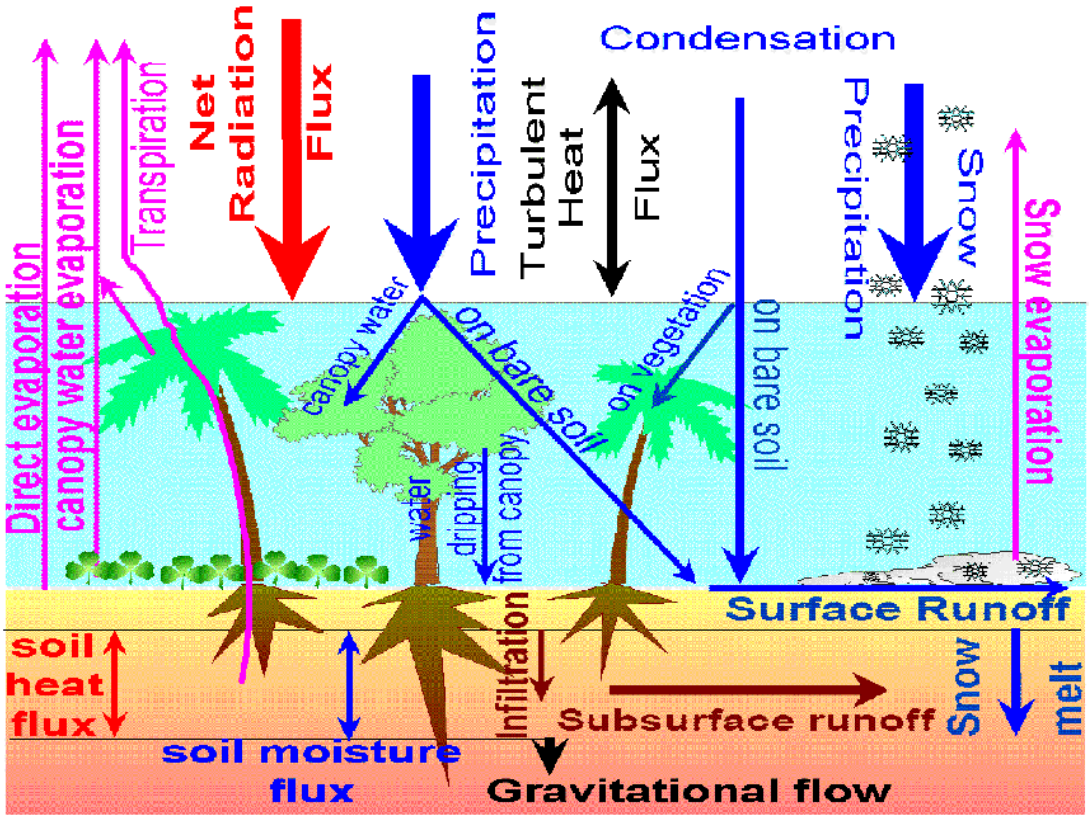
Direct evaporation
canopy water evaporation
Transpiration
Net Radiation Flux
Precipitation
Turbulent Heat Flux
Condensation
Precipitation
Snow
Snow evaporation
canopy water
on bare soil
on vegetation
on bare soil
water dripping from canopy
Surface Runoff
soil heat flux
soil moisture flux
Infiltration
Subsurface runoff
Snow melt
Gravitational flow

Figure 4.4

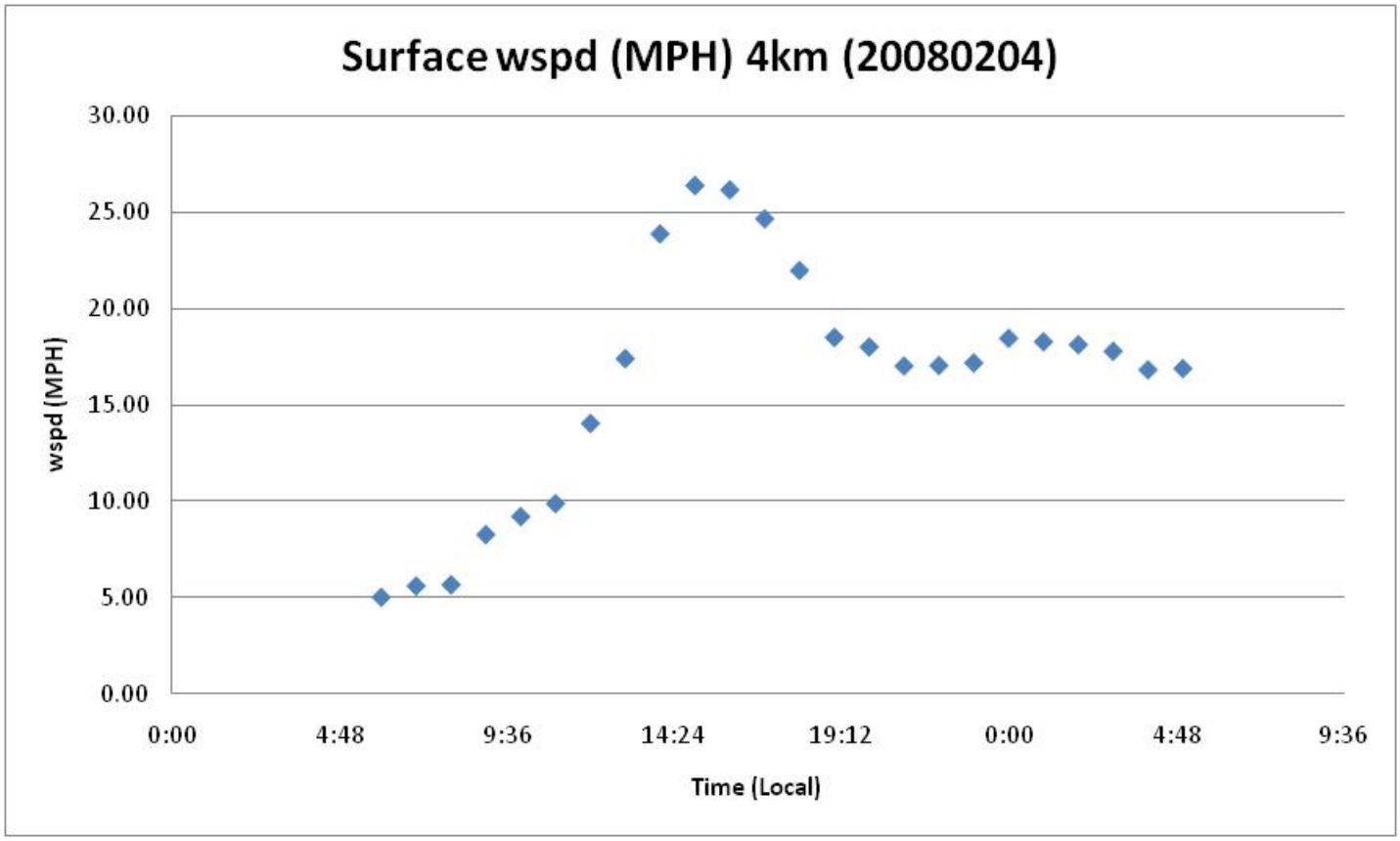
Surface wspd (MPH) 4km (20080204)
30.00
25.00
20.00
15.00
10.00
5.00
0.00
wspd (MPH)
0:00
4:48
9:36
14:24
19:12
0:00
4:48
9:36
Time (Local)

Figure 4.5

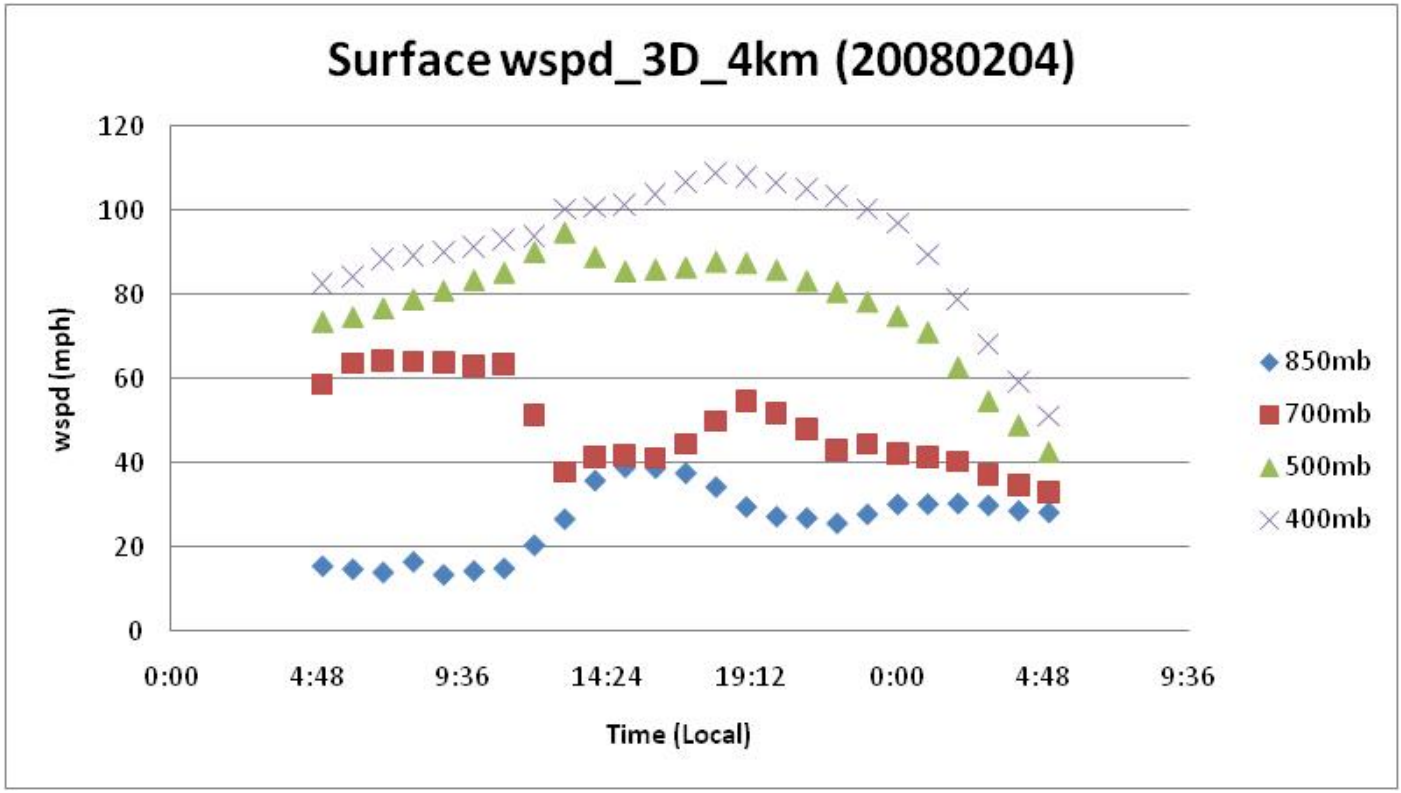
Surface wspd_3D_4km (20080204)
120
100
80
60
40
20
0
wspd (mph)
0:00
4:48
9:36
14:24
19:12
0:00
4:48
9:36
Time (Local)
850mb
700mb
500mb
400mb

Figure 4.6

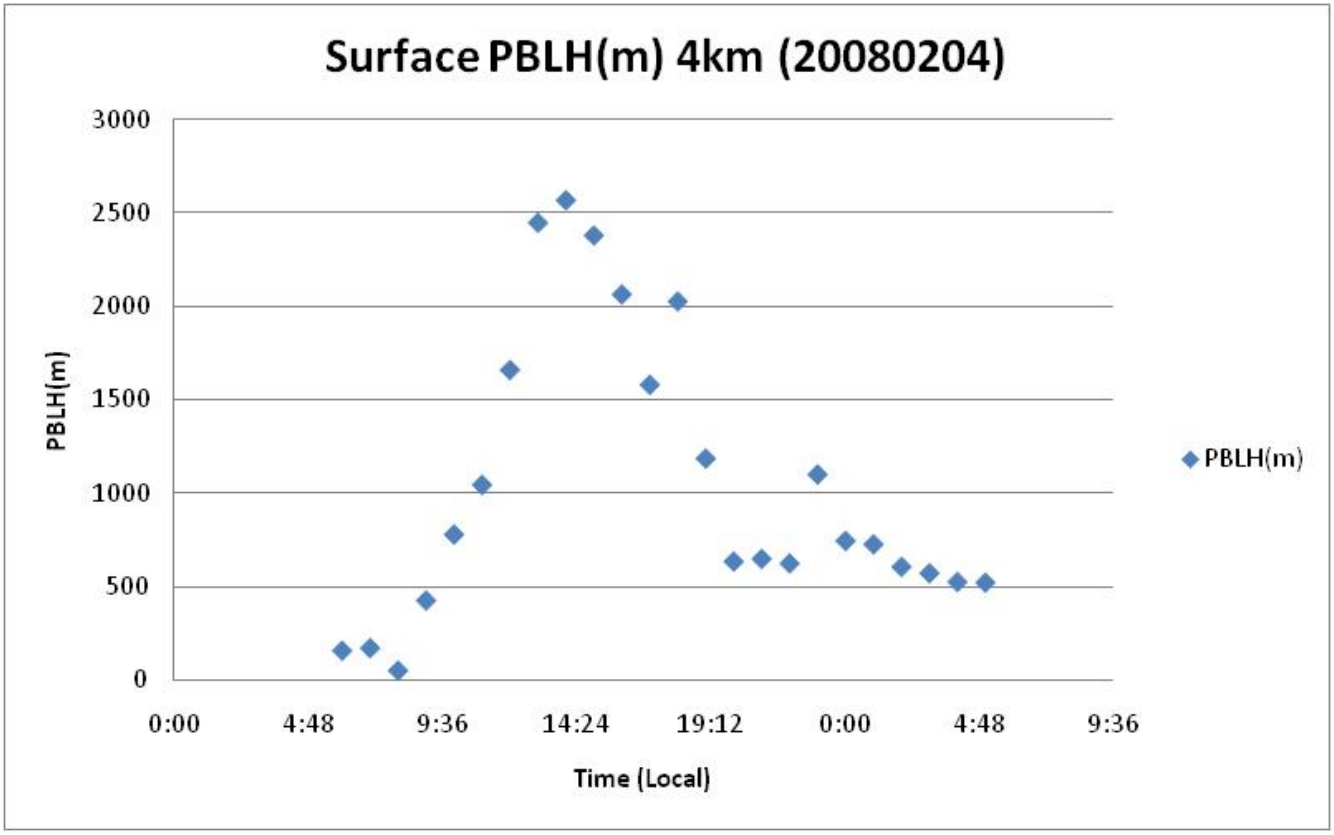
Surface PBLH(m) 4km (20080204)
3000
2500
2000
1500
1000
500
0
PBLH(m)
0:00
4:48
9:36
14:24
19:12
0:00
4:48
9:36
Time (Local)
PBLH(m)

Figure 4.7

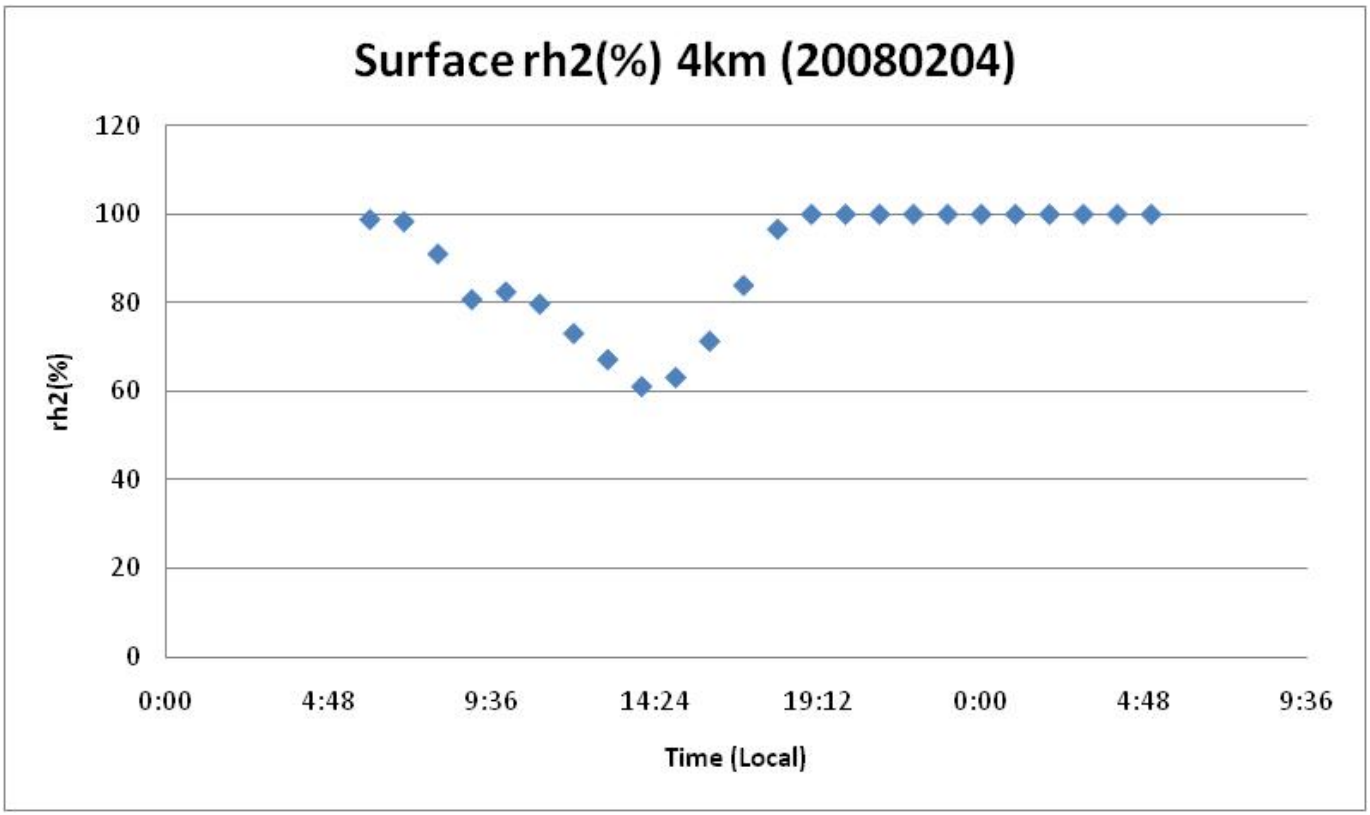
Surface rh2(%) 4km (20080204)
120
100
80
60
40
20
0
rh2(%)
0:00
4:48
9:36
14:24
19:12
0:00
4:48
9:36
Time (Local)

Figure 4.8

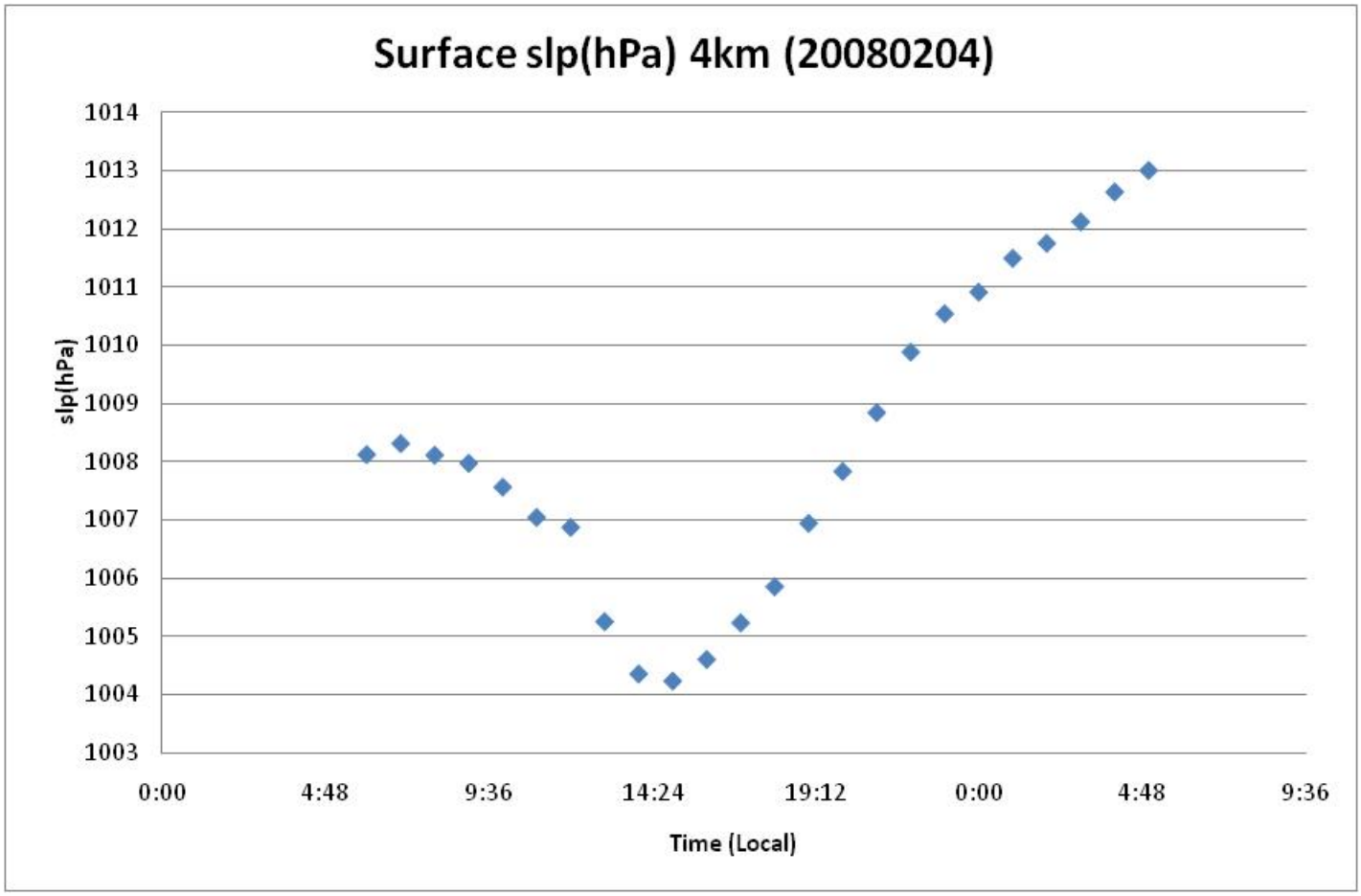
Surface slp(hPa) 4km (20080204)
slp(hPa)
1014
1013
1012
1011
1010
1009
1008
1007
1006
1005
1004
1003
0:00
4:48
9:36
14:24
19:12
0:00
4:48
9:36
Time (Local)

Figure 4.9

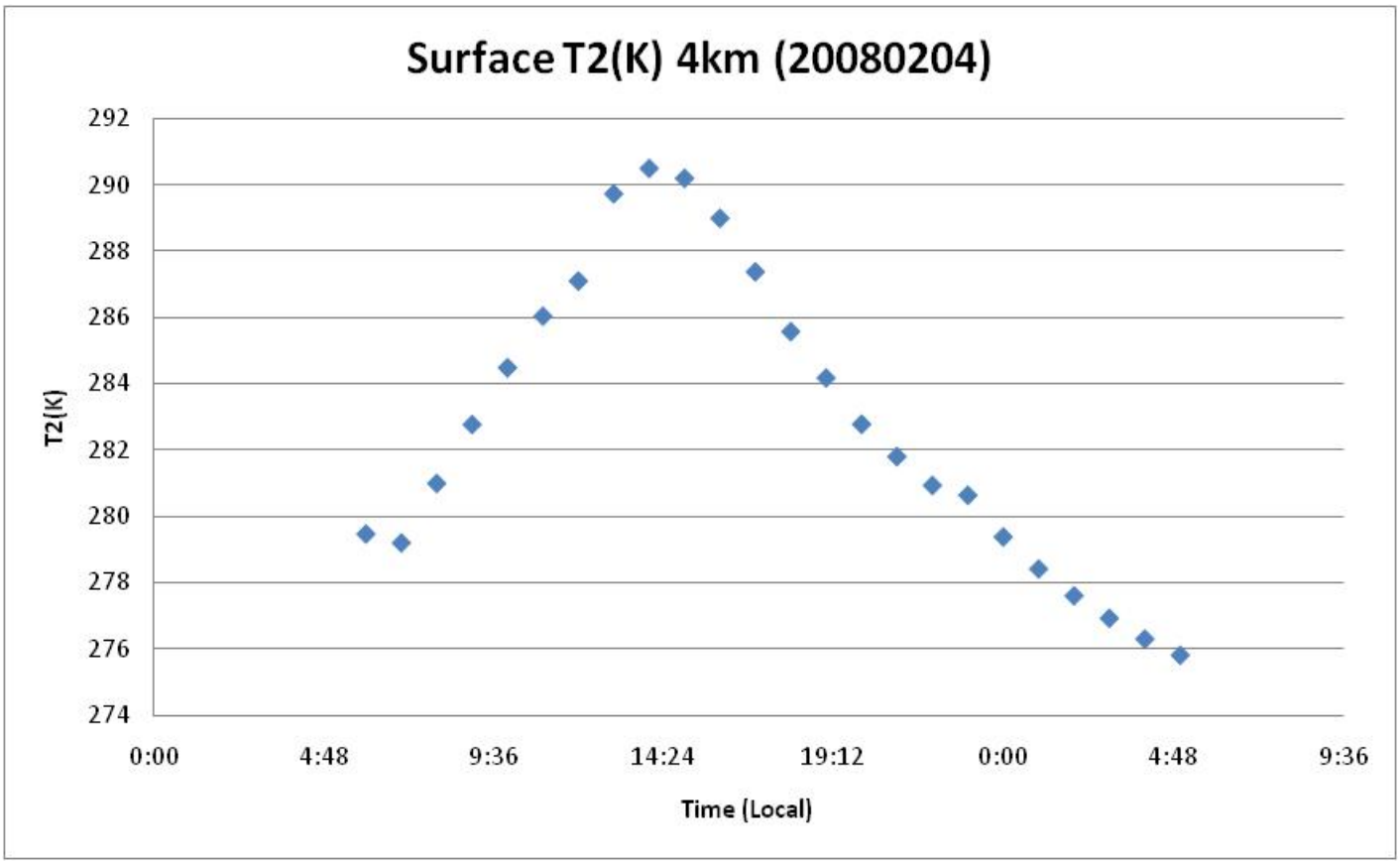
Surface T2(K) 4km (20080204)
292
290
288
286
284
282
280
278
276
274
T2(K)
0:00
4:48
9:36
14:24
19:12
0:00
4:48
9:36
Time (Local)

Figure 4.10

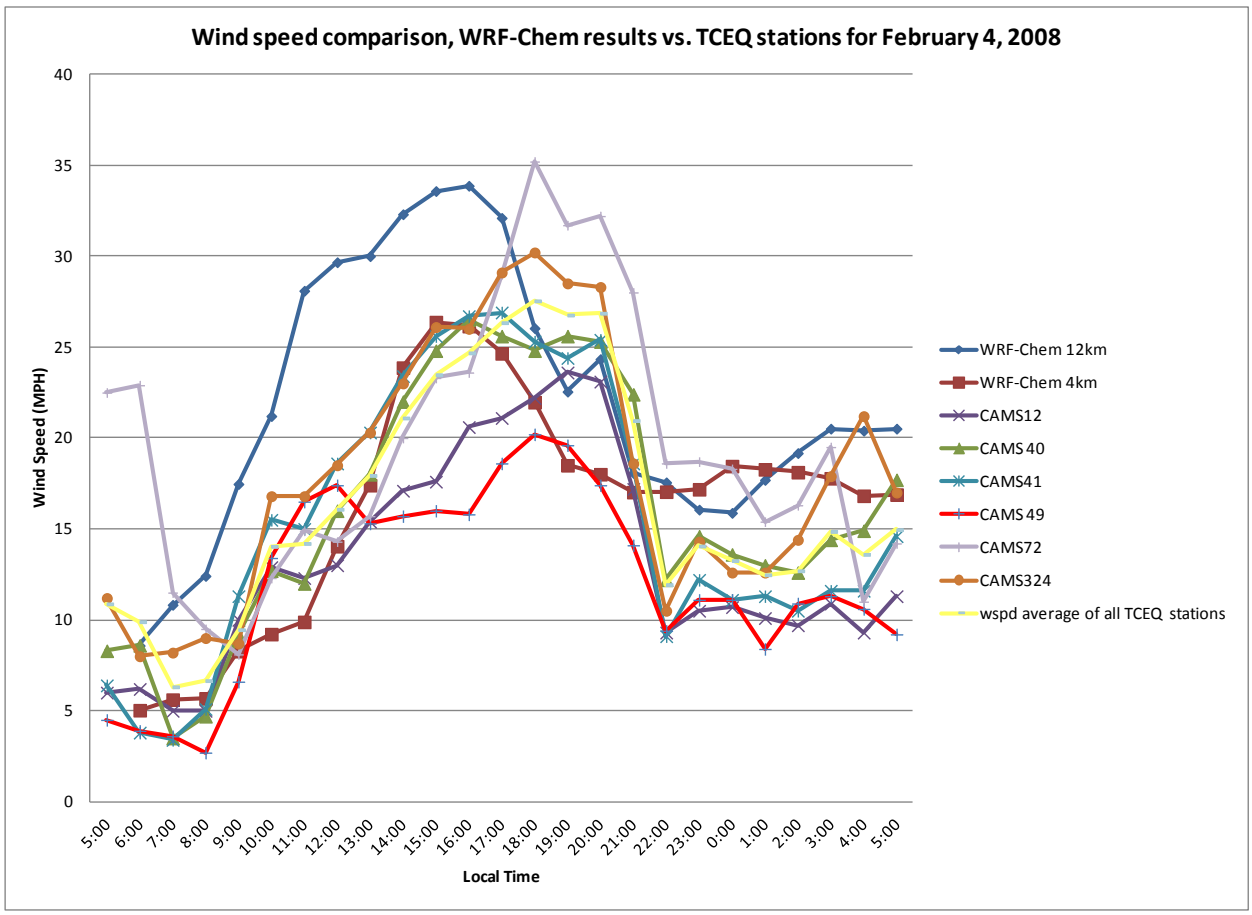
Wind speed comparison, WRF-Chem results vs. TCEQ stations for February 4, 2008
Wind Speed (MPH)
Local Time
WRF-Chem 12km
WRF-Chem 4km
CAMS12
CAMS 40
CAMS41
CAMS 49
CAMS72
CAMS324
wspd average of all TCEQ stations

Figure 2.11

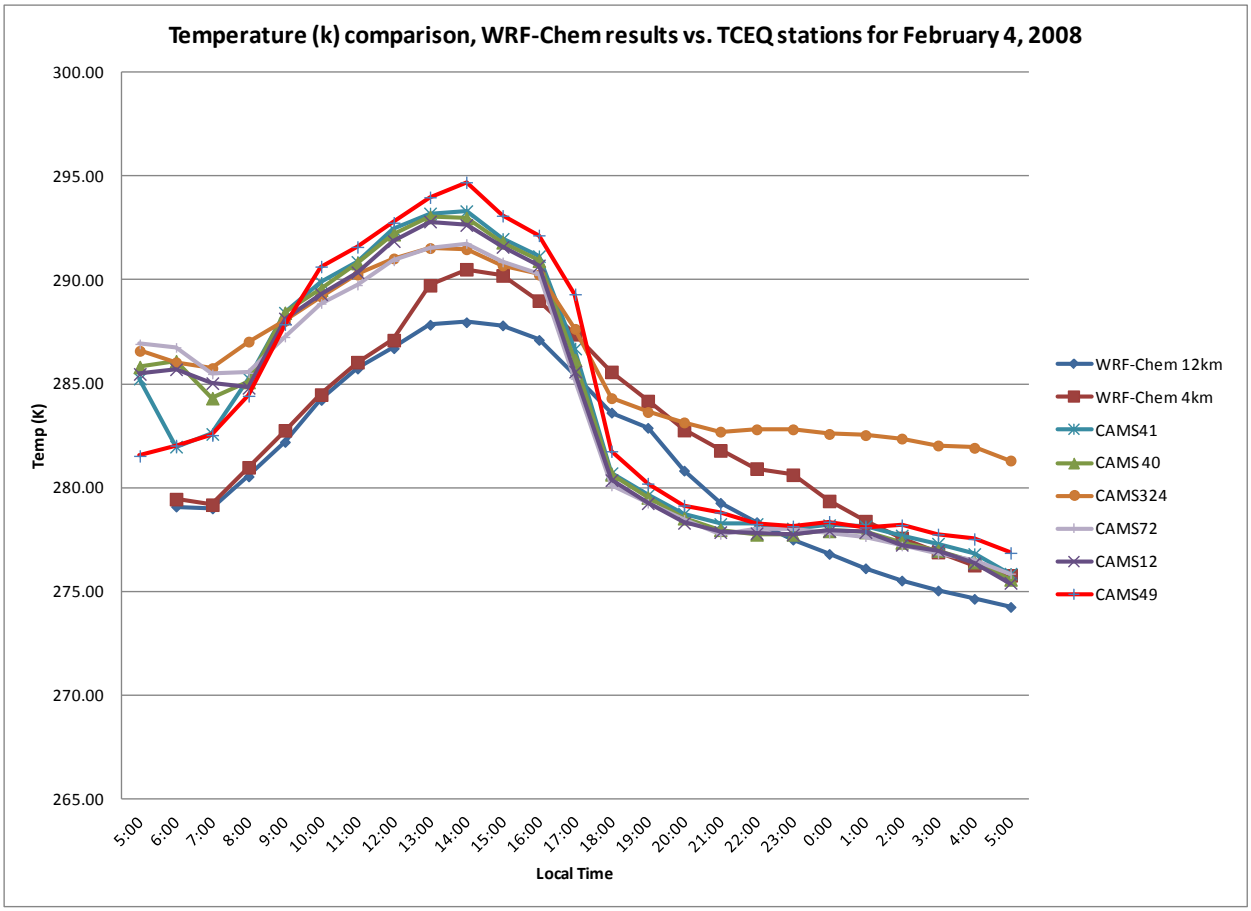
Temperature (k) comparison, WRF-Chem results vs. TCEQ stations for February 4, 2008
300.00
295.00
290.00
285.00
280.00
275.00
270.00
265.00
Temp (K)
5:00
6:00
7:00
8:00
9:00
10:00
11:00
12:00
13:00
14:00
15:00
16:00
17:00
18:00
19:00
20:00
21:00
22:00
23:00
0:00
1:00
2:00
3:00
4:00
5:00
Local Time
WRF-Chem 12km
WRF-Chem 4km
CAMS41
CAMS 40
CAMS324
CAMS72
CAMS12
CAMS49

Figure 4.12

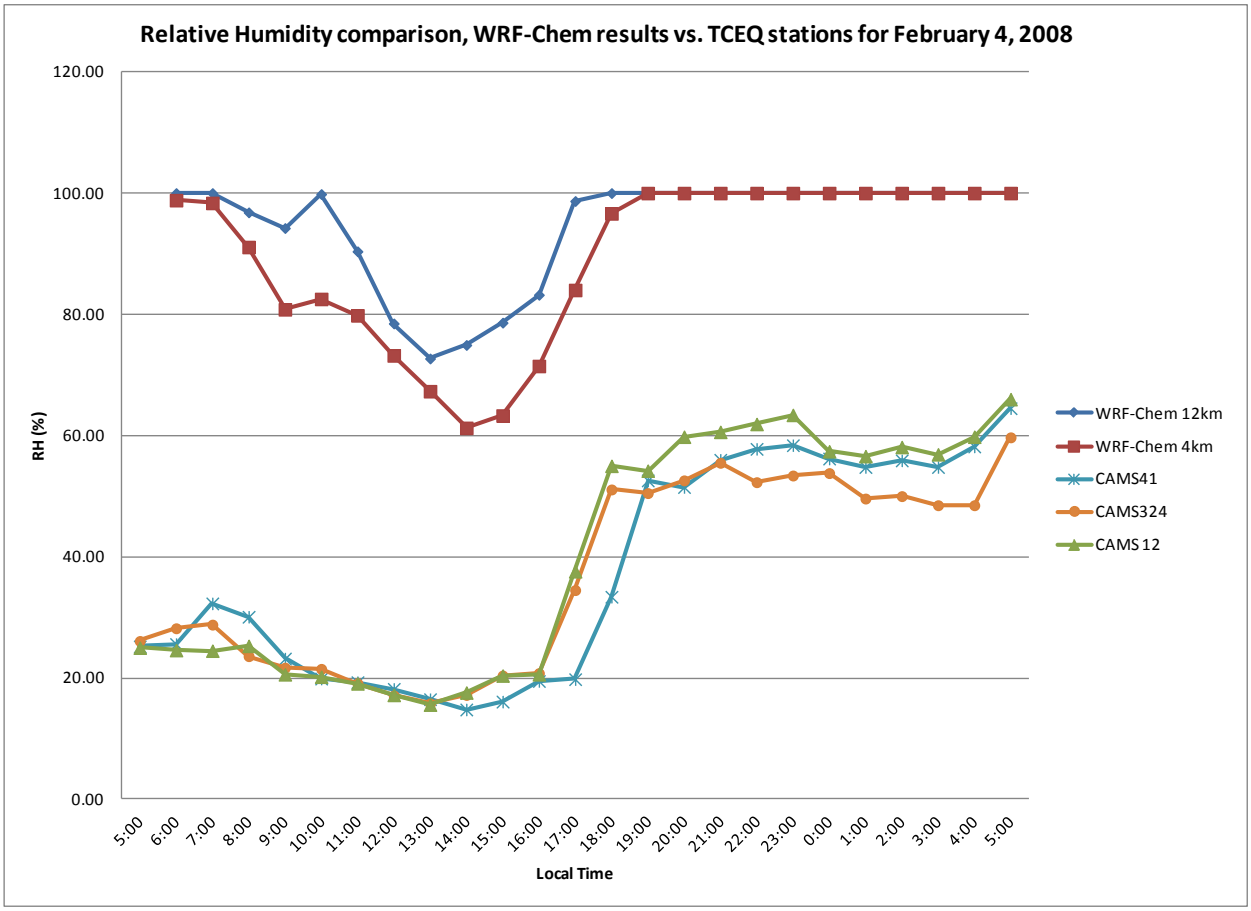
Relative Humidity comparison, WRF-Chem results vs. TCEQ stations for February 4, 2008
120.00
100.00
80.00
60.00
40.00
20.00
0.00
RH (%)
5:00
6:00
7:00
8:00
9:00
10:00
11:00
12:00
13:00
14:00
15:00
16:00
17:00
18:00
19:00
20:00
21:00
22:00
23:00
0:00
1:00
2:00
3:00
4:00
5:00
Local Time
WRF-Chem 12km
WRF-Chem 4km
CAMS41
CAMS324
CAMS 12

Figure 4.13

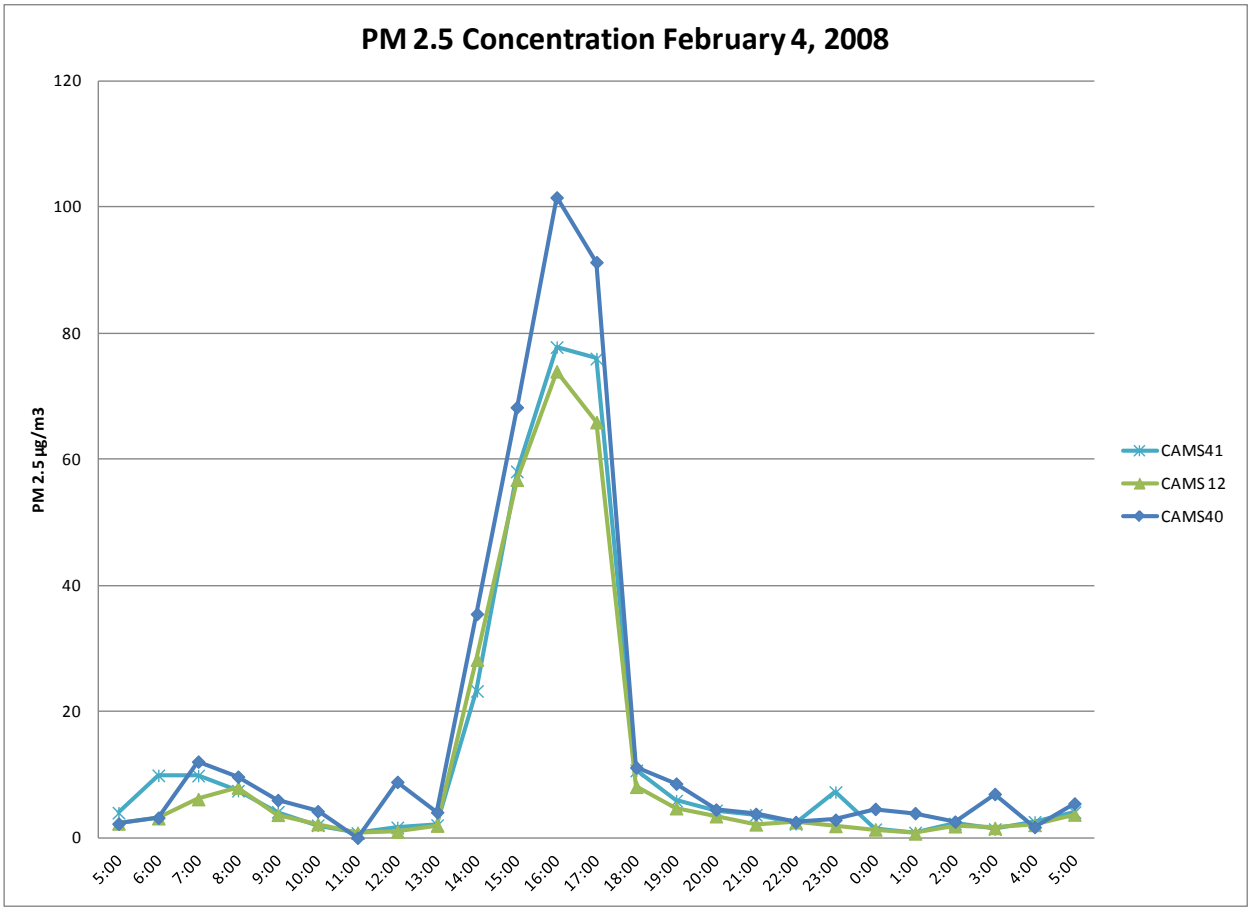
PM 2.5 Concentration February 4, 2008
PM 2.5 µg/m3
120
100
80
60
40
20
0
5:00
6:00
7:00
8:00
9:00
10:00
11:00
12:00
13:00
14:00
15:00
16:00
17:00
18:00
19:00
20:00
21:00
22:00
23:00
0:00
1:00
2:00
3:00
4:00
5:00
CAMS41
CAMS 12
CAMS40

Figure 4.14

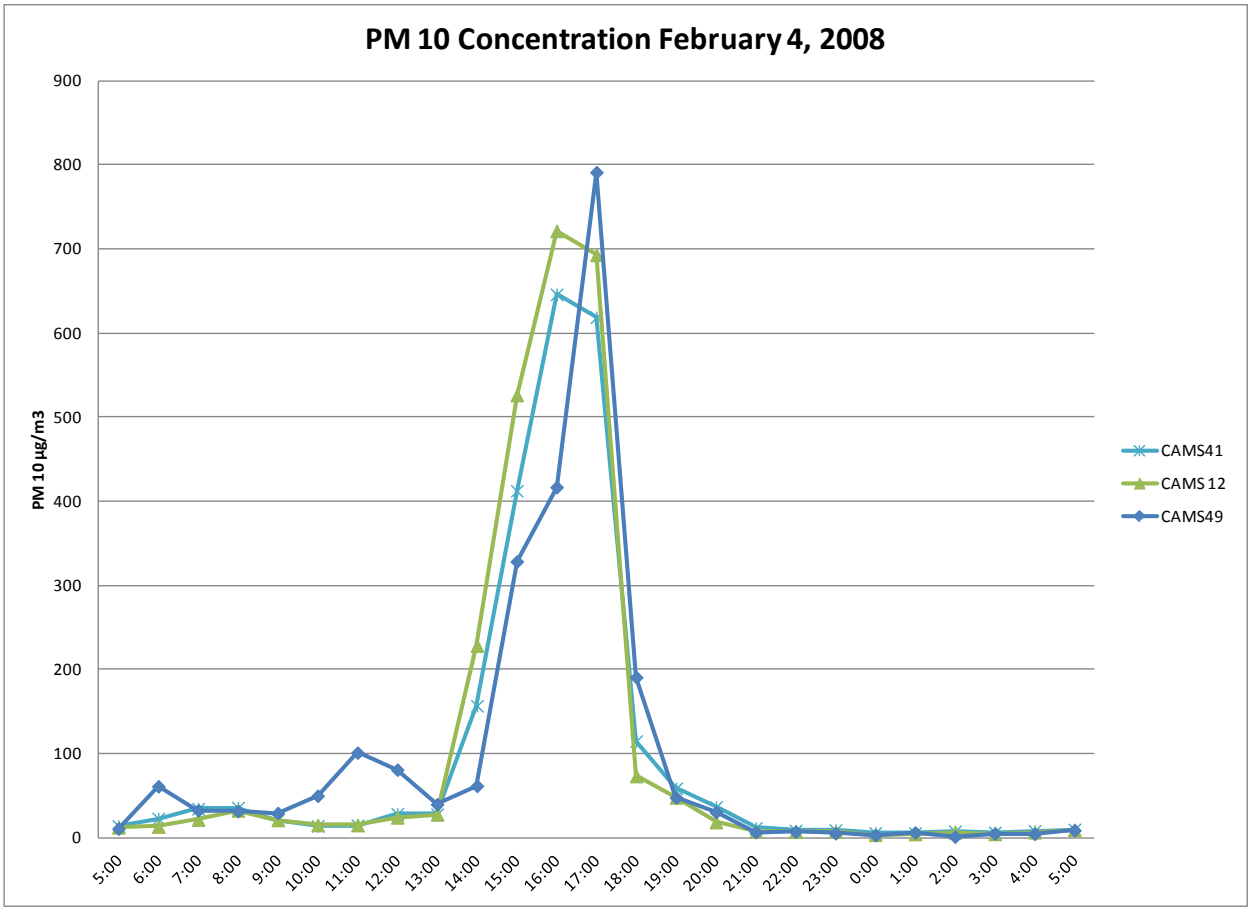
PM 10 Concentration February 4, 2008
PM 10 µg/m3
900
800
700
600
500
400
300
200
100
0
5:00
6:00
7:00
8:00
9:00
10:00
11:00
12:00
13:00
14:00
15:00
16:00
17:00
18:00
19:00
20:00
21:00
22:00
23:00
0:00
1:00
2:00
3:00
4:00
5:00
CAMS41
CAMS 12
CAMS49

Figure 3

Table I:

Surface wspd (MPH) 4km (20080204)				
Date and Time(UTC)	Time (UTC)	Local Time	wspd(m/s)	wspd (MPH)
2008020412	12	5:00		
2008020413	13	6:00	2.25	5.03
2008020414	14	7:00	2.51	5.61
2008020415	15	8:00	2.54	5.68
2008020416	16	9:00	3.7	8.28
2008020417	17	10:00	4.12	9.22
2008020418	18	11:00	4.42	9.89
2008020419	19	12:00	6.28	14.05
2008020420	20	13:00	7.78	17.40
2008020421	21	14:00	10.67	23.87
2008020422	22	15:00	11.79	26.37
2008020423	23	16:00	11.69	26.15
2008020500	0	17:00	11.02	24.65
2008020501	1	18:00	9.82	21.97
2008020502	2	19:00	8.27	18.50
2008020503	3	20:00	8.05	18.01
2008020504	4	21:00	7.61	17.02
2008020505	5	22:00	7.62	17.05
2008020506	6	23:00	7.68	17.18
2008020507	7	0:00	8.25	18.45
2008020508	8	1:00	8.17	18.28
2008020509	9	2:00	8.1	18.12
2008020510	10	3:00	7.95	17.78
2008020511	11	4:00	7.52	16.82
2008020512	12	5:00	7.55	16.89

Table II:

Surface wspd_3D_4km (20080204)												
								Converted to MPH				
Date and Time(UTC)	Time (UTC)	Local Time	850mb	700mb	500mb	400mb		Local Time	850mb	700mb	500mb	400mb
2008020412	12	5:00	6.85	26.24	32.97	36.97		5:00	15.32301	58.6972	73.75178	82.69952
2008020413	13	6:00	6.53	28.49	33.46	37.72		6:00	14.60719	63.73031	74.84788	84.37723
2008020414	14	7:00	6.18	28.78	34.4	39.57		7:00	13.82426	64.37902	76.9506	88.51556
2008020415	15	8:00	7.31	28.66	35.36	39.9		8:00	16.352	64.11059	79.09806	89.25375
2008020416	16	9:00	5.93	28.57	36.25	40.27		9:00	13.26503	63.90926	81.08893	90.08141
2008020417	17	10:00	6.35	28.16	37.4	40.92		10:00	14.20454	62.99212	83.66141	91.53542
2008020418	18	11:00	6.61	28.35	38.19	41.63		11:00	14.78615	63.41714	85.42859	93.12365
2008020419	19	12:00	9.07	22.98	40.39	42.03		12:00	20.28901	51.40479	90.34985	94.01842
2008020420	20	13:00	11.84	16.94	42.46	44.85		13:00	26.48532	37.8937	94.9803	100.3266
2008020421	21	14:00	15.92	18.51	39.84	45.03		14:00	35.61202	41.40569	89.11953	100.7292
2008020422	22	15:00	17.32	18.64	38.34	45.3		15:00	38.74373	41.69649	85.76413	101.3332
2008020423	23	16:00	17.25	18.43	38.52	46.51		16:00	38.58715	41.22673	86.16677	104.0399
2008020500	0	17:00	16.7	19.87	38.74	47.77		17:00	37.35683	44.44792	86.6589	106.8584
2008020501	1	18:00	15.25	22.29	39.36	48.69		18:00	34.11327	49.8613	88.0458	108.9164
2008020502	2	19:00	13.13	24.52	39.21	48.37		19:00	29.37097	54.84967	87.71026	108.2006
2008020503	3	20:00	12.11	23.11	38.47	47.67		20:00	27.08929	51.69559	86.05493	106.6347
2008020504	4	21:00	11.95	21.47	37.3	47.06		21:00	26.73139	48.02702	83.43771	105.2702
2008020505	5	22:00	11.39	19.22	36.15	46.2		22:00	25.4787	42.99391	80.86524	103.3464
2008020506	6	23:00	12.35	19.89	35.09	44.84		23:00	27.62616	44.49266	78.49408	100.3042
2008020507	7	0:00	13.4	18.92	33.59	43.36		0:00	29.97494	42.32283	75.13868	96.99354
2008020508	8	1:00	13.43	18.46	31.85	40.01		1:00	30.04205	41.29384	71.24641	89.49981
2008020509	9	2:00	13.49	18.01	28.14	35.21		2:00	30.17627	40.28722	62.94738	78.76252
2008020510	10	3:00	13.3	16.68	24.53	30.52		3:00	29.75125	37.31209	54.87204	68.27129
2008020511	11	4:00	12.71	15.51	21.96	26.48		4:00	28.43146	34.69488	49.12311	59.23407
2008020512	12	5:00	12.55	14.83	19.1	22.86		5:00	28.07355	33.17376	42.72548	51.13636

Table III:

Surface PBLH(m) 4km (20080204)			
Date and Time(UTC)	Time (UTC)	Local Time	PBLH(m)
2008020412	12	5:00	
2008020413	13	6:00	161.28
2008020414	14	7:00	175.14
2008020415	15	8:00	55.39
2008020416	16	9:00	429.77
2008020417	17	10:00	782.46
2008020418	18	11:00	1047.69
2008020419	19	12:00	1661.09
2008020420	20	13:00	2447.04
2008020421	21	14:00	2567.21
2008020422	22	15:00	2379.21
2008020423	23	16:00	2064.74
2008020500	0	17:00	1582.01
2008020501	1	18:00	2026.9
2008020502	2	19:00	1187.48
2008020503	3	20:00	638.06
2008020504	4	21:00	652.17
2008020505	5	22:00	627.98
2008020506	6	23:00	1102.59
2008020507	7	0:00	747.92
2008020508	8	1:00	729.88
2008020509	9	2:00	609.02
2008020510	10	3:00	574.67
2008020511	11	4:00	528.68
2008020512	12	5:00	525.55

Table IV:

Surface rh2(%) 4km (20080204)			
Date and Time(UTC)	Time (UTC)	Local Time	rh2(%)
2008020412	12	5:00	
2008020413	13	6:00	98.83
2008020414	14	7:00	98.37
2008020415	15	8:00	91.1
2008020416	16	9:00	80.82
2008020417	17	10:00	82.53
2008020418	18	11:00	79.82
2008020419	19	12:00	73.21
2008020420	20	13:00	67.31
2008020421	21	14:00	61.26
2008020422	22	15:00	63.3
2008020423	23	16:00	71.47
2008020500	0	17:00	84.01
2008020501	1	18:00	96.64
2008020502	2	19:00	100
2008020503	3	20:00	100
2008020504	4	21:00	100
2008020505	5	22:00	100
2008020506	6	23:00	100
2008020507	7	0:00	100
2008020508	8	1:00	100
2008020509	9	2:00	100
2008020510	10	3:00	100
2008020511	11	4:00	100
2008020512	12	5:00	100

Table III:

Surface slp(hPa) 4km (20080204)			
Date and Time(UTC)	Time (UTC)	Local Time	slp(hPa)
2008020412	12	5:00	
2008020413	13	6:00	1008.13
2008020414	14	7:00	1008.32
2008020415	15	8:00	1008.12
2008020416	16	9:00	1007.98
2008020417	17	10:00	1007.57
2008020418	18	11:00	1007.05
2008020419	19	12:00	1006.88
2008020420	20	13:00	1005.26
2008020421	21	14:00	1004.36
2008020422	22	15:00	1004.24
2008020423	23	16:00	1004.61
2008020500	0	17:00	1005.24
2008020501	1	18:00	1005.86
2008020502	2	19:00	1006.95
2008020503	3	20:00	1007.84
2008020504	4	21:00	1008.85
2008020505	5	22:00	1009.89
2008020506	6	23:00	1010.55
2008020507	7	0:00	1010.92
2008020508	8	1:00	1011.5
2008020509	9	2:00	1011.76
2008020510	10	3:00	1012.13
2008020511	11	4:00	1012.64
2008020512	12	5:00	1013.01

Table IVI:

Surface T2(K) 4km (20080204)			
Date and Time(UTC)	Time (UTC)	Local Time	T2(K)
2008020412	12	5:00	
2008020413	13	6:00	279.46
2008020414	14	7:00	279.19
2008020415	15	8:00	280.99
2008020416	16	9:00	282.77
2008020417	17	10:00	284.49
2008020418	18	11:00	286.05
2008020419	19	12:00	287.11
2008020420	20	13:00	289.75
2008020421	21	14:00	290.52
2008020422	22	15:00	290.22
2008020423	23	16:00	289.01
2008020500	0	17:00	287.39
2008020501	1	18:00	285.58
2008020502	2	19:00	284.18
2008020503	3	20:00	282.78
2008020504	4	21:00	281.8
2008020505	5	22:00	280.93
2008020506	6	23:00	280.63
2008020507	7	0:00	279.37
2008020508	8	1:00	278.4
2008020509	9	2:00	277.59
2008020510	10	3:00	276.91
2008020511	11	4:00	276.28
2008020512	12	5:00	275.79

Table VII:

CAMS 12					
wind speed average (m/h)	RH %	Temp °F	Temp K	PM 2.5 ug/m3	PM 10 ug/m3
6	25	54.2	285.48	2.27	12.31
6.2	24.6	54.6	285.71	3.1	13.35
5	24.5	53.4	285.04	6.13	21.59
5	25.3	53	284.82	7.96	32.48
10	20.6	59	288.15	3.64	21.11
12.9	20.2	61.1	289.32	2.17	15.13
12.3	19.1	63	290.37	0.8	15.09
13	17.2	65.7	291.87	0.96	24.2
15.4	15.6	67.4	292.82	1.93	27.72
17.1	17.6	67.1	292.65	28.24	228.46
17.6	20.4	65.2	291.59	56.75	526.27
20.6	20.6	63.6	290.71	73.94	721.47
21.1	37.6	54.4	285.59	65.88	692.99
22.2	55	45	280.37	8.08	73.33
23.6	54.2	43	279.26	4.69	47.98
23.1	59.8	41.3	278.32	3.42	18.53
17.2	60.6	40.5	277.87	2.13	7.58
9.3	61.9	40.4	277.82	2.45	7.12
10.5	63.4	40.3	277.76	1.87	7.31
10.7	57.4	40.6	277.93	1.32	3.48
10.1	56.6	40.5	277.87	0.69	4.33
9.7	58.1	39.4	277.26	1.83	6.45
10.9	56.9	38.9	276.98	1.56	4.55
9.3	59.8	37.8	276.37	2.04	6.44
11.3	66	36.1	275.43	3.69	9.43

Table VIII:

CAMS 40					
wind speed average (m/h)	RH %	Temp °F	Temp K	PM 2.5	PM 10
8.3	No data	54.8	285.82	2.23	
8.6		55.3	286.09	3.18	
3.5		52.1	284.32	12.07	
4.7		53.5	285.09	9.68	
9.2		59.5	288.43	5.98	
12.7		61.5	289.54	4.21	
12		63.8	290.82	QAS	
16		66.3	292.21	8.85	
18		67.8	293.04	4.05	
22		67.7	292.98	35.48	
24.8		65.6	291.82	68.24	
26.5		64	290.93	101.5	
25.6		55.4	286.15	91.24	
24.8		45.5	280.65	11.14	
25.6		43.5	279.54	8.58	
25.3		41.7	278.54	4.47	
22.4		40.7	277.98	3.78	
12.2		40.3	277.76	2.49	
14.6		40.3	277.76	2.85	
13.6		40.6	277.93	4.57	
13		40.5	277.87	3.9	
12.6		39.6	277.37	2.55	
14.4		38.9	276.98	6.94	
14.9		37.9	276.43	1.71	
17.7		36.4	275.59	5.43	

Table IX:

CAMS 41					
wind speed average (m/h)	RH %	Temp °F	Temp K	PM 2.5	PM 10
6.4	25.2	53.8	285.26	3.98	13.89
3.8	25.6	47.9	281.98	9.89	22.78
3.4	32.3	49	282.59	9.85	34.46
5.1	30.1	53.8	285.26	7.46	35.8
11.3	23.2	59.5	288.43	4.12	21.28
15.5	19.9	62.1	289.87	1.98	14.1
15	19.3	63.9	290.87	0.75	14.72
18.6	18.2	66.7	292.43	1.64	28.34
20.3	16.5	68.1	293.21	2.01	28.09
23.4	14.8	68.3	293.32	23.27	156.92
25.6	16.1	65.9	291.98	58.08	412.48
26.7	19.5	64.4	291.15	77.78	646
26.9	19.8	56.4	286.71	75.96	618.76
25.3	33.4	45.6	280.71	10.67	114.97
24.4	52.6	43.7	279.65	5.88	58.67
25.4	51.5	42.1	278.76	4.33	36.54
18.6	56	41.2	278.26	3.63	11.67
9.1	57.8	41.2	278.26	2.2	8.53
12.2	58.4	40.8	278.04	7.24	9.11
11.1	56.2	41.1	278.21	1.34	5.74
11.3	54.8	41	278.15	0.82	5.59
10.5	55.9	40.2	277.71	2.24	7.56
11.6	54.8	39.5	277.32	1.37	6.25
11.6	58.2	38.6	276.82	2.52	8.12
14.6	64.5	36.9	275.87	4.06	9.76

Table X:

CAMS 49							
wind speed average (m/h)	Resultant wind speed (m/h)	Resultant Wind Direction	Maximum Wind Gust (m/h)	Temp °F	Temp K	PM 2.5	PM 10
4.5	4.4	158	7.7	47.1	281.54		10.88
3.9	3.5	119	9.2	48	282.04		61.16
3.6	3.4	148	6.2	48.9	282.54		32.64
2.7	2.3	87	6.5	52.3	284.43		31.68
6.6	3.8	200	24.5	58.5	287.87		29.44
13.4	12.8	212	27.1	63.5	290.65		49.9
16.5	15.8	223	31.5	65.2	291.59		101.19
17.4	16.8	223	36	67.3	292.76		80.94
15.3	14.6	214	30.8	69.5	293.98		39.85
15.7	14.6	252	32.5	**70.8**	294.71		61.68
16	15.4	271	29.8	67.9	293.09		328.47
15.8	15.2	265	30.4	66.2	292.15		416.85
18.6	17.6	277	40.8	61.1	289.32		**791.24**
20.2	19.7	297	38	47.5	281.76		190.78
19.6	19	300	33.8	44.7	280.21		47.76
17.4	16.9	296	35.1	42.8	279.15		30.54
14.1	13.7	291	25.7	42.2	278.82		6.61
9.4	9.1	281	19.4	41.2	278.26		7.16
11.1	10.7	280	21.7	***41***	278.15		***5.27***
11.1	10.7	280	22.7	41.4	278.37		3.17
8.4	7.9	277	18.3	40.9	278.09		6.24
10.9	10.4	278	24.4	41.1	278.21		***1.24***
11.3	10.9	277	22.2	40.3	277.76		5.07
10.6	10.2	273	22.7	39.9	277.54		4.63
9.2	8.7	274	20.3	38.7	276.87		8.93

Table XI:

CAMS 72					
wind speed average (m/h)	RH %	Temp °F	Temp K	PM 2.5	PM 10
22.5		56.8	286.93		
22.9		56.5	286.76		
11.5		54.2	285.48		
9.5		54.3	285.54		
8.1		57.4	287.26		
12.3		60.3	288.87		
14.9		61.9	289.76		
14.3		64	290.93		
15.7		65.1	291.54		
20		65.5	291.76		
23.3		63.9	290.87		
23.6		62.8	290.26		
29		53.8	285.26		
35.2		44.5	280.09		
31.7		43	279.26		
32.2		41.6	278.48		
28		40.3	277.76		
18.6		40.8	278.04		
18.7		40.8	278.04		
18.3		40.4	277.82		
15.4		40.1	277.65		
16.3		39.3	277.21		
19.5		38.6	276.82		
11		38	276.48		
14.2		36.9	275.87		

Table XII:

CAMS 324					
wind speed average (m/h)	RH %	Temp °F	Temp K	PM 2.5	PM 10
11.2	26.1	56.2	286.59		
8	28.2	55.2	286.04		
8.2	28.8	54.7	285.76		
9	23.6	57	287.04		
8.7	21.7	58.8	288.04		
16.8	21.5	60.9	289.21		
16.8	19.1	62.8	290.26		
18.5	17.1	64.2	291.04		
20.3	15.8	65.1	291.54		
23	17.2	65	291.48		
26.1	20.4	63.6	290.71		
26	20.8	62.8	290.26		
29.1	34.5	58.1	287.65		
30.2	51.1	52.1	284.32		
28.5	50.5	50.9	283.65		
28.3	52.6	50	283.15		
18.6	55.5	49.2	282.71		
10.5	52.3	49.4	282.82		
14.3	53.4	49.4	282.82		
12.6	53.8	49	282.59		
12.6	49.6	48.9	282.54		
14.4	50	48.6	282.37		
17.9	48.5	48	282.04		
21.2	48.5	47.8	281.93		
17	59.7	46.7	281.32		

Chapter 5

5.1 Conclusion

A synoptic climatology of significant dust event was compiled at the National Weather Service Office of El Paso, TX, based on observational data from El Paso International Airport collected since 1932. As seen in the analysis of this data, El Paso, TX dust record appears to follow a regular annual dust cycle, characterized by frequent dust events throughout the spring season and fewer during the summer and winter. This annual dust cycle results from seasonal changes in environmental conditions. The environmental factors studied here related to these seasonal changes were particulate matter, wind speed, relative humidity and precipitation. Most of the dust events studied were associated with periods of low relative humidity (<35%), no precipitation and wind speeds greater than 10 mph. Most dust events are associated with a combination of strong winds, non surface coverage, and dry conditions, all of which occur most frequently during the spring season. Wind speed alone cannot be a perfect indicator of high dust levels, since other environmental factors such as surface cover and moisture can significantly reduce regional dust levels, even during high wind speeds.

The concentration of particulate matter with a size from 2.5 up to 10 micrometers in El Paso/Juarez metropolitan area on windy days is a clear proxy for blowing dust in the atmosphere. As expected in this research, the Non-Convective cases had a higher PM 10 concentration and lower PM 2.5 concentration, as non-convective cases can be larger in space and time and allow for a greater probability for obtaining larger particles. It was also suspected that the earlier in the season storms would have a larger concentration of smaller particles; which over a single season

might decrease in time, at least for the same source region, as they are depleted from the source soils as observed in Figures 2.6 (b-e). As seen in the PM plots, on Convective days we had more PM 2.5 (Finer particle) meaning that this type of cases can affect more the community because those smaller particles are the ones we breathe and can affect people's health, specially the kids and the elderly. Also this can raise the public's awareness of potential dust hazards and their causes in order to help residents be better prepared for action when needed.

As previously seen in chapter 3, 24-hour air mass back trajectories into El Paso, Texas during 2001- 2005 were largely symmetrical in their distribution around the city, for days in which dust was observed during this drought period (about 12% of all days), the trajectories were most associated with southwesterly flow from an area of known dust sources in the Chihuahuan Desert. An area with source contribution function >1 (more likely than random upwind location for air residence), during dust days, existed in northwest Chihuahua, Mexico near the eastern slope of the Sierra Madre Occidental.

Convectively-driven dust events, most frequent in El Paso during the summer North American Monsoon, were most prevalent with airflow from the south and east, as opposed to Gulf of California moisture surges which bring heavy precipitation and convection that is less dusty. The fastest- moving trajectories during days with dust in El Paso advected a distance of >600 km in 24-hours (7 m/sec), consistent with air parcels moving toward intensifying lee cyclones over the southwestern Great Plains or (for convectively-driven dust events) moisture surges from the Gulf of Mexico region.

This type of modeling and analysis has high utility in dust weather forecasting. When meteorological and land-surface conditions are conducive to dust storm generation, then a mean wind vector can be generated from the surface (around 880 mb at El Paso) to the forecast mixing height, which is usually around 700-600 mb. If this vector is within a high source contribution area identified here, then the meteorologist can have increased confidence of a potential dust event, which would have implications for air quality, aviation, and health and safety through high particulate concentration and visibility reduction. The recognition of these characteristic air mass trajectories will aid in forecasting dust storms in the Paso del Norte metropolitan area, and similar methodologies could be followed for other dust-prone cities.

Back trajectory analysis is just one piece in a weight-of-evidence approach. The approach we have used (probability modeling of HYSPLIT trajectories) has not been used before for dust transport pathways and is intended to be a preliminary step to show where to look for on the ground sampling. Some scientists disagree that the model of physical systems can be wrong to some degree, but when a variety of independent methods all point to the same conclusion, that conclusion is more likely to be valid (Oreskes et al., 1994; Oreskes and Belitz, 2001). Back trajectory methods are certainly independent of chemical analyses of dust.

Many models have been developed to study dust storms and their effects like the WRF-Chem model mentioned in chapter 4. These models are designed to serve both operational forecasting and atmospheric research needs; allowing researchers the ability to conduct simulations reflecting either real data or idealized configurations. My focus in this part was not to obtain PM results using an Air Quality Model, since it is well known that Air Quality Models don’t perform well under extreme circumstances, such as those exhibited during a dust storm.

Instead, my concentration was to examine the meteorological conditions predicted in a model conducive of a dust storm and compare them to measurements obtained by the ground stations and see how well or bad the model performed. As seen in the previous graphs, the model did well predicting the wind speeds and temperature when compared to the TCEQ stations' data. When looking at the Relative humidity data, there was a big discrepancy between the model and the ground data. This discrepancy could be because the model used Relative Humidity averages from all the stations around El Paso, TX and not one station in particular.

As future work, some health effects studies of convective vs. non-Convective dust events can be useful to identify which type of event is more harmful to the community. Also the analysis of other dust events cases with different strengths can be done using an updated version of the WRF-Chem, to see if the model performs well in any condition, Convective or Non-Convective.

It has been known that dust storms are environmental hazards that cause air quality and visibility problems across the southwestern part of the United States. Defining and studying the environmental/meteorological factor that help that produce dust events is very important because it will aid in forecasting dust storms in the El Paso, TX/Juarez, Chihuahua, MX metropolitan area, and similar studies could be followed for other dust-prone cities. Also, an evaluation of the climatology of dust-prone cities can help the meteorological community to improve their forecasting of extreme dust events around the world.

References

Ackerman, S.A. (1997). Remote sensing aerosols using satellite infrared observations. Journal of Geophysical Research, 102 (D14), 17069- 17079.

Adams, D.K., and Comrie, A.C. (1997). The North American Monsoon. Bull. Amer. Met. Soc. 78: 2197- 2213.

Alfaro, S.C., Gaudichet, A., Gomes, L., and Maille, M. (1997). Modeling the size distribution of a soil aerosol produced by sandblasting. J. Geophys. Res., 102 (D10), 11239– 11249.

Apodaca, K., and Morris, V. R. (2009). Analysis of aerosol number size distribution and hygroscopic growth factors as functions of ambient relative humidity during the North American Monsoon. AMS 89th Annual Conference, JP 2.15, Phoenix, AZ

Apodaca, K., Morris, V.R., Lozano, A.Y., Negrete, J., Fitzgerald, R.M. (2007). Interaction between dust storms, precipitation and Gulf of California moisture surges in the Paso del Norte region. Abstracts, 19th Conference on Climate Variability and Change, American Meteorological Society, no. JP2.13.

Ashbaugh, L.L., Malm, W.C., and Sadeh, W.Z. (1985). A residence time probability analysis of sulfur concentrations at Grand Canyon National Park. Atmos. Environ., 19, 1263- 1270.

Bach, A.J., Brazel, A.J., Lancaster, N. (1996). Temporal and spatial aspects of blowing dust in the Mojave and Colorado deserts of southern California, 1973–1994. Physical Geography 17, 329-353.

Baddock, M. C., Gill, T. E. Bullard, J. E., Dominguez-Acosta, M., Rivera Rivera, N. I. (2011). Geomorphology of the Chihuahuan Desert on potential dust emissions. Journal of Maps, 249-259.

Barnum, B. H., Winstead, N. S., Wesely, J., Hakola, A., Colarco, P. R., Toon, O. B., Ginoux, P., Brooks, G., Hasselbarth, L., and Toth, B. (2004). Forecasting dust storms using the CARMA-dust model and MM5 weather data. Environmental Modeling and Software, 19, 129–140.

Belsman, L. O. (2004). Satellite data for air quality forecaster. The Aerospace Corporation.

Bernier, S.A., Gill, T.E. and Peterson, R.E. (1998). Climatology of dust in the Southern High Plains of Texas. In: Busacca, A., Lilligren, S. and Newell, K. (eds), Dust aerosols, loess soils and global change: An interdisciplinary conference and field tour on dust in ancient environments and contemporary environmental management, October 1998, Seattle, Washington, Washington State University College of Agriculture and Home Economics Miscellaneous Publication no. 190, pp. 4-7

Brandalli, H. W., Ashman, J. P., and Reinke, D. L. (1977). Pictures of the month; Texas dust moves into Florida. Monthly Weather Review. vol. 105, pp. 1068-1070.

Brazel, A.J., Nickling, W.G. (1987). Dust storms and their relation to moisture in the Sonoran Mojave Desert region of the Southwestern United States. Journal of Environmental Management 24, 279–291.

Brazel, A.J. & Nickling, W.G. (1986). The relationship of weather types to dust storm generation in Arizona (1965}1980). Journal of Climatology, 6: 255-275.

Brown, M.J., Krauss, R.K. & Smith, R.M. (1968). Dust deposition and weather. Weatherwise, 21:66-70.

Cahill, T. A., Gill T. E., Gillette, D. A., Gearhart, E. A., Reid, J. S., and Yau, M-L. (1994). Generation, Characterization, and Transport of Owens (Dry) Lake Dusts, Final Report. Contract No. A132–105, Air Quality Group, Crocker Nuclear Laboratory, Univ. of Calif.

Calvo, A.I., Alves, C., Castro, A., Pont, V., Vicente, A.M., Fraile, R. (2012). Research on Aerosol Sources and Chemical Composition: Past, Current and Emerging Issues. Atmospheric Research, doi: 10.1016/j.atmosres.2012.09.021

Castalgia, P. J. and Fawcett, P. J. (2006). Large Holocene lakes and climate change in the Chihuahuan desert. Geology. 34 (2), 113-116.

Changery, M.J. (1983). A dust climatology of the western United States. Published by the NationalClimatic Data Center, Asheville, NC, for the Division of Health, Siting and Waste ManagementOffice, U.S. Nuclear Regulatory Commission.

Christopher, S. A., Gupta, P., Johnson, B., Ansell, C., Brindley, A., Haywood, J. (2011). Multi-sensor satellite remote sensing of dust aerosols over North Africa during GERBIL. Quarterly Journal of Royal Meteorological Society. Vol. 137, No. 658: 1168-1178.

.

CLiMET (1996). CI-500 Innovation, Laser Particle Counter Operations Manual. 1.0 CFM.

Connell, B.H. and Prata, F. (2006). Detecting volcanic ash and blowing dust using GOES, MODIS, and AIRS imagery. In: 14th Conference on Satellite Meteorology and Oceanography, American Meteorological Society, Preprints, P3.8, 7 pp.

Darmenova, K., Sokolik, I.N. and Darmenov, A. (2005). Characterization of east Asian dust outbreaks in the spring of 2001 using ground based and satellite data. Journal of Geophysical Research, 110, D02204, doi:10.1029/2004JD004842.

DeMott, P.J., Prenni, A.J., Liu, X., Kreidenweis, S.M., Petters, M.D., Twohy, C.H., Richardson, M., Eidhammer, T., Rogers, D. (2010). Predicting global atmospheric ice nuclei distributions and their impacts on climate. P. Natl. Acad. Sci. USA 107, 11217.

Doggett, A.L., Gill, T.E., Peterson, R.E., Bory, A.J.M., and Biscaye, P.E. (2002). Meteorological characteristics of a severe wind and dust emissions event: southwestern USA, 6-7 April 2001.

Preprints, 21st Conference on Severe Local Storms, August 2002, San Antonio, TX, published by American Meteorological Society, Boston, pp. 78-80.

Dominguez Acosta, M., (2009). The Pluvial Lake Palomas- Samalayuca Dunes system. Doctoral Dissertation, Geology, University of Texas at El Paso, United States.

Doyle, M., Dorling, S. (2002). Satellite and ground based monitoring of aerosol plumes. Water Air and Soil Pollution Focus 2, 615- 629.

Draxler, R.R., and Hess, G.D. (2004). Description of the HYSPLIT_4 modeling system. NOAA Tech. Memo. ERL ARL-224, 1- 28.

Draxler, R.R., and Rolph, G.D. (2003). HYSPLIT (HYbrid Single-Particle Lagrangian Integrated Trajectory). Model accessed via NOAA ARL READY Website (http://www.arl.noaa.gov/ready/hysplit4.html). NOAA Air Resources Laboratory, Silver Spring, MD.

Draxler, R.R., Gillette, D.A., Kirkpatrick, J.S., and Heller, J. (2001). Estimating PM10 air concentrations from dust storms in Iraq, Kuwait and Saudi Arabia. Atmos. Environ., 35, 4315-4330.

Fengmei, Y. and Chongyi, E. (2010). Correlation analysis between sand-dist events and meteorological factors in Shapotou, Northern China. Environmental Earth Science, 59: 1359-1365. doi 10.1007/s12665-009-0123-4

Field, R. D., van der Werf, G. R., and Shen, S. S. P. (2009). Human amplification of drought-induced biomass burning in Indonesia since 1960, Nature Geoscience, 2, 185–188, doi:10.1038/ngeo443.

Formenti, P., Schuetz, L., Balkanski, Y., Desboeufs, K., Ebert, M., Kandler, K., Petzold, A., Scheuvens, D., Weinbruch, S., Zhang, D. (2011). Recent progress in understanding physical and chemical properties of mineral dust. Atmos. Chem. Phys. 11, 8231-8256.

Gill, T.E., Dominguez Acosta, M., and Rivera Rivera, N.I. (2008). The Lake Palomas basin: dust engine of the Chihuahuan Desert. Geol. Soc. Amer. Abst. Prog., 40(6), 78.

Gill, T. E., Westphal, D. L., Stephens, G., and Peterson, R. E. (2000). Integrated assessment of regional dust transport from West Texas and New Mexico, Spring 1999. American Meteorological Society, 11th Conference on Air Pollution Meteorology Preprints, 370-375.

Gillette, D.A., (1999). A qualitative geophysical explanation for “Hot Spot” dust emitting source regions. Cont. Atmos. Phys., 72, 67 - 77.

Gillette, D. A. and Walker, T. (1977). Characteristic of airborne particles produced by wind erosion of sandy soil, High Plains of West Texas. Soil Science, vol. 123, pp. 97-110.

Ginoux, P., J. M. Prospero, T. E. Gill, N. C. Hsu, and Zhao, M. (2012), Global-scale attribution of anthropogenic and natural dust sources and their emission rates based on MODIS Deep Blue aerosol products, Rev. Geophys., 50, RG3005, doi:10.1029/2012RG000388.

Ginoux, P., Chin, M., Tegen, I., Prospero, J.M., Holben, B.N., Dubovik, O., and Lin, S.J. (2001). Sources and distribution of dust aerosols with the GOCART model. Journal of Geophysical Research 106: 20255-20273.

Goudie, A. S. (2009). Dust Storms: Recent Developments. Journal of Environmental Management, 90, 89-94.

Grell, G. A., Peckham, S. E., Schmitz, R., McKeen, S. A., Frost, G., Skamarock, W. C., and Eder, B. (2005). Fully coupled "online" chemistry within the WRF model. Atmospheric Environment, 39, 6957-6975.

Griffin, D. W. (2007). Atmospheric Movement of Microorganisms in Clouds of Desert Dust and Implications for Human Health. Clinical Microbiology Reviews. Vol. 20, No. 3, 459-477.

Grineski, S. E., Staniswalis, J. G., Bulathsinhala, P., Peng, Y., Gill, T. E. (2011). Hospital admissions for asthma and acute bronchitis in El Paso, Texas: Do age, sex and insurance status modify the effects of dust and low wind events. Environmental Research, 111, 1148-1155.

Grini, A., Myhre, G., Zender, C. S., and Isaksen, S. A. (2005). Model simulation of dust sources and transport in the global atmosphere: Effects of soil erodibility and wind speed variability. Journal of Geophysical Research, 110, D02205, doi:10,1029/2004JD005037.

Grini, A., Zender, C.S., Colarco, P.R. (2002). Saltation Sandblasting behavior during mineral

Guenther, A., Zimmerman, P., and Wildermuth, M. (1994). Natural volatile organic compound emission rate estimates for US woodland landscapes. Atmospheric Environment, 28, 1197–1210.

Harvey, G. (2007). Excel 2007 Workbook for Dummies (2nd ed.). Wiley. pp. 296 ff. ISBN 0470169370.

Henderson, D. E., Milford, J. B. and Miller, S. L. (2005). Prescribed burns and wildfires in Colorado: Impacts of mitigation measures on Indoor air particulate matter. Journal of the Air and Waste Management Association, 55, 1516-1526.

Hernández-Cadena, L., Téllez-Rojo, M. M., Sanín-Aguirre, L. H., Lacasaña-Navarro, M., Campos, A., Romieu, I. (2000). Relación entre consultas a urgencias por enfermedad respiratoria y contaminación atmosférica en Ciudad Juárez, Chihuahua. Salud Pública de México. Vol. 42, no. 4, 288-297.

Ho, W-C.,Hartley, W. R., Myers, L., Lin, M-H., Lin, Y-S., Lien, C-H., Lin, R-S. (2007). Air pollution, weather, and associated risk factors related to asthma prevalence and attack rate. Environmental Research, 104, 402-409.

Holben, B. N., Eck, T. F., Slutsker, I., Tanré, D., Buis, J. P., Setzer, A., Vermote, E., Reagan, J. A., Kaufman, Y. J., Nakajima, T., Laven, F., Jankowiak, I. and Smirnov, A. (1998). AERONET – A Federated Instrument Network and Data Archive for Aerosol Characterization. Remote Sensing of the Environment, 66,1–16.

Holcombe, T.L., Ley, T., Gillette, D.A. (1997). Effects of prior precipitation and source area characteristics on threshold wind velocities for blowing dust episodes, Sonoran Desert 1948–1978. Journal of Applied Meteorology 36, 1160–1177.

Hussein, T., Hämeri, K., Aalto, P., Asmi, A., Kakko, L. and Kulmala, M. (2004). Particle size characterization and the indoor-to-outdoor relationship of atmospheric aerosols in Helsinki. Scandinavian Journal of Work Environmental Health, 30(2), 54-62.

Jackson, M.L., Gillette, D.A., Danielson, E.F., Blifford, I.H., Bryson, R.A. & Syers, J.K. (1973). Global dustfall during the Quaternary as related to environments. Soil Science, 116: 135-145.

Janugani, S., Jayaram, V., Cabrera, S. D., Rosiles, J. G., Gill, T. E. and Rivera Rivera, N. I. (2009). Directional Analysis and Filtering for Dust Storm detection in NOAA-AVHRR Imagery. Proceedings of the SPIE Vol. 7334, 73341G-1.

Jauregui, E. (1989). Meteorological and environmental aspects of dust storms in northern Mexico. Erdkunde, 43: 141-147.

Idso, S., Ingram, R.S., and Pritchard, J.M. (1972). An American haboob. Bull. Amer. Meteor. Soc., 53, 930–935.

Kondratyev, K. Ya., Grigoryev, A. A., and Pokrovsky, O. M. (1983). The effects of aerosols on climate and aerosol climatology on the basis of observations from space. Advances in Space Research, 2 (5), 3-10.

Kopone, IK, Asmi, A, Keronen, P, Puhto, K, and Kulmala, M. (2001). Indoor air measurement campaign in Helsinki, Finland 1999 - the effect of outdoor air pollution on indoor air. Atmospheric Environment, 35, 1465–77.

Lancaster, N., Helm, P. (2000). A test of a climatic index of dune mobility using measurements from the southwestern United States. Earth Surface Processes and Landforms 25, 197–207.

Lee, J. A., Baddock, M. C., Mbuh, M. J., Gill, T. E. (2012). Geomorphic and land cover characteristics of Aeolian dust sources in West Texas and eastern New Mexico, USA. Aeolian Research, 3, 459-466.

Lee, J. A., Gill, T. E., Mulligan, K. R., Domínguez Acosta, M., and Perez, A. E. (2009). Land Use/Land Cover and Point Sources of the December 15 2003 Dust Storm in Southwestern North America. Geomorphology, 105, 18- 27.

Lee, J.A. & Tchakerian, V.P. (1995). Magnitude and frequency of blowing dust on the Southern High Plains of the United States, 1947-1989. Annals of the Association of American Geographers,85: 684-693.

Lee, J.A., Allen, B.L., Peterson, R.E., Gregory, J.M. & Moffett, K.E. (1994). Environmental controls on blowing dust direction at Lubbock, Texas, U.S.A. Earth Surface Processes and Landforms, 19: 437-449.

Legrand, M., Plana-Fattori, A. and N'doumé, C. (2001). Satellite detection of dust using the IR imagery of Meteosat, 1, Infrared difference dust index. Journal of Geophysical Research, vol. 106, no. D16, pp. 18251-18274, doi:10.1029/2000JD900749.

Liu, H.Y., Tian, Y.H., and Ding, D., (2003). Contributions of different land cover types in Otindag Sandy Land and Bashang area of Hebei Province to the material source of sand stormy weather in Beijing. Chinese Science Bulletin 48 (17), 1853–1856.

Littmann, T.J. (1991). Dust storm frequency in Asia: climatic control and variability. International Journal of Climatology 11, 393–412.

Lozano, A.Y., Negrete, J., Fitzgerald, R.M., Apodaca, K., and Morris, V.R. (2007). Correlation between precipitation, dust storms and Gulf of California moisture surges in the Paso del Norte region during the North American Monsoon. Abstracts, 21st Conference on Hydrology, American Meteorological Society, P2.11.

Lu, H. (1999). An integrated wind erosion modeling system with emphasis on dust emission and transport. Ph.D. thesis, the University of New South Wales, Sydney.

MacMahon, J.A., and Wagner, F.H. (1985). The Mojave, Sonoran and Chihuahuan Deserts of North America. In: Evenari, M., Noy-Meir, I., and Goodall, D.W. (Eds.), Hot Deserts and Arid Shrublands. Ecosystems of the World Series, Elsevier, 12A: 105- 202.

McMurry, P. H. (2000). A review of atmospheric aerosol measurements. Atmospheric Environment, 34, 1959-1999.

Mahowald, N.M., Kloster, S., Engelstaedter, S., Moore, J.K., Mukhopadhyay, S., Mcconnell, J.R., Albani, S., Doney, S.C., Bhattacharya, A., Curran, M.a.J., Flanner, M.G., Hoffman, F.M., Lawrence, D.M., Lindsay, K., Mayewski, P.A., Neff, J., Rothenberg, D., Thomas, E., Thornton, P.E., Zender, C.S. (2010). Observed 20th century desert dust variability: impact on climate and biogeochemistry. Atmos. Chem. Phys. 10, 10875-10893.

Mahowald, N. M., Ballantine, J. A., Feddema, J., and Ramankutty, N. (2007). Global trends in visibility: implications for dust sources, Atmos. Chem. Phys., 7, 3309–3339, doi:10.5194/acp-7-3309-2007.

Mahowald, N. M., Muhs, D. R., Levis, S., Rasch, P. J., Yoshioka, M., Zender, C. S., and Luo, C. (2006). Change in atmospheric mineral aerosols in response to climate: Last glacial period,

preindustrial, modern, and doubled carbon dioxide climates. Journal of Geophysical Research. Vol. 111, D10202, doi:10.1029/2005JD006653.

Makra, L., Sánta, T., Matyasovszky, I., Damialis, A., Karatzas, K., Bergmann, K-C. and Vokou, D. (2010). Airborne pollen in three European cities: Detection of atmospheric circulation pathways by applying three-dimensional clustering of backward trajectories. Journal of Geophysical Reseach, 111, D24220, doi:10.1029/2010JD014743.

Middleton, N. J., Goudie, A. S., and Wells, G. L. (1986). The frequency and source areas of dust storms. Aeolian Geomorphology, Allen and Unwin, Boston, pp. 237-259.

Middleton, N.J. (1984). Dust storms in Australia: frequency, distribution and seasonality. Search, 15: 46-47.

Miller, S.D. (2003). A consolidated technique for enhancing desert dust storms with MODIS. Geophysical Research Letters, vol. 30, no. 20, pp. 2071, doi:10.1029/2003GL018279.

Moran, J. M., (2006). Weather Studies, Introduction to Atmospheric Science. 3rd Edition American Meteorological Society, Boston, MA.

National Weather Service (NWS) Glossary (2010).

http://www.weather.gov/glossary/

Natsagdory, L., Jugder, D., and Chung, Y.S., (2003). Analysis of dust storms observed in Mongolia during 1937–1999. Atmospheric Environment vol. 37, no. 9–10, pp. 1401–1411.

Nichovic, S., Kallos, G., Kakaliagou, O., and Jovic, D. (1997). Aerosol production/transport/deposition processes in the Eta model: Desert cycle simulations. In Proceedings of the Symposium on Regional Weather Prediction on Parallel Computer Environments, . Athens, Greece (pp. 137–145) [Preprints].

Nicole Pauly, H. (2009). Impaired visibility: the air pollution people see, Atmos. Environ., 43, 182–195, doi:10.1016/j.atmosenv.2008.09.067.

Nilgun, K., Nickovic, S., (2000). An illustration of the transport and deposition of mineral dust onto the eastern Mediterranean. Atmospheric Environment vol. 34, pp. 1293–1303.

Novlan, D.J., Hardiman, M., Gill, T.E., (2007). A synoptic climatology of blowing dust events in El Paso, Texas from 1932-2005. Preprints, 16th Conference on Applied Climatology, American Meteorological Society, J3.12, 13 pp.

Okin, G. S., Bullard, J. E., Reynolds, R. L., Ballantine, J-A. C., Schepanski, K., Todd, M. C., Benalp, J., Baddock, M. C., Gill, T.E. and Miller, M. E. (2011). Dust emission: small-scale processes with global-scale consequences. Eos, Transactions of the American Geophysical Union 92(29):241- 242.

Okin, G., Reheis, M. (2002). An ENSO predictor of desertification in the southwestern United States. Geophysical Research Letters 29, doi: 10.1029/2001GL014494

Orgill, M.M. & Sehmel, G.A. (1976). Frequency and diurnal variation of dust storms in the contiguous U.S.A. Atmospheric Environment, 10: 813-825.

Ostro, B., Lipsett, M.J., Wiener, M.B., and Selner, J.C. (1991). Asthmatic responses to airborne acid aerosols. American Journal of Public Health 81, 694–702.

Park, S. H., Gong, S.L., Zhao, T.L., Vet, R.J., Bouchet, V.S., Gong, W., Makar, P.A., Moran, M.D., Stroud, C., Zhang, J. (2007). Simulation of entrainment and transport of dust particles within North America in April 2001 ("Red Dust Episode"). J. Geophys. Res., 112, D20209, doi:10.1029/2007JD008443.

Pecille, J.A. (1973). Wind and dust study for Lubbock, Texas. NOAA Technical Memorandum NWS SR-70, US Department of Commerce.

Peckham, S. E., and Grell, G. A. (2008) WRF-Chem Status. Retrieved from: http://ruc.noaa.gov/wrf/WG11/status.htm

Peckham, S. E., Grell, G. A., McKeen, S. A., Fast, J. D., Gustafson, W. I., Ghan, S. J., Zaveri, R., Easter, R. C., Bernard, J., Champman, E., Wiedinmyer, C., Schmitz, R., Salzmann, M., and Freitas, S. R. (2009). WRF/Chem Version 3.1 User's Guide.

Pelletier, J. D. (2006). Sensitivity of playa windblown-dust emissions to climatic and anthropogenic change. Journal of Arid Environment, 66, 62-75.

Peng, Yanlei, Staniswalis, J.G., Grineski, S.E., and Gill, T.E. (2010). A retrospective analysis of the association of dust storms and respiratory hospitalizations in El Paso, Texas, using a case-crossover study design. Abstracts, 1st Environment and Health Symposium, American Meteorological Society, J20.7.

Poirot, R.L., Wishinski, P.R., Hopke, P.K., and Polissar, A.V. (2001). Comparative application of multiple receptor methods to identify aerosol sources in northern Vermont. Env. Sci. Tech, 35, 4622- 4636.

Pollard, M.C. (1977). An Investigation of dust storm generation in the Southern Great Plains. M.Sc. thesis, Texas A&M, College Station. 75 pp.

Pope III, C. A. and Dockery, D. W. (2006). Health Effects of Fine Particulate Air Pollution: Lines that Connect. Journal of the Air &Waste Management Association. 56: 709-742.

Pope III, C. A., Brunnet, R. T., Thun, M. J., Calle, E. E., Krewski, D., Ito, K., and Thurston, G. D. (2002). Lung cancer, cardio-pulmonary mortality, and long-term exposure to fine particulate air pollution. The Journal of the American Medical Association. 287 (9), 1132-1141.

Pope, C. A., Dockery, D.W., Spengler, J.D., and Raizenne, M. (1991). Respiratory health and PM10: a daily time-series analysis. American Review of Respiratory Disease 46, 90–97.

Prospero, J. M., Ginoux, P., Torres, O., Nicholson, S.E., and Gill, T. E., (2002). Environmental characterization of global sources of atmospheric soil dust identified with the Nimbus 7 Total Ozone Mapping Spectrometer (TOMS) absorbing aerosol product. Reviews of Geophysics, 40 (1), 1002, doi:10.1029/2000RG000095.

Prospero, J. M. Charlson, R. J., Mohnen, V., Jaenicke, R., Delany, A. C., Moyers, J., Zoller, W. and Rahn, K. (1983). The Atmospheric Aerosol System: An Overview. Reviews of Geophysics and Space Physics, 21 (7), 1607-1629.

Pye, K. (1987). Aeolian Dust and Dust Deposits. Academic Press Inc. London. 334.

Raman, A. and Arellano, A. F. (2011). Modeling and Data Analysis of 2011 Phoenix Dust Storm. 15th Conference on Atmospheric Chemistry. 93 AMS Annual Meeting, Paper 5.5. Austin, TX.

Reheis, M., Budahn, J. R. and Lamothe, P. J. (2002). Geochemical evidence for diversity of dust sources in the Southwestern United States. Geochimica et Cosmochimica Acta, 66, 1569–1587.

Rivera Rivera, N. I., Gill, T. E., Hand, J. L., and Bleiweiss, M. P. (2010) Source characteristics of hazardous Chihuahuan Desert dust outbreaks. Atmospheric Environment, In Press.

Rivera Rivera, N. I., Gill, T. E., Gebhart, K. A., Hand, J. L., Bleiweiss, M. P. , and Fitzgerald, R. M. (2009). Wind modeling of Chihuahuan Desert dust outbreaks. Atmospheric Environment, 43, 347-354.

Rivera Rivera, N.I. (2006). Detection and characterization of dust source areas in the Chihuahuan Desert, southwestern North America. Masters. Thesis, University of Texas at El Paso, United States.

Reheis, M., Budahn, J. R. and Lamothe, P. J. (2002). Geochemical evidence for diversity of dust sources in the Southwestern United States. Geochimica et Cosmochimica Acta, 66, 1569–1587.

Rosmond, T. E., Teixeira, J., Peng, M., Hogan, T. F., and Pauley, R. (2002). Navy Operational Global Atmospheric Prediction System (NOGAPS): Forcing for ocean models. Oceanography, 15(1), 99–108.

Salvador, P., Artinaño, B., Pio, C., Alfonso, J., Legrand, M., Puxbaum, H., and Hammer, S., (2010). Evaluation of aerosol sources at European high altitude background sites with trajectory statistical methods. Atmos. Environ., 44, doi:10.1016/j.atmosenv.2010.03.042

Samet, J. M., Dominici, F., Curriero, F. C., Coursac, I., and Zeger, S. L. (2000). Fine particle air pollution and mortality in 20 US cities, 1987-1994. The New England Journal of Medicine, 343, 1742-1749.

Sapkota, J., Symons, J. M., Kleissl, J., Wang, L., Parlange, M. B., Ondov., J., Breysse., P. N., Diette, G. B., Eggleston, P. A. and Buckley, T. J. (2005). Impact of the 2002 Canadian forest fires on particulate matter air quality in Baltimore City. Environmental Science and Technology, 39, 24-32.

Schepanski, K., I. Tegen, B. Laurent, B. Heinold, and A. Macke. (2007). A new Saharan dust source activation frequency map derived from MSG-SEVIRI IR-channels, Geophysical Research Letters, 34(18).

Schichtel, B.A., Gebhart, K.A., Barna, M.G., and Malm, W.C., (2006). Association of airmass transport patterns and particulate sulfur concentrations at Big Bend National Park, Texas. Atmos. Environ., 40, 992- 1006.

Schmidt, R. H. (1986). Chihuahuan Climate. Second Symposium on Resources of the Chihuahuan Desert, Chihuahuan Desert Institute, Alpine, Texas, pp. 40-63.

Schmidt, R. H., Jr. (1979). A climatic delineation of the "real" Chihuahuan Desert. Journal of Arid Environments, 2, 243-250.

Seager, R., and Heim, R.R. (2009). Early 21st-century drought in Mexico. Eos- Trans. AGU 90 (11), 89 – 90.

Shao Yaping, Wyrwoll, K.-H., Chappell, A., Huang Jianping, Lin Zhaohui, McTainsh, G.H., Mikami, M., Tanaka, T.Y., Wang Xulong and Yoon Soonchang. (2011). Dust cycle: An emerging core theme in Earth system science. Aeolian Research 2(4):181-204, doi:10.1016/j.aeolia.2011.02.001

Shao, Y. (2000). Physics and Modeling of Wind Erosion. Kluwer Academic Publisher, Dordrecht, Netherlands.

Simpson, D., Guenther, A., Hewitt, C.N., and Steinbrecher, R. (1995). Biogenic emissions in Europe, 1: Estimates and uncertainties. Journal of Geophysical Research, 100D, 22875–22890.

Skamarock, W. C., Klemp, J. B., Dudhia, J., Gill, D. O.,Barker, D. M., Wang, W., and Powers, J. G. (2005). A description of the Advance Research WRF Version 2. NCAR Technical Note, NCAR/TN-468+STR.

Smith, R.M., Twiss, P.C., Kraus, R.K. & Brown, M.J. (1970). Dust deposition in relation to site, season and climatic variables. Soil Science Society of America Proceedings, 34: 112-117.

Sotiriou, M., Ferguson, S. F., Davey, M., Wolfson, J. M., Demokritou, P., Lawrence, J., Sax, S. N., and Koutrakis, P. (2008). Measurement of particle concentrations in a dental office. Environmental Monitoring and Assessment, 137, 351–361.

Stensrud, D.J., Gall, R.L., and Nordquist, M.K. (1997). Surges over the Gulf of California during the Mexican Monsoon. Mon. Wea. Rev., 125, 417– 437.

Stout, J. E. (2001). Dust and Environment in the Southern High Plains of North America. Journal of Arid Environment, 47:425-441.

Stull, R. B. (1988). An Introduction to Boundary Layer Meteorology, Kluwer AcademicPublisher, 666 p.

Tegen, I., Werner, M., Harrison, S.P., Kohfeld, K.E. (2004). Relative importance of climate and land use in determining present and future global soil dust emission. Geophysical Research Letters 31, L05105. doi:10.1029/2003GL019216.

Texas Commission on Environmental Quality (TCEQ-CAMS) website (2012) http://www.tceq.state.tx.us/compliance/monitoring/air/monops/hourly_data.html.

Texas Commission on Environmental Quality (TCEQ) (2009). Continuous Air monitoring Stations (CAMS). Retrieved from: http://www.tceq.com/compliance/monitoring/cams.html

Tong D.Q., Dan M., Wang T. and Lee P. (2012). Long-term dust climatology in the western United States reconstructed from routine aerosol ground monitoring. Atmospheric Chemistry and Physics 12:5189-5205.

Vautard, R., Yiou, P., and van Oldenborgh, G. J. (2009). Decline of fog, mist and haze in Europe over the past 30 years, Nature Geosci., 2, 115–119, doi:10.1038/ngeo414.

Varsik, J. R., Seigmund, W. A. and Berger, D. H. (1997). Telescope mirror contamination and airborne dust. http://www.bbso.njit.edu/~varsik/dust/absindex.html.

Vedal, S., Petkau, J., White, R., and Blair, J. (1998). Acute effects of ambient inhalable particles in asthmatic and nonasthmatic children. American Journal of Respiratory Critical Care Medicine, 157, 1034–1043.

Vedal, S. (1997). Ambient particles and health: lines that divide. Journal of the Air & Waste ManagementAssociation 47, 551–581.

Villanova, C. A. and Creech-Eakman, M. J. (2007). Looking for Correlations between Dust Events and Weather at Observatories in New Mexico. Publications of the Astronomical Society of the Pacific, 119, 1179- 1185.

Wang, K. C., Dickinson, R. E., Su, L., Trenberth, K. E. (2012). Contrasting trend of mass and optical properties of aerosols over the Northern Hemisphere from 1992 to 2011. Atmos.Che,. Phys., 12, 9387-9398. Doi:10.5194/acp-12-9387-2012.

Wang, K., Dickinson, R. E., and Liang, S. (2009). Clear sky visibility has decreased over land globally from 1973 to 2007, Science, 323, 1468–1470, doi:10.1126/science.1167549.

Warn, G.F. & Cox, W.H. (1951). A sedimentary study of dust storms in the vicinity of Lubbock, Texas. American Journal of Science, 249: 553-568.

Warner, T. T. (2004). Desert Meteorology. Cambridge University Press. Cambridge, U.K.

Washington, R., Todd, M.C. (2005). Atmospheric controls on mineral dust emission from the Bodélé Depression, Chad: The role of the low level jet. Geophys. Res. Lett. 32, L17701.

Washington, R., Todd, M., Middleton, N. J., and Goudie, A. S. (2003). Dust-storms source areas determined by the Total Ozone Monitoring Spectrometer and Surface Observations. Annals Association of American Geographers, 93 (2), 297-313.

Watson, J. G. (2002). Visibility: science and regulation, J. Air & Waste Manage. Assoc., 52, 628–628.

Watson, J. G., J. C. Chow, D. Dubois, M. Green, N. Frank, and M. Pitchford (1997). Guidance for Network Design and Optimum Site Exposure for PM 2.5 and PM 10 . Prepared for the Office of Air Quality Planning and Standards, United State Environmental Protection Agency, Research Triangle Park, NC 27711.

Wigner, K. A. and Peterson, R. E. (1987). Synoptic climatology of blowing dust on the Texas South Plains, 1947-84. Journal of Arid Environment, No. 13, pp. 199-209.

Wise, E.K., and Comrie, A.C. (2005). Meteorologically adjusted urban air quality trends in the Southwestern United States. Atmos. Environ., 39, 2969- 2980.

Wong, M. S., Nichol, J. E. and Lee, K. H. (2012). Estimation of aerosol sources and aerosol transport pathways using AERONET clustering and backward trajectories: a case study of Hong Kong, International Journal of Remote Sensing, 34:3, 938-955

WRF – The Weather and Research Forecasting Model. (2009). Retrieved from:

http://wrf-model.org/index.php

WRF-chem. (2009). Pacific Northwest National Laboratory (PNNL). Retrieved from:

http://www.pnl.gov/atmospheric/research/wrf-chem/

Xia, X.C., and Yang, G.S. (1996). Dust storms and its control in Northwest China. Chinese Environmental Press, Beijing, 128 pp.

Xiao J., and Chang, C. (2008). Dust storm's characters and correlation with meteorological data. 2008 International Workshop and Education Technology and Training & 2008 International Workshop on Geoscience and Remote Sensing. IEEE Computer Society, vol. 1, pp. 563- 566, doi:10.1109/ETTandGRS.2008.188 .

Xie, J., Yang, C., Zhou, B. and Huang, Q. (2009). High-performance computing for the simulation of dust storms. Computer, Environment and Urban System. doi:10.1016/j.compenvurbsys.2009.08.002

Yin, D., Nickovic, S., and Sprigg, W.A. (2007). The impact of using different land cover data on wind-blown desert dust modeling results in the southwestern United States. Atmos. Environ

Yin, D., Nichovic, S., Barbaris, B., Chandy, B., and Sprigg, W. A. (2005). Modeling wind-blown desert dust in the southwestern United States for public health warning: A case study. Atmospheric Environment,. 39, 6243-6254.

Yu, B., Hesse, P.P., Neil, D.T. (1993). The relationship between antecedent regional rainfall conditions and the occurrence of dust events at Mildura, Australia. Journal of Arid Environments 24, 109–124.

Zhang, R., Shen, Z., Cheng, T., Zhang, M., Liu, Y. (2010). The elemental composition of atmospheric particles at Beijing during Asian dust events in spring 2004. Aerosol Air Qual. Res. 10, 67-75.

Zhang, X.Y., Arimoto, R., and An, Z.S., (1997). Dust emission from Chinese desert liked to variations in atmospheric circulation. Journal of Geophysical Research - Atmosphere vol. 102 no. D23, 28, pp. 041–28,047.

Zhao, T. X-P., Ackerman, S. and Guo, W. (2010). Dust and Smoke Detection for Multi-Channel Imager. Remote Sensing, 2, 2347-2368.

Zender, C. S., and Kwon, E.Y. (2005). Regional contrast in dust emission responses to climate. Journal of Geophysical Research. Vol. 110, D13201, doi:10.1029/2004JD005501.

Zobeck, T.M., and Van Pelt, R.S. (2005). Erosion: Wind-induced. In: Hillel, D., editor.Encyclopedia of Soils in the Environment. Oxford, UK;Elsevier, Ltd., pp. 470-478.

Vita

Nancy I. Rivera Rivera was born in Rio Piedras, Puerto Rico. The third child of Gil M. Rivera Mercado and Tomasita Rivera Rivera, she graduated from Luis Muñoz Marín High School, Barranquitas, Puerto Rico in the spring of 1999 and entered to The University of Puerto Rico, Mayagüez Campus in the fall. While pursuing a bachelor's degree in Geology, she worked at the Puerto Rico Seismic Network as a data analyst. During the summers she was an intern in the Significant Opportunities in Atmospheric Research and Science (SOARS) program in Boulder, CO. In the fall of 2004, she entered the Graduate School at The University of Texas at El Paso (UTEP) where she completed a Master's Degree in Environmental Science in winter 2006. In the fall semester of 2007 she entered the Environmental Science and Engineering PhD. Program at UTEP. During her studies at UTEP in 2008 she met and dated Command Sergeant Major Lynch from the United States ARMY. They got married in March 2010. While pursuing her PhD. at UTEP she was supported as a NOAA Center for Atmospheric Sciences (NCAS) fellow, published several peer reviewed papers and participated in several international conferences.

Permanent address: P. O. Box 426
Barranquitas, P. R. 00794

This thesis/dissertation was typed by Nancy I. Rivera Rivera